UCL Université catholique de Louvain

École polytechnique de Louvain (EPL)

Synergistic effect between phenoxy and CNTs on the delamination toughness of modified epoxy based composites

Dissertation presented by
Iman BABAEI

for obtaining the Master's degree in
Chemical and Materials Engineering
Option(s): Functional Advanced materials Engineering (FAME)

Supervisor(s)
Christian BAILLY, Wael BALLOUT

Reader(s)
Jacques DEVAUX, Pascal VAN VELTHEM

Academic year 2015-2016

Rue Archimède, 1 bte L6.11.01, 1348 Louvain-la-Neuve **www.uclouvain.be/epl**

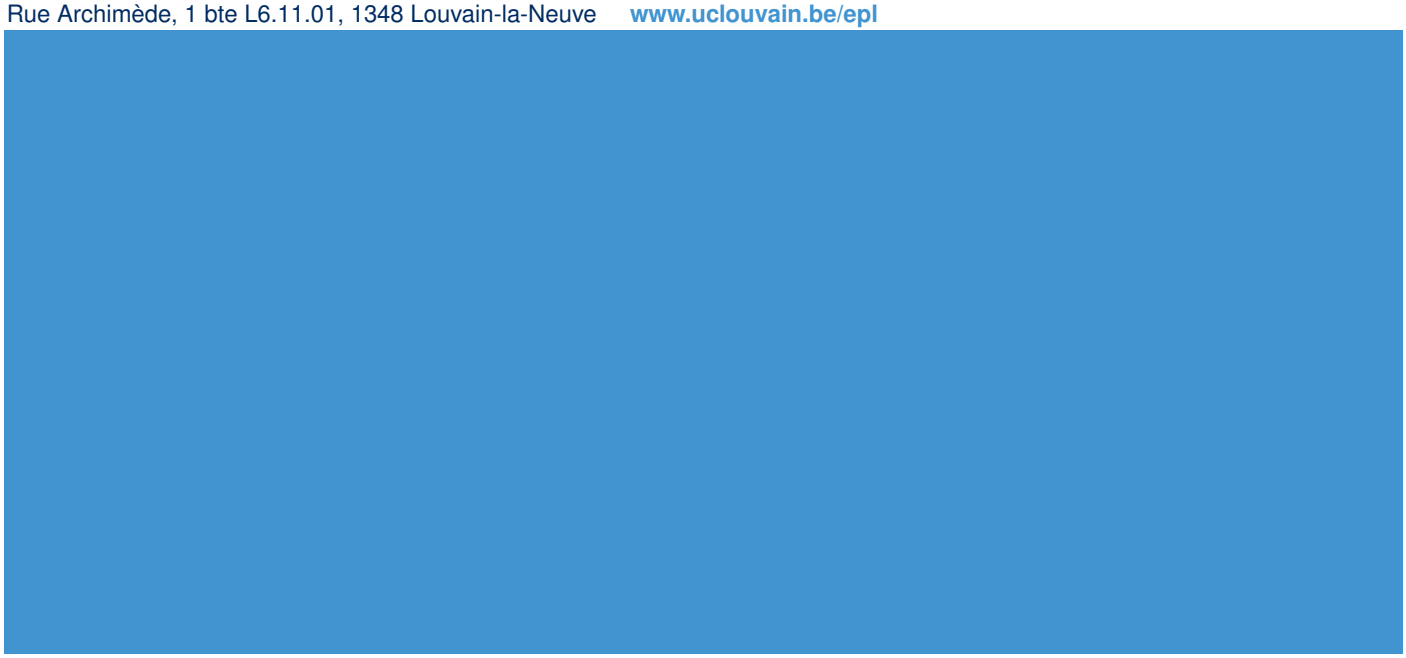

Abstract

Epoxy resins are horse-work of the advanced polymer matrix composites (PMC) which are widely used in automotive and aerospace industries. High mechanical properties with low density and excellent chemical resistance are main advantages of these PMCs. On the other hand due to high crosslinked network, these PMCs are inherently brittle and have limited fracture toughness and impact resistance compared to metallic alternatives. Among resin additives, thermoplastics and nanoparticles have been used as toughening agents for the past decades.

In this work synergistic effect of thermoplastic phenoxy phase and multi- walled carbon nanotubes (MWCNTs) as toughening agents of epoxy system made of tetraglycidyl 4,4′-diaminodiphenylmethane (TGDDM) and 4,4′-diaminodiphenylsulfone (DDS) has been studied.

Two different methods are used for epoxy modifications, one is adding them separately and the other one is using nanocomposites of phenoxy and CNTs. Three points SENB tests are done to evaluate the fracture toughness. Transmission electron microscopy (TEM) is used to study microstructure and degree of dispersion of the bulk of the samples and scanning electron microscopy (SEM) is used to study fracture surfaces and figure out toughening mechanisms.

It is observed that in the case of adding separately, synergistic effect only exists when 0.3 wt% CNTs and 9.7 wt% phenoxy is added and 114% increase in G_{Ic} is achieved. On the other hand when nanocomposites are used synergistic effect is seen when adding 0.6 wt% CNTs and 9.4 wt% phenoxy; with 107% increase in G_{Ic}.

TEM observations prove that in the case of using nanocomposites CNTs are more at the interfaces of phenoxy nodules after reaction phase induce separation (RIPS). SEM shows that at the lower amounts of CNTs, 0.1 wt%, toughening mechanisms is mainly crack path deflection, and in samples with higher amounts on CNTs beside crack path deflection shear banding due to pull out of MWCNTs is also identified as toughening mechanism.

Key words: Epoxy, Toughening, Carbon Nanotubes (CNTs), Phenoxy

Acknowledgements

I would like to first thank my thesis advisor Prof. Christian Bailly of the Bio- and Soft Matter (BSMA) of the Institute of Condensed Matter and Nanosciences (IMCN) of the University of Louvain. Amongst the many reason to thank him I can mention trusting in me to do this master thesis, his advices through the whole academic year 2015-2016, and especially keeping me in the right direction while writing this thesis.

Second I would like to thank Pascal Van Velthem and Wael Ballout for their daily advice and supervisions. Together they brightened my pass through all different stages of this master thesis. They were reliable backups whenever I was facing a problem.

Also I would like to thank Mrs. Pascale Lipnik, for her help in sample preparation for TEM observations, and Mr. Jean Marc, for preparing SENB samples.

Finally and most importantly, I would like to thank my family. Without them I would not even start my master studies two years ago. Their unbounded love and support in these last two years were my only fortune to not only pass my darkest period of life but also obtain a master degree.

Table of Contents

List of Tables

List of Figures and Illustrations

List of Symbols, Abbreviations and Nomenclature

Symbol	Definition
CNTs	Carbon nanotubes
DDM	Diamino diphenyl methane
DDS	Diaminodiphenyl sulfone
DGEBA	Diglycidyl ether of bisphenol-A
DWCNTs	Double-walled carbon nanotubes
G_{IC}	Critical strain energy release rate
K_{IC}	Critical stress intensity factor
MDA	Methylene dianiline
MWCNTs	Multi-walled carbon nanotubes
PKHP	Phenoxy powder
RIPS	Reaction induced phase separation
SEM	Scanning electron microscopy
SWCNTs	Single-walled carbon nanotubes
TEM	Transmission electron microscopy
T_g	Glass transition temperature
TGDDM	Tetraglycidyl-4,4’ diamino-diphenol methane
TGpAP	Triglycidyl p-aminophenol
TP	Thermoplastic
UCST	Upper critical solution temperature
α	Degree of conversion

CHAPTER 1 INTRODUCTION

A composite material is defined as a combination of two or more materials, matrix and reinforcements, that make the final material with better properties and also each of these materials keep their own physical, chemical, and mechanical properties. (F.C. Campbell 2010) Their main advantage over bulk materials is their higher strength and stiffness beside lower density. This has made them an interesting alternative for heavy metallic alloys which can also cause in lower fuel consumption and therefore greener planet.

Based on the matrix, composites are divided into three groups: metallic matrix composite (MMC), ceramic matrix composite (CMC), and polymer matrix composite (PMC). MMCs are mainly used in automobile industry, the matrix is usually aluminum and reinforced with silicon carbide. CMCs are used in places with really high ambient temperatures, like heat shield in spacecraft. The matrix and reinforcement are often the same material such as alumina, mullite, and silicon carbide. PMCs are most common composites with polymer based resins as matrix and fibers such as glass, carbon, or aramid for reinforcement.

Generally some main advantages of PMCs are high specific strength, good thermal insulation, medium to high productivity rate, and good impact, compression, fatigue, and electrical achievable properties. On the other hand some of their disadvantages can be stated that properties are affected by temperature and moisture, vulnerable to delamination or ply segregation, poor strength in out of plane direction, and difficult to be repaired.

Even though both thermoset and thermoplastic polymers can be used as matrix in PMCs; still thermosets are used far more than thermoplastics. For instance 95% of aerospace prepregs are thermosets. (D. Brosius, 2015) Historical use of thermosets in composites industry can be mentioned as the main reason for this huge gap in application percentage. Some other advantages of thermosets are: lower processing viscosities, high adhesion to fibers, and high thermal resistance. On the other hand some disadvantages might be: limited shelf lives, carefully controlled process needed to reach the desired curing, and once they are made, they are made. Figure 1.1 shows the percentage of materials used in Boeing 787 that among them composites' portion is 50 wt%.

Amongst different thermosets used as matrices for PMCs; epoxy and polyester are the dominants, approximately 85%. Epoxy is more expensive than polyester, used mainly in aerospace industry and called "work horse" for high performance composites. Some good properties of epoxies are high resistance to heat and maintaining properties at high temperatures, excellent adhesion to reinforcement, tailored elasticity, and excellent finishing and resistance to solvents and corrosives.

On the other hand some of their drawbacks are low shelf life at room temperature, long processing time, low strain-to-failure, low impact resistance, and difficult to recycle. As being thermoset; once polymerized cannot be remolded or reshaped. (Jasmin Stein, 2013) The main disadvantages of advanced composites

based on epoxy resins are low thermal and electrical conductivity and limited fracture toughness due to high density of crosslinking.

For decades scientists have tried different methods and materials, such as rubbers, thermoplastics, copolymers, and nanoparticles, to enhance the fracture toughness of epoxy based systems. Each of these methods have their own cons and pros. For example using copolymers decreases Young's modulus or rubbers are good options for ductile systems.

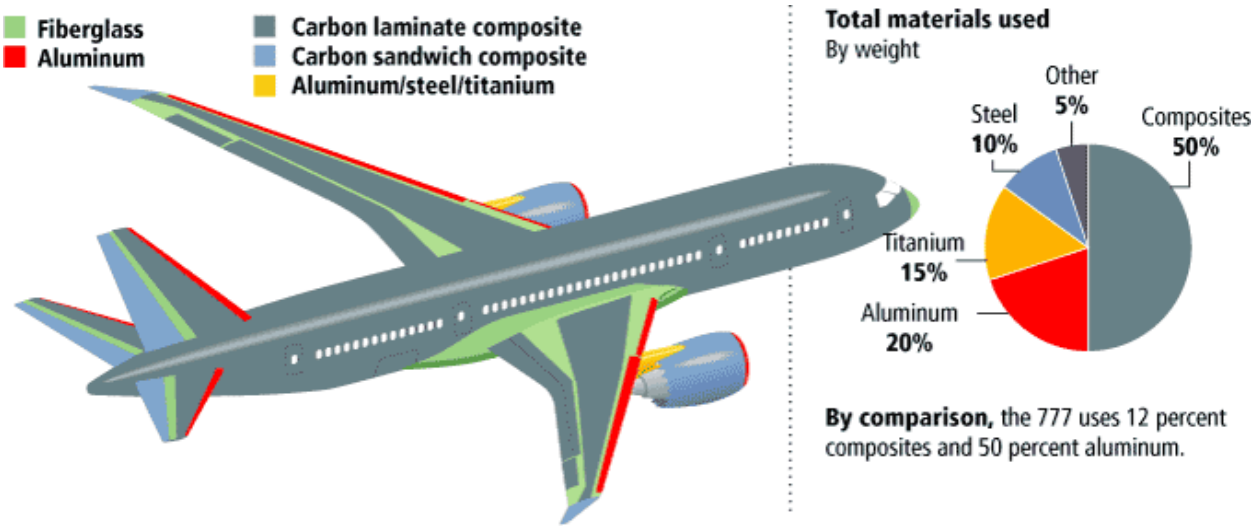

Figure 1.1 Weight percentage of materials used in Boeing 787 showing the interest in high performance composites applications[1].

A new method can be using two different materials at the same time and try to combine their advantages. Different thermoplastics and nanoparticles have been studied and proved to be good toughening agents for epoxy based systems. For example *Zeng et al.* studied simultaneous effects of nano-silica and nano-rubbers on the interlaminar fracture toughness of epoxy composites. (*Zeng et al. 2012)*

The main objectives of this master thesis are: examining if there is a synergistic effect between carbon nanotubes and thermoplastic phenoxy phase on fracture toughness of epoxy systems, if there is what are the specific formulations for this synergy, and as well as understanding toughening mechanisms that improve the fracture toughness of the modified system.

The methodologies to reach these objectives were to make blends containing both of toughening agents and check their properties with blends containing only one of the additives. Also two make the blends to different methods were used, either CNTs and phenoxy were added separately or nanocomposites of

[1] http://modernairliners.com/boeing-787-dreamliner/boeing-787-dreamliner-specs#boeing-787-specs-dreamliner-materials-pictorial

phenoxy and CNTs were used. At the end transmission and scanning electron microscopy (TEM and SEM) were applied to study the microstructure and understand the toughening mechanisms.

The presented manuscript is the result of this study and divided in five chapters. After introduction, in the state of the art previously published works by other institutions and scientist and also previous works done at UC Louvain are reviewed. Then in the third chapter the materials and techniques which are used are described. In the fourth chapter results are given and fully discussed with the help of second chapter. And finally some conclusions are drawn in the fifth chapter, followed by references.

CHAPTER 2 STATE OF THE ART

In this chapter first a brief review of different epoxies and hardeners and the transformations happening through their curing process is given. Then fracture toughness is described briefly and after that different methods of toughening like rubber modification, block copolymers, thermoplastics, hard inclusions as well as the association of at least two of them (ternary systems) are presented. The corresponding toughening mechanisms are discussed as well. Finally studies done at UCL about epoxy hardening are summarized.

Epoxy Systems

As stated in the introduction, when it comes to PMCs, epoxies are the best candidates to be used as matrix; especially for high performance composites used in aerospace field. Some properties of epoxy, beside mechanical and chemical resistance properties, which has made it so favorable are low viscosity, ease of cure, low shrinkage while curing, and excellent adhesion to carbon fibers. [1]

Epoxy resins, or as some references call them polyepoxides, are reactive polymers containing epoxide groups. Epoxide groups, shown in figure 2.1, are strained and highly reactive and due to their existence in epoxy resins curing can occur if the conditions are met. There are different ways to synthesis epoxide groups such as heterogeneously or homogenously catalyzed oxidation reaction of reactants like alkenes. Due to different methods there are different products but mainly epoxide groups are ethylene oxide and propylene oxide. [2]

Epoxy resins are not cured or just partly cured and they completely cure in special conditions. Some types cure by themselves, catalytic homopolymerisation, but others need additive such as polyfunctional amides, acids, phenols etc. to crosslink and cure. To reach the desired properties of the epoxy systems these additives must be added as close as possible to their stoichiometric proportion which depends on the density of the epoxide groups.

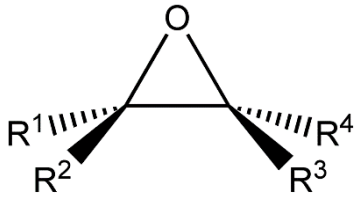

Figure 2.1 Chemical structure of epoxide group. [2]

First epoxy resins synthesized in Switzerland and United States in 1930s was diglycidyl ether of bisphenol-A (DGEBA), it is still most common in industry. It is linear polymerizing molecule with functionality 2 available with different viscosities, as illustrated in figure 2.2 (a). [1] Composites based on DGEBA resins have operation temperatures around 150 ° C. [3] Pure compound is colorless solid, unlike yellow commercial ones, and melts a bit above room temperature. [4]

Another kind of epoxy resins are triglycidyl p-aminophenol (TGpAP) which has a functionality 3 and so is more viscous than DGEBA. Its chemical structure is shown in figure 2.2 (b). It is also more brittle with higher T_g, compared with DGEBA, due to higher density of crosslinking. TGpAP is often used with DGEBA or TGDDM to improve their properties. [3]

Finally, epoxy resins with functionality 4 are tetraglycidyl-4,4' diamino-diphenol methane (TGDDM) or tetraglycidyl methylene dianiline (TGMDA) which have higher degree of crosslinking. Figure 2.2 (c) shows it's chemical structure. They are brittle with higher T_g; TGDDM hardened with DDS has T_g around 260-290 ° C, and often used with toughening agents. [3]

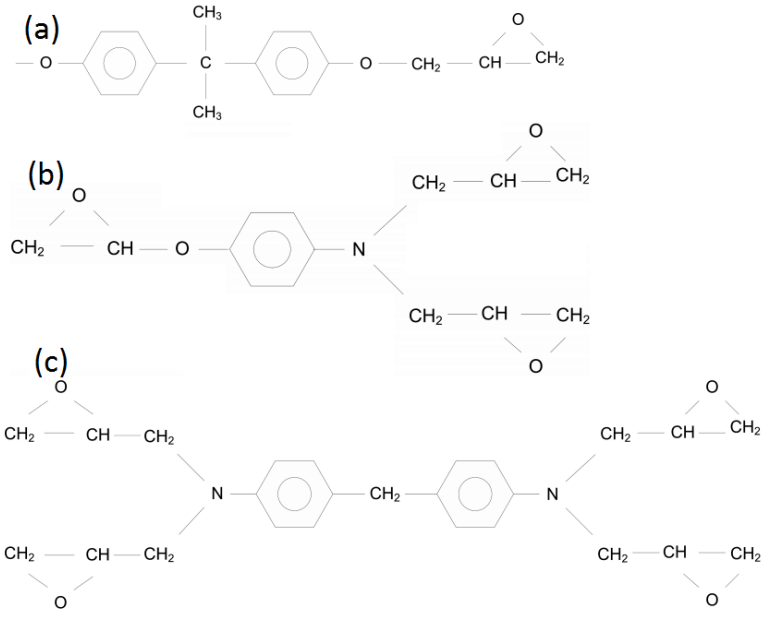

Figure 2.2 Chemical structures of different kinds of epoxies with different functionalities; DGEBA with functionality 2, (a), TGpAP with functionality 3, (b), and TGDDM with functionality 4, (c). [3]

As said, some epoxy resins need hardeners or initiators to cure. There are different hardeners with different prices which give the final cured epoxy products different properties. [4] Amine crosslinking agents are widely used and have two categories; aliphatic and aromatic. Aromatic amine groups cure at higher temperatures and cause the cured epoxy to have more strength and be less tough with higher T_g; compared with ones cured by aliphatic amine agents. [3] Good chemical resistance and long pot life are these agents' advantages while being solid, toxicity and long curing cycles are disadvantages. [4]

Some aromatic amine curing agents are diamino diphenyl methane (DDM), methylene dianiline (MDA) and diaminodiphenyl sulfone (DDS) which have phenyl groups and at least one nitrogen atom. Figure 2.3 shows chemical structure of these aromatic curing agents. [4] Among them DDS gives excellent thermal stability and higher T_g, so it is used more often than other curing agents. To reach the best thermal and

mechanical properties, hardeners should be used in stoichiometric portions. Mechanical properties of TGDDM cured by DDS are shown in table 1.

Table 2.1 Some properties of TGDDM epoxy resins cured with DDS [5]

Property	Value
T_g	260-290 ^oC
Density	1.29 gr/cm^3
Tensile modulus	5.03 GPa

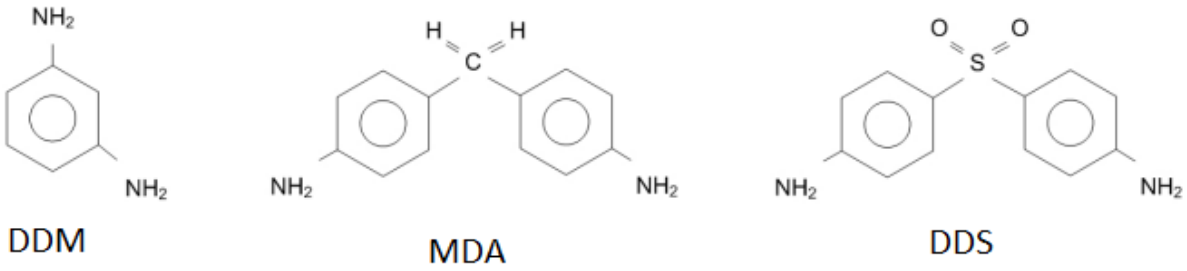

Figure 2.3 Chemical structure of three common aromatic diamine curing agents for epoxy resins. [3]

Curing of epoxy can be done by step or chain polymerization or by both kinds or by etherification. Epoxies with high functionality are more probable to be cured by etherification because of proximity of their epoxy groups. By changing the functionality of resins or molar ratio of reactive groups; polymerization process can be changed. [3]

In order to be aware and control the transformations happening during curing cycle, time-temperature-transformation (TTT) diagram, shown in figure 2.4, should be taken into account. Gelation, vitrification, full cure, and degradation are changes during curing cycle which are illustrated in TTT diagrams. Three important parameters of these diagrams are T_{g0}, glass transition temperature of uncured polymer with degree of conversion (α) equals to 0, $T_{g\infty}$, glass transition temperature for fully cure polymer with $\alpha=1$, and $_{gel}T_g$, T_g for gel with $\alpha=\alpha_{gel}$.

Based on these three important temperature and curing temperature four different results can occur: [6]

$T_c<T_{g0}$: No chemical reaction

$T_{g0}<T_c<{}_{gel}T_g$: Vitrification without gelation

${}_{gel}T_g<T_c<T_{g\infty}$: Gelation and then vitrification

$T_{g\infty}<T_c$: Gelation until fully curing the mixture

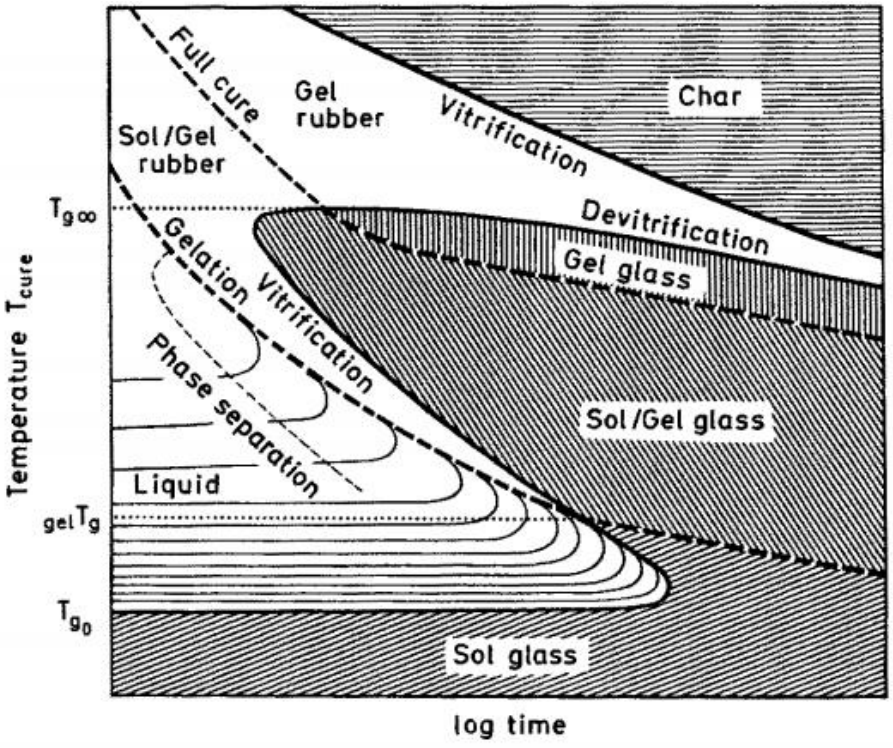

Figure 2.4 Time-temperature-transformation (TTT) isothermal cure diagram for a thermosetting system showing gelation, vitrification, and full cure line. Also to critical temperatures of T_{g0} and $T_{g\infty}$ are illustrated on the diagram.[6]

Gelation is an important transition that occurs during polymer network formation illustrated by large macromolecular network or in other words change from liquid to solid state. It is schematically illustrated in figure 2.5. After gelation starts the mixture is combination of sol and gel, until full conversion ($\alpha=1$) when there is no sol. From the processing point of view, gelation should only start only after the final shape of material is reached, desired mold is completely full of resin. Therefore having knowledge about when gelation occurs is important. [3]

Gel-time is the time that takes for gelation to occur from the beginning of polymerization. Of different ways to calculate this critical parameter; rheological tests are common. Dynamical shear properties are measured as a function of time and frequency at the desired temperature. Then to calculate the gel-time, based on

ASTM D 4473, there are two ways: one is the time for η^* to reach 100 mPaS, and another one is the cross point of G' and G". [5]

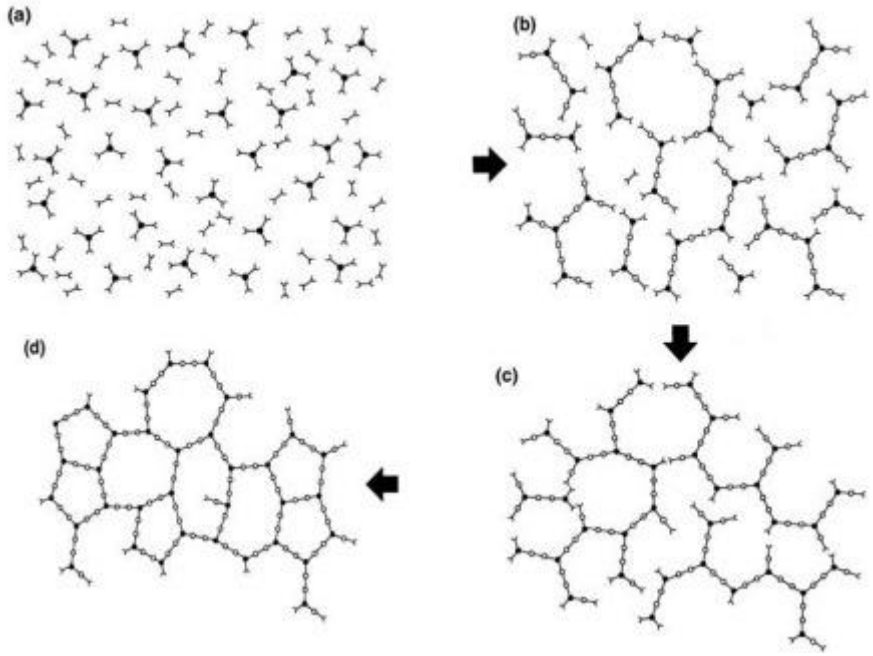

Figure 2.5 Schematically showing transformations happening through curing cycle; (a) monomers, (b) early stages, (c) approximately gelation, and (d) is complete network formation [6]

Fracture Toughness: K_{IC} & G_{IC}

As mentioned, usually epoxies used in high performance composites are so brittle, have low fracture toughness, due to high density of crosslinking. Fracture toughness of a material depends on volume of material that can deform plastically before the fracture, which as shown in figure 2.6 depends on thickness of the sample. Higher fracture toughness for thinner samples is related to lower degree of plastic constraint of these samples at the crack tip. [1]

As illustrated in figure 2.6 there are three different modes of fracture indicated by Roman numeral. Most common one of these modes is mode I where largest tensile loading is perpendicular to crack plane. Stress intensity factor for this mode, K_I, equals to:

$$K_I = \sigma\sqrt{\pi a \beta}$$

Where σ is applied stress, a is the length of the crack, and β is dimensionless parameter depending on structural geometry. [5] Critical stress intensity factor K_{Ic} is defined as lowest stress intensity for crack propagation to occur. It is used as a parameter to compare fracture toughness of materials, lower K_{Ic} values mean more brittle fracture and vice versa.

G_{Ic} is related to fracture toughness by:

$$G_{Ic} = \frac{K_{Ic}^2}{E'}$$

Where E' equals to E for plane stress and equals to $E/(1 - v^2)$ and v is poisons ratio.

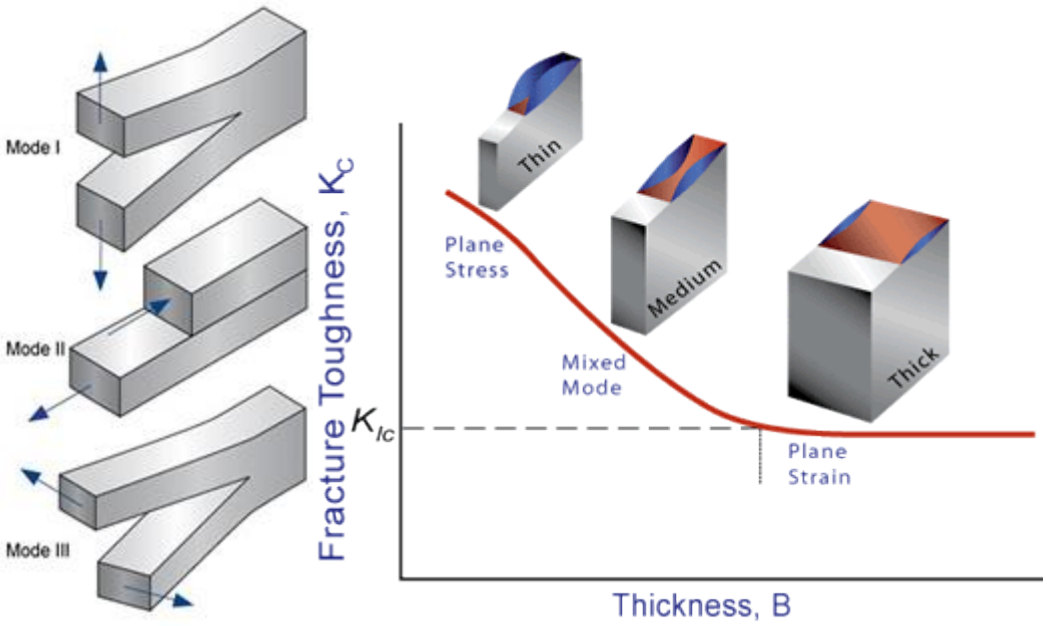

Figure 2.6 Three modes of fracture are schematically shown on the left and importance of thickness on the measured value of fracture toughness is shown on the right. [7]

Single edge notch bend (SENB or three-point bend) is a common way to test the toughness of bulk metals or polymers. Schematic of this test's sample is shown in figure 2.7. To be considered as a plain strain this criteria should be met:

$$B \geq 2.5\left(\frac{K_{IC}}{\sigma_y}\right)^2$$

Where B is the thickness of sample and σ_y is the yield strength. ASTM D5045 is a common standard test method for plane strain fracture toughness which makes it possible to test and compare results for different materials illustrated if figure 2.7.

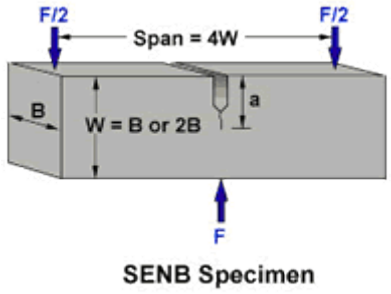

Figure 2.7 Dimensions of SENB sample for standard ASTM three points bending test to measure fracture toughness is shown schematically. [7]

Toughening Methods

As stated in the previous paragraphs epoxy systems have low fracture toughness, are brittle, which is one of their most important drawbacks. Many efforts have been made to increase their fracture toughness by different methods like rubber modification, copolymerization, thermoplastic application, and using hard inclusion. In the next paragraphs of this part these methods are discussed; mainly focused on the last two methods. Toughening mechanism of thermoplastic and hard inclusion methods are also stated in details.

Rubber modified

Rubbers used in this method can be either reactive rubbers, like copolymer of butadiene and acrylonitrile, or preformed rubber particle, like core shell rubbers (CSR). In 1969 *McGarry et al.* published the first work done to toughen epoxy with the help of rubbers. After that many works are done by other scientists on the different aspects of this method. The basic of this method is that a rubber is dissolved in epoxy, there might be also a chemical reaction between them, and after curing the dissolved rubber particles precipitate and improve the toughness. Some of the parameters affecting the final results in this method are matrix ductility, rubber concentration, and particle-matrix interface.

One of the most attractive rubbers used in this method is a copolymer of butadiene and acrylonitrile; with different acrylonitrile contents ranging from 0% to 26%. The low molecular weight butadiene acrylonitrile rubbers, (3400-4000g/mol), are soluble in liquid diglycidyl ether of bisphenol-A (DGEBA) epoxy resins. It can be synthesized with carboxylic acid or amine groups at the chain ends, CTBN and ATBN respectively. Chemical structures of these two kinds of rubber are illustrated in figure 2.8.

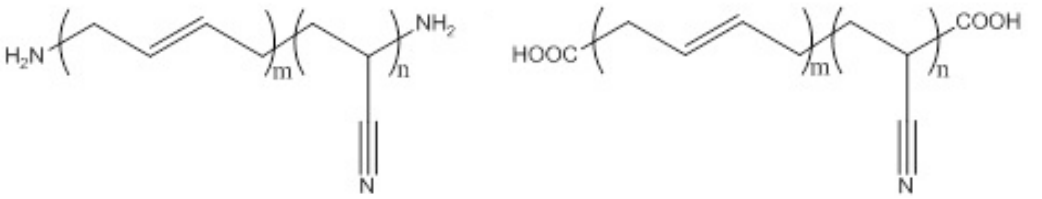

Figure 2.8 Chemical structures of ATBN and CTBN rubbers [8]

Bagheri et al. has reviewed the work of other scientist and published the results at 2009. [9] They claim that only epoxy systems which are ductile and lightly crosslinked, can be toughened by this method. They also state matrix shear yielding is the most potent mechanism in this method. Even though most of the scientists mentioned in reference [9] believe that higher monomer molecular weight means lower density of crosslinking and more ductility; *Arias et al.* believe that better indicator of ductility is T_g; due to different chemical nature of curing agents which might neutralize density of crosslinking. [10] Figure 2.10 shows the effects of the monomer molecular weight on fracture toughness of both neat epoxy and epoxy modified with elastomers. [11]

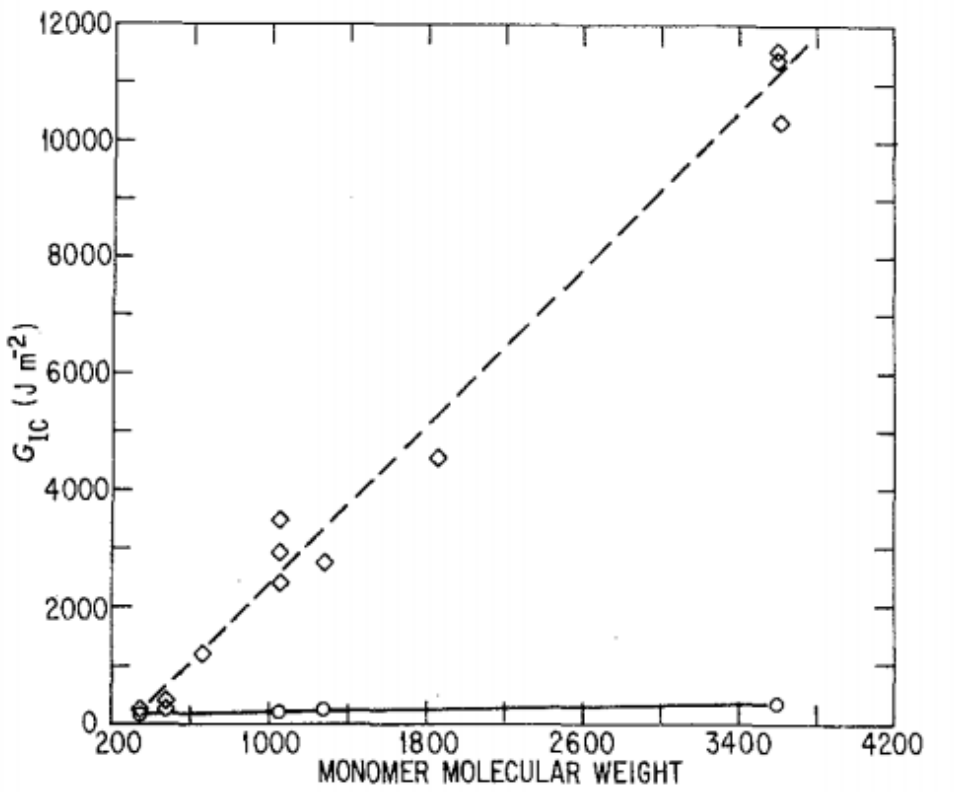

Figure 2.9 Effect of monomer molecular weight on the toughness of rubber modified systems, squares, and neat epoxy blends, circles. As can be seen monomer molecular weight does not affect the fracture toughness of neat epoxy, but linearly increases the fracture toughness of rubber modified sample [11]

It is shown by finite element analysis and also proven by experiments that until 20 vol% there is a linear relation between decrease in Young's modulus and yield stress with concentration of rubbers. This linear relation exist also for increasing in toughness with addition of rubbers but after a specific amount it does not increase anymore or even decreases. [9] *He et al.* concluded in their article that there is a dramatically improve in toughness of epoxy by addition of a small amount of acrylic rubber in the form of micrometer size particles; maximum reached and remained relatively constant between 12.5 phr and 25 phr of the rubber. At higher rubber concentrations toughness dropped gradually. Figure 2.11 shows the results of their studies. [12]

Lina et al. worked on the modification of epoxy resin with carboxyl-terminated polybutadiene (CTPB) liquid rubber. Besides the mechanical properties they investigated chemical reaction between oxirane ring of epoxy and carboxyl group of CTPB. The resulting pre-polymers were cured using methyl hexahydrophthalic anhydride and SEM application showed uniformly dispersed CTPB particles in epoxy matrix. They state the optimum mechanical strength and toughness is achieved when 20 phr CTPB is used. Higher electrical resistivity and breakdown strength, and lower dielectric permittivity and loss were also claimed by them for the CTPB-modified epoxy blends. [13]

Baiuk et al. studied bond properties of rubber modified epoxy systems by using two types of reactive liquid polymers, CTBN and ATBN. The purpose of their work was to overcome the premature failure, debonding, when using carbon fibers with epoxy resins. Samples were tested under the shear-lap test conditions and the results were as follows: ideal modifier was ATBN which has the highest ductility and toughness, 2.2 and 2.4 time more than the neat sample respectively. [14]

Yahyaie et al examined the toughening mechanisms of rubber modified epoxies, both bulk and thin film, by synthetizing and utilizing epoxy terminated polybutadiene (ETPB). Their results show that highest fracture toughness is achieved by using 7.5% of ETPB. Toughening mechanisms in the bulk material are claimed to be mainly cavitation and shear yielding mechanisms. In contrast, for the epoxy thin film they argue the main active toughening mechanism are crack arresting and shear yielding which led to improvement of adhesion and mechanical properties by energy dissipation. [15]

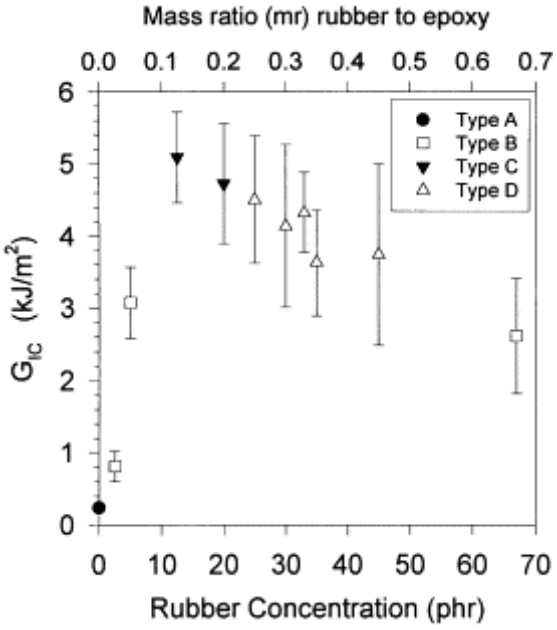

Figure 2.10 Strain release energy of modified epoxy system with acrylic rubber versus the concentration of the rubber [12]

Abadyan et al examined the effect of loading rate on toughness mechanisms in rubber modified epoxy using amine-terminated butadiene acrylonitrile (ATBN) rubber. At lower rates, 1-10 mm/min, of loading rate the toughening mechanism observed by them was shear yielding and cavitation in the plastic zone around the crack tip. It is stated that in this region fracture toughness decreases by increasing loading rate. Then there is a transition region, 10-100 mm/min, where there is no effect of loading rate on fracture toughness and toughening mechanisms are cavitation, shear yielding, and branching. Beyond this region fracture toughness drops dramatically to the level of unmodified epoxy. [16]

Guicun Qi et al showed in their work that if rubber modified plastics have a special morphology it can result in enhancing toughness and heat resistance cooperatively. The morphology they suggested is when in situ interface formed between plastic matrix and rubber particles have higher hardness than matrix. Hard interface cover rubber nanoparticles and protect them from deforming at high temperature, besides covalent integration with matrix improves the total toughness. [17]

Copolymers

The basic principle of this method is a copolymer compromised of one block that is miscible in epoxy, before and after curing, and one block that is miscible in uncured epoxy and during curing when the high conversions are reached becomes immiscible. [1] Important parameters in this method are nature of the copolymer's blocks, their relative length, and the hardener used. [18] *Dean et al.* studied different morphologies of copolymers inside epoxy resins, spherical micelle, wormlike micelle, and vesicle. [19]

They also stated that by increasing the volume fraction of epoxy miscible blocks the phase transition from vesicle to spherical micelle occurs. [20] Figure 2.12 illustrates these different morphologies.

Dean et al. also showed in their articles that by adding 2.5 wt% of PEO-PEP di-block copolymer block K_{IC} increases up to 45% with the help of mechanisms like localized matrix deformation, crack deflection, and possibly crack-bridging. They also studied the effect of copolymer morphology and claim that spherical micelles are better than vesicles and wormlike micelles is the best in improving G_{Ic}, fourfold improvement by wormlike micelles morphology. [19, 20]

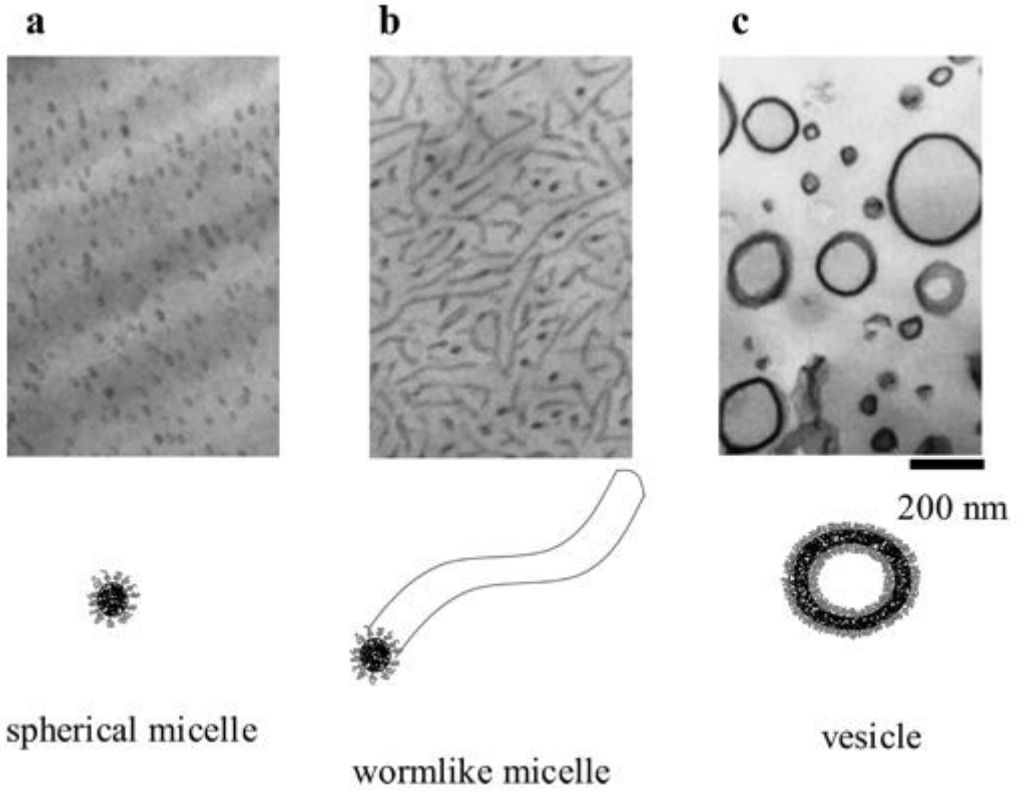

Figure 2.11 Representation of the block copolymer modified epoxy morphologies [20]

Li et al. investigated microstructure and mechanical properties of a bisphenol-A epoxy with a bio-derived amine hardener (Cardolite® NC-541LV) system modified with series of poly(ethylene oxide)-b-poly(butylene oxide) (PEOPBO) diblock copolymers. Chemical structure of these materials are shown in figure 2.13. They claim reaching nine times greater G_{IC} and modest increase in the glass transition temperature without significant reduction in the elastic modulus by using 5 wt % of intermediate molecular weight PEO-PBO due to a branched wormlike morphology. [21]

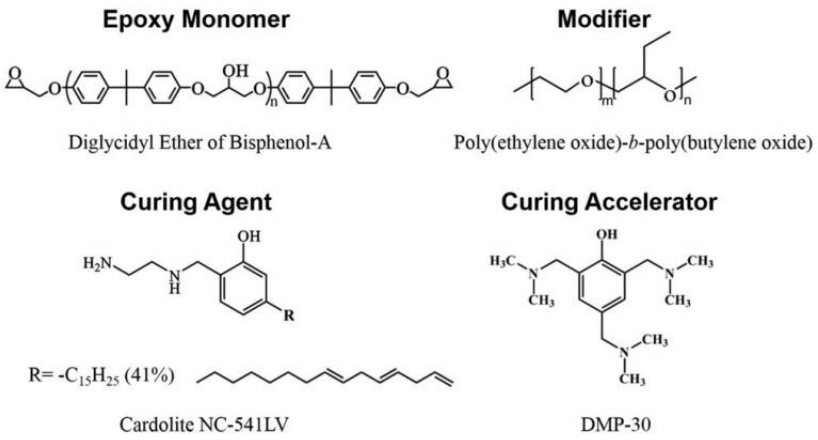

Figure 2.12 Chemical structures of thermoset resin ingredients and block copolymer modifier [21]

Downy et Drzal, worked on toughening DGEBA based epoxy polymer systems with di- and tri-functional aliphatic epoxy copolymers, figure 2.14 illustrates their chemical structures. They state the increase of 56–77% in Izod impact strength test values over neat epoxy with small amount of additives, around 1 wt %, and not dramatically affecting other properties like glass transition temperature and flexural properties. [22]

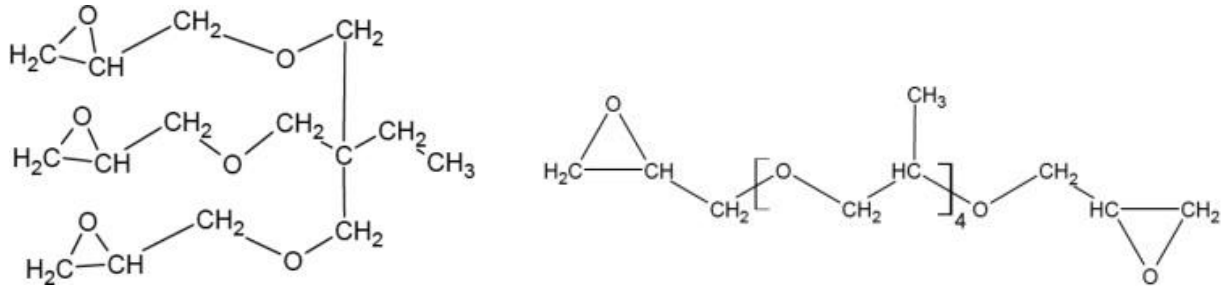

Figure 2.13 Trimethylolpropane triglycidyl ether (tri-functional aliphatic), left, and Polypropylene glycol diglycidyl ether (di-functional aliphatic), right. [22]

Romeo et al. studied the effect of the curing cycle on the on the morphology of the block copolymer epoxy system. They state that during curing cycle thermoset shifts from good solvent to poor one and finally to nonsolvent because average molar mass increases before gelation and after that crosslink density increases which increase the conversion. They have experienced a solution of 20 wt % PS-b-PMMA (M_n= 67100, Φ_{PS}= 0.69) in a stoichiometric mixture of DGEBA and 4,4′-methylenebis (2,6-diethylaniline)(MDEA). With different curing cycles different morphologies from dispersion of spherical micelles to a dual morphology were achieved which affect properties of material such as transparency and toughness. [23]

Redline et al. examined two different copolymers of PS-PEO and PEP-PEO, shown in figure 2.15, added to epoxy resins. Both copolymers self-assembled into spherical micelles with PEO coronas but one with rubbery PEP cores and the other with glassy PS cores. Until 2 wt % of loading both systems acted similar

to each other but above that PEP-PEO copolymers outperformed PS-PEO ones by approximately a factor of two. Again they claim that more ductile matrix can reach higher toughness and main toughening mechanism is matrix shear yielding. [24]

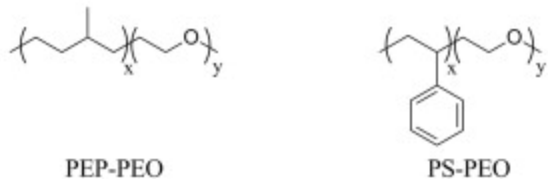

Figure 2.14 Chemical structures of PEP-PEO and PS-PEO diblock copolymers. [24]

Thermoplastics

Another method to toughen highly crosslinked epoxy resins is using thermoplastics which has been studied since 1980s. The main advantage of this method is that while improving the toughness, no significant decrease in properties like tensile modulus or strength is observed, unlike the case of using rubbers. [1] *Hodgkin et al.* has reviewed effects of parameters like thermoplastic endgroups, material's morphology, and ductility of the matrix and the chemical structure of the thermoplastic on the final improvements of toughness of the system. [25]

In order to achieve a good thermoplastic toughening these materials should have a thermally stable backbone, not necessarily reactive endgroups, which is soluble in uncured epoxy and will phase separate during curing. Different morphologies depend on concentrations and molecular weights. Lower concentrations of second phase lead to dispersed thermoplastic morphologies, while higher concentration will cause phase inverted morphologies. Between these two extremes, cocontinuous morphologies are occurred with intermediate concentrations. Figure 2.16 schematically illustrates dissolving and then phase separation of epoxy resin and thermoplastic modifiers. Rate of phase separation alongside with rate of curing reactions causes a homogenous or heterogeneous morphology to form. [26]

Girard-Reydet et al. studied phase separation mechanisms in DGEBA/DDS and DGEBA/MDA systems modified with polyetherimide. By using cloud point curves (CPC) they found the thermodynamic critical point of the CPC for PEI in both systems to be ϕ_{Mcrit}=9.8 wt% and 10.7 wt%, respectively for system hardened with DDS and MDA. They claimed that for concentrations near these values phase separation was proceeded by spinodal demixing, while for modifier concentrations higher than these critical values nucleation and growth was mechanism of the phase separation. They stated that post-cure stage due to devitrification of phases and further epoxy-amine reactions helps the phase separation process to continue to happen. [27]

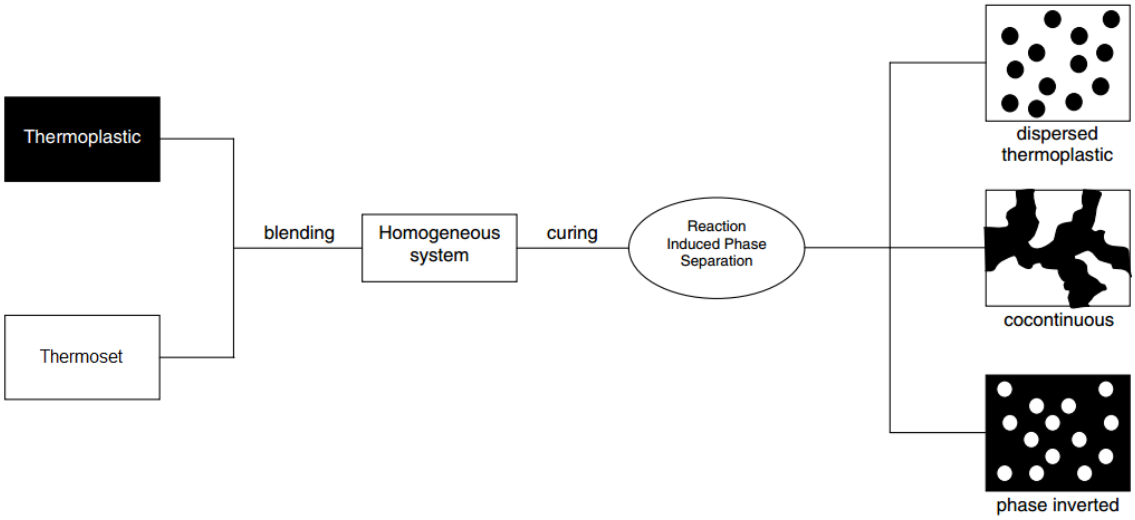

Figure 2.15 Morphology evolution of thermoset/thermoplastic blends upon curing [26]

Williams et al. reviewed articles and works about generation of two-phase morphologies in modified thermoset polymers. They stated that two main procedures in order to generate these morphologies are reaction-induced phase separation (RIPS) and dispersion of second phase in starting monomers. They also used CPC diagram and stated that mostly modified systems exhibit an upper-critical-solution-temperature (UCST) behavior. Each concentration of modifiers, ϕ_M, is not miscible in the system below a temperature, T_r, and RIPS occurs when system reaches the point (ϕ_M , T_r), as shown in figure 2.17. [28]

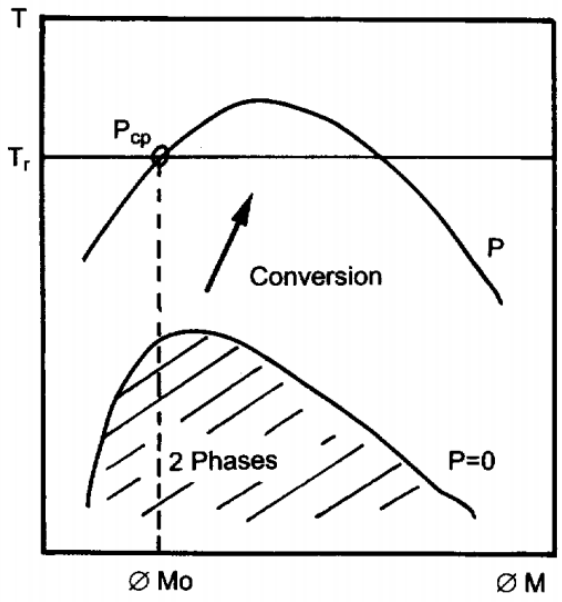

Figure 2.16 Reaction induced phase separation in a modified system with UCST behavior and effect of conversion (P) on miscibility gap. [28]

Considering morphology, toughness improvement is optimized by reaching co-continuous or phase inverted morphology. Thermoplastics with higher molecular weight better increase the system toughness. Unlike rubbers, thermoplastic toughening is more effective in highly crosslinked matrix. [25]

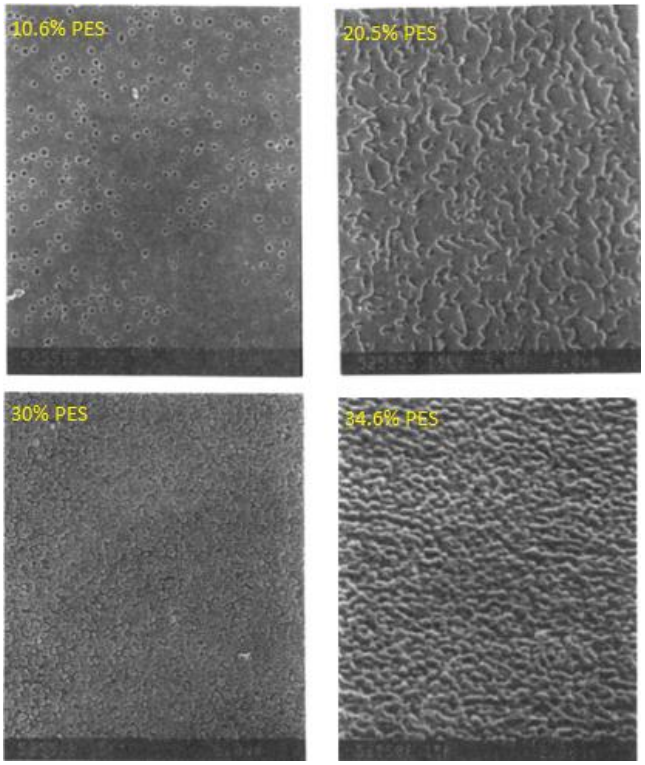

Figure 2.17 Effect of PES on the morphology in epoxy resin system [29]

Polyethersulfone (PES), polyetherimide (PEI), phenoxy, Poly(ether ether ketone) (PEEK), and polysulfone (PSF) are among the thermoplastic toughening materials which have been deeply studied.

Polyetherimide (PEI) is an amorphous, amber-to-transparent thermoplastic which may exist in epoxies as particulate, co-continuous, or phase-inverted morphologies. [30] *Gilbert and Bucknall* claimed almost tenfold increasing of G_{IC}, from 0.055 to 0.530 kj.m^{-2}, and slight increasing in Young's modulus by using up to 30 wt% of PEI. Results of their study is shown in table 2.2 They state particle bridging as a major toughening mechanism and crack pinning as a minor one. Adding more than 30 wt% of PEI caused phased separation in the system and formation of PEI-based system which resulted in lower K_{IC}. [31]

Table 2.2 Results of using PEI as toughening agent [31]

Blend	K_{IC} [MPa.m$^{1/2}$]	E [MPa]	G_{IC} [kJ.m^{-2}]
Neat PEI	3.56	3.30	3.303
Unmodified Epoxy	0.48	3.59	0.055
5phrPEI	0.73	3.52	0.131
10phr PEI	0.82	3.62	0.160
20phr PEI	1.17	3.47	0.340
30phr PEI	1.53	3.80	0.530

Table 2.3 Results of adding 10% PESU to epoxy system (TGDDM hardened with MTHPA) [32]

Material	G_c (J/m^2)	$G_{c,rel}$ (%)
EP	151 ± 21	100 ± 14
EP/PESU-L 10%	185 ± 13	122 ± 7
EP/PESU-M 10%	180 ± 30	119 ± 17
EP/PESU-H 10%	369 ± 45	244 ±12

Aravand et al. studied polyoxymethylene (POM) as thermoplastic toughening material. They observed different morphologies like particulate (5-10 wt% POM), co-continuous (15 wt% POM) and phase inverted (20-25 wt% POM) based on the amount of composition. Blends with co-continuous or phase inverted morphologies had no improvement in fracture toughness. They state Young's modulus and T_g stayed preserved while G_{IC} of the sample with 10 wt% POM increased almost four times. Particle crack bridging, matrix shear yielding, and particle debonding with subsequent void growth are claimed to be main toughening mechanisms. [33]

Giannotti et al. researched on the effect of using two thermoplastics at the same time. They studied epoxy system modified with polysulfone and poly(ether imide). For not facing preparation problems due to high viscosity they kept the total amount of thermoplastic 10-15 wt% and concluded adding small amount of PSF changes the morphology of system. For example in the case 10 wt% PEI when 25 % of PEI was replaced by PSF, particulate morphology changed into co-continuous and up to 40 % improvement in G_{IC} was achieved. Suggested toughening mechanisms by them were ductile tearing of the TP phase, crack bridging, and crack pinning. [34]

Francis et al. studied epoxy system toughened with poly poly(ether ether ketone) with pendent methyl groups and claimed similar results about morphology and its effects on toughness. They observed two times increase of K_{IC} in sample with 15 wt% percent of PEEKM and linked it with the co-continuous morphology of the blend with no deterioration in thermal stability. Toughening mechanisms suggested to be crack pinning, crack path deflection, crack bridging by the dispersed domains and particle tearing. [26]

Teng and Chang studied homogenous, transparent, and inhomogeneous, opaque, phenoxy/epoxy blends by kinetically controlling the curing reaction. The reason for this phase separation is that phenoxy is miscible in epoxy monomers and low molecular weight epoxy chains but not in high molecular weight crosslinked epoxy. Viscosity of the blend during curing cycle and before this phase separation plays an important role in final morphology. [35] They found that toughness increases by increasing the amount of phenoxy and homogeneous blends showed the highest increase. They suggested localized shear plastic deformation around crack tip as toughening mechanism. [36] In another study by *Siddhamalli et al.* interconnected globular morphology was suggested as a favorable morphology to improve toughness by stretching and tearing of the phenoxy phase. [37] Table 2.4 shows effect of phenoxy concentration on mechanical properties of epoxy system.

Table 2.4 Effects of phenoxy concentration on epoxy-phenoxy blends properties [36]

Blend	Phase separation	Tensile strength (MPa)	Tensile modulus (GPa)	Tensile strain (%)	K_{Ic} (MPam$^{1/2}$)
Epoxy/DDS	-	33 ± 3	3 ± 0.1	1.9 ± 0.6	0.7
Phenoxy/Epoxy/DDS 10 wt% phenoxy	Droplet	41± 3	3 ± 0.1	2.8 ± 0.4	0.9 ± 0.2
Phenoxy/Epoxy/DDS 20 wt% phenoxy	Interconnected globules	74 ± 10	2.9 ± 0.1	6.7 ± 1.3	3.2 ± 0.9
Phenoxy/Epoxy/DDS 30 wt% phenoxy	Phase inverted	62 ± 5	2.8 ± 0.1	5.6 ± 0.7	2.3 ± 0.3
Phenoxy/Epoxy/DDS 40 wt% phenoxy	Phase inverted	47	2.5	3.4 ± 0.3	1.1 ± 0.1

Toughening Mechanisms of thermoplastic modified systems

As *Pearson and Yee* [2] has shown in the figure 2.18, there are at least six different mechanisms that causes epoxy based systems to toughen. Some of them were mentioned in previous paragraphs and in the coming ones "crack bridging", "crack pinning", "crack path deflection", and "particle induced shear bending" are mechanisms discussed more in details.

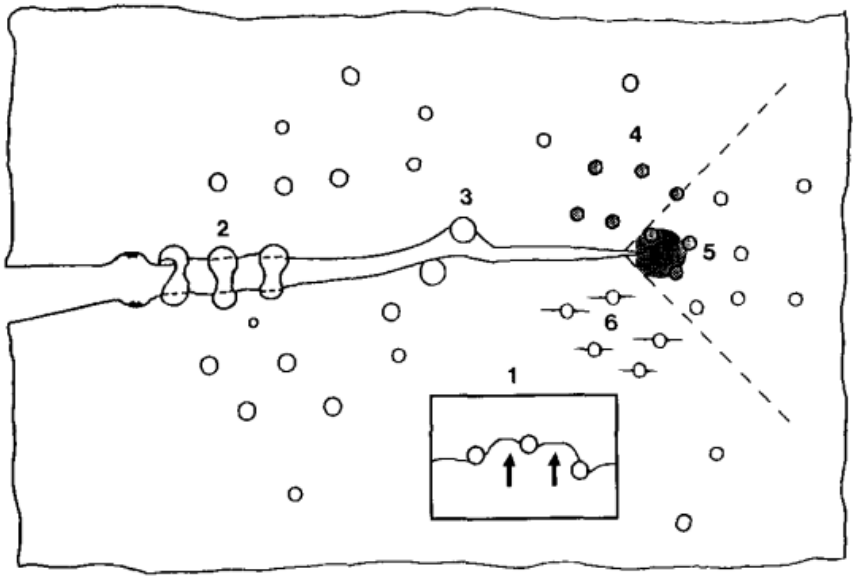

Figure 2.18 Different toughening mechanisms in thermoplastic modified epoxies. [38]

Crack Bridging

Pearson and Yee stated in their article that one of the ways thermoplastic particles increase the toughness is by spanning the crack surfaces and lowering the stress at crack tip, it is shown in figure 2.19. They also stated plastic deformation of thermoplastic phase might be the reason of toughening in this mechanism. [10] Cardwell and Yee worked on toughening of epoxies through thermoplastic crack bridging and published SEM results of their experiments showing crack bridging as a toughening mechanism. [39]

Scientists have tried to make a quantitative models for this mechanism based on crack opening displacement, how ductile phase behaves, and the stress distribution in bridging zone. One the models is done by *Przystupa and Courtney* on Co-CoAl alloys. [40] They have stated that apparent fracture toughness of a brittle material containing ductile inclusions, K_C, can be calculated as:

$$K_C = K_{EX} \geq AK_{CRM} + K_p$$

Where K_{EX} is the stress intensity of external forces, K_{CRM} is the critical stress intensity of the matrix, K_p is the stress intensity of unbroken particles, and A equals to: $\frac{A_1 A_2}{A_3}$ where A_1, A_2, and A_3 are corrections due to crack bowing, particle penetrability, and secondary slip within particles; respectively. [40] They also managed to show the similarity between their model and experimental results.

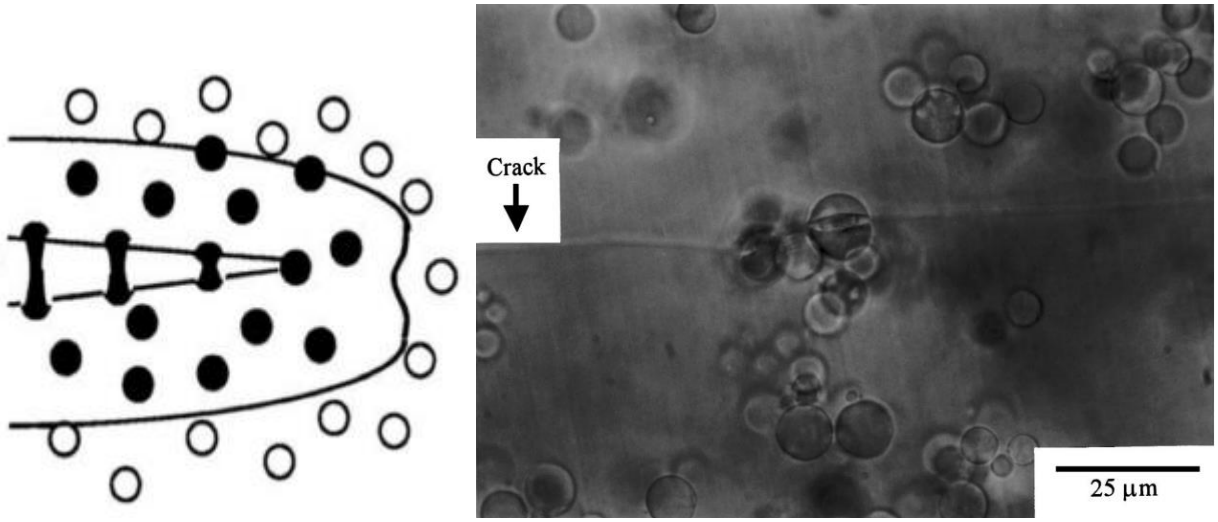

Figure 2.19 Schematically (left) and experimentally (right) showing crack bridging mechanism. [38, 39]

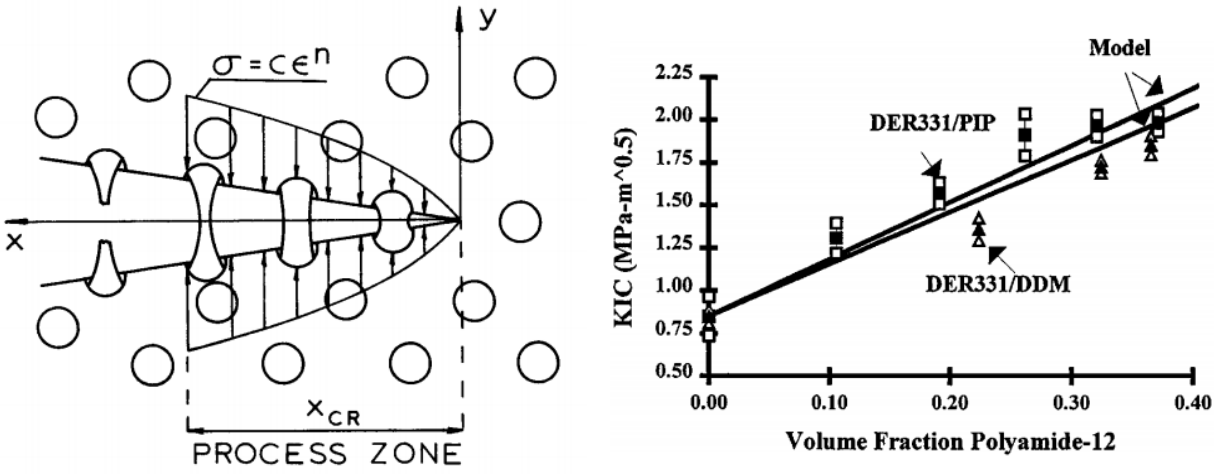

Figure 2.20 Schematic of the quantitative model by Przystupa and Courtney and showing the results obtained by experiments and by theory in one graph. [38, 40]

Crack Pinning

In this mechanism thermoplastic particles do not let the cracks to penetrate and make them to bow out which results in extra energy consumption, shown schematically in figure 2.21. [38] This is true when there is a huge difference in toughness between thermoplastic and brittle phase. As illustrated in figure 2.21 from reference [14]; this mechanism is observed as particles with tails in SEM images.

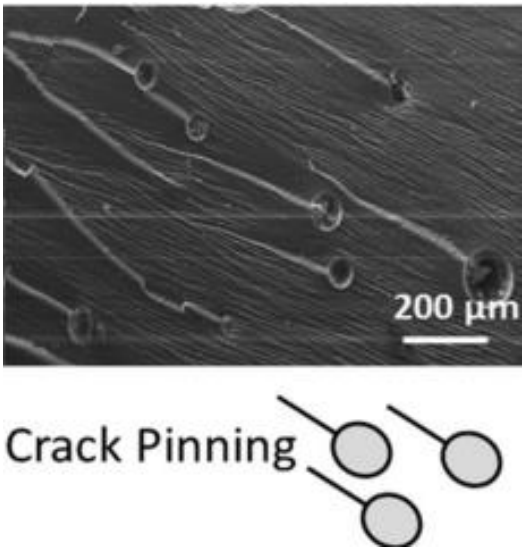

Figure 2.21 Schematic and SEM image of crack pinning mechanism [41]

Based on the work published by *Lange* at 1970, the toughening effect due to crack pinning can be calculated as:

$$\frac{G_{IC}}{G_0} = 1 + \frac{T}{d_s G_0}$$

Where G_{IC} is the fracture toughness of the modified epoxy, G_0 is the fracture toughness of the unmodified epoxy, T is the line energy per unit crack front (line tension), and d_s is the center-to-center distance between particles which is calculated as:

$$d_s = \frac{2d_p(1-f)}{3f}$$

Where d_p is the diameter of the particles and f is the volume fraction of particles. [42]

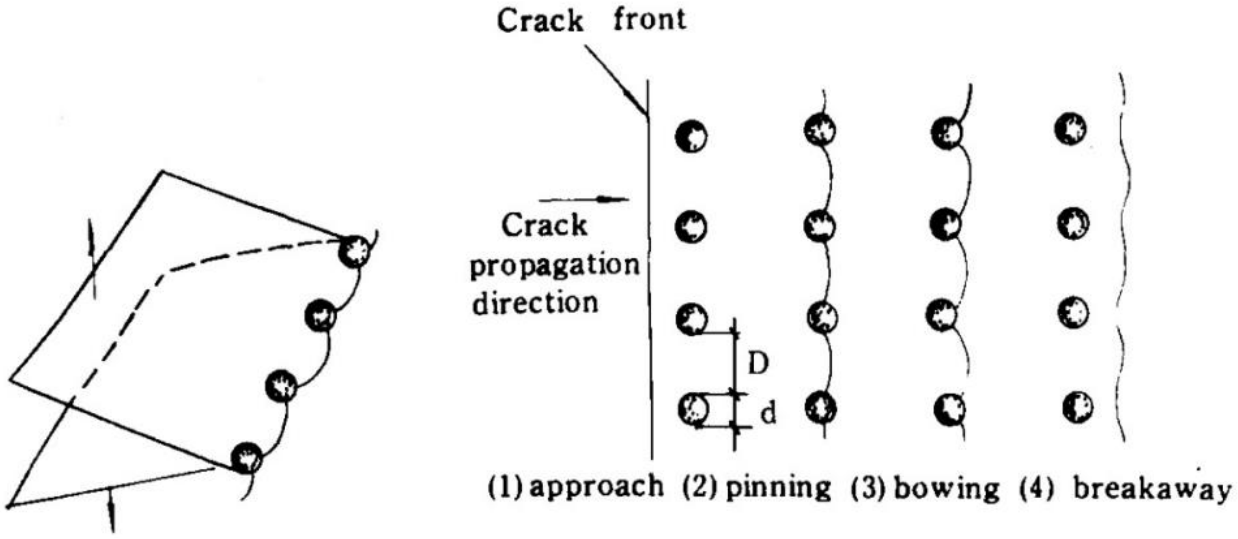

Figure 2.22 Crack propagation and its interaction with dispersed particles [38]

Crack path deflection

As can be seen schematically in figure 2.23 in this mechanism rigid thermoplastic particles make the crack change its plane in order to propagate which increases the surface area that finally results in more energy for crack propagation. [38]

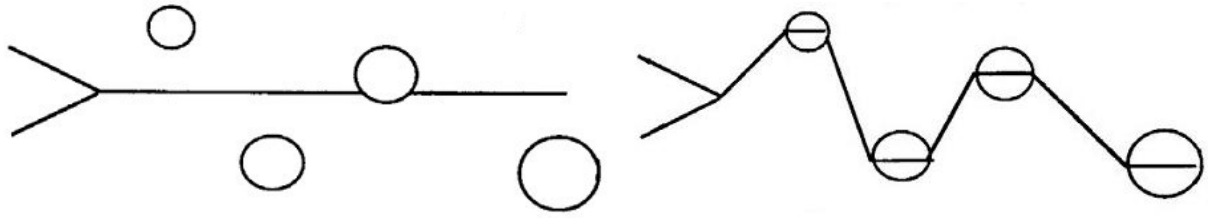

Figure 2.23 Schematically showing of crack path deflection [38]

For Quantitative modeling of this mechanism, suggested by *Faber and Evans* (1983), the equation is:

$$\frac{K_c}{K_0} = \left(\frac{E_0}{E_c}\left(1 + 0.87V_f\right)\right)^{1/2}$$

Where K_c is the fracture toughness of modified epoxy, K_0 is fracture toughness of neat epoxy, E_c is the Young's modulus of modified epoxy, E_0 is the Young's modulus of neat epoxy, and V_f is the volume fraction of the particles. As maximum volume fraction of thermoplastic particles is not more that 30% and there is not a large difference in Young's moduli of neat and modified epoxy; this model states that crack path deflection does not have big portion in toughness increasing, $\frac{K_c}{K_0} \approx 1.12$. [43]

Figure 2.24 illustrates SEM results of a system toughened by this mechanism.

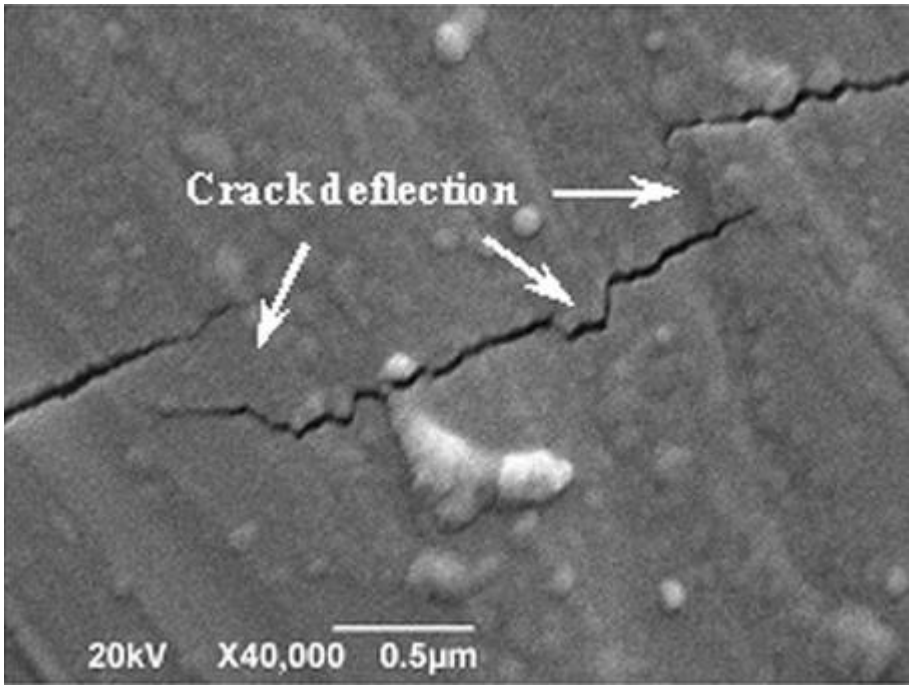

Figure 2.24 SEM result of a sample toughened by crack path deflection mechanism by graphene in the sintered nano-58S bioactive glass scaffold samples. [44]

Particle induced shear bending

Kim and Brown (1987) shown in their article that in modified epoxy resins with glassy second component when modifier contents are low the mechanism which helps toughening is particle induced shear bending. As schematically shown in the figure 2.25, in this mechanism particles initiate local yielding in epoxy matrix and this yielding of epoxy is the main deformation process and dissipates the failure energy. [45]

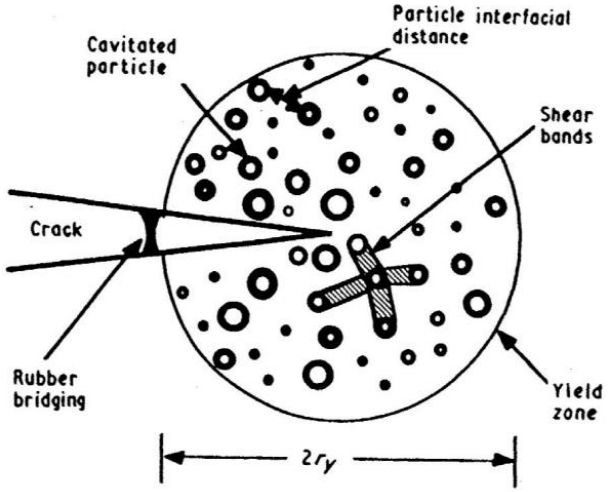

Figure 2.25 Schematic of particle induce shear bending mechanism [38]

Figure 2.26 shows how this mechanism looks on the fracture surface of a modified system.

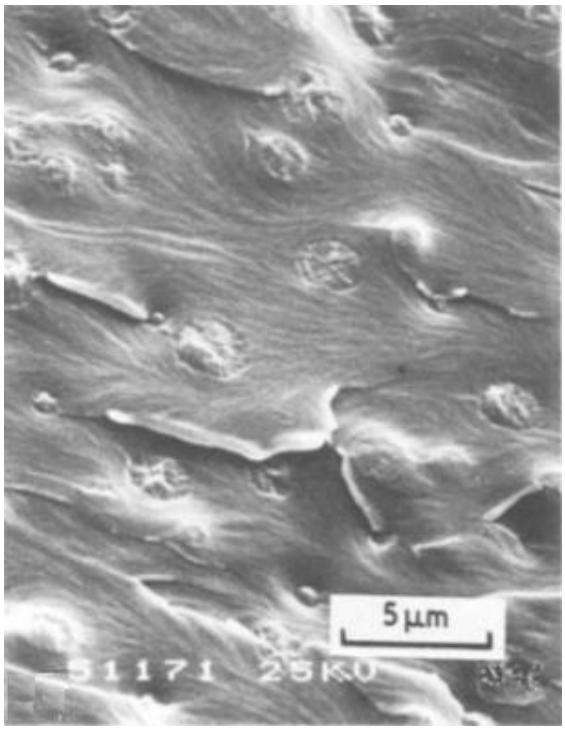

Figure 2.26 SEM result of induced shear bending as a toughening mechanism in epoxy system modified with glassy second component. [45]

Hard inclusions

Hard inclusions such as silicates, clays, and carbon nanotubes have been studied as toughening agents. The effects of these method is highly depending on dispersion state and shape factor of the inclusions. [18] Nano particles due to high surface to volume ratio, which is helpful in stress transfer from matrix to fillers, are the best shape of hard inclusions. [46] In the following paragraphs first modification with clays, silica, and carbon nanotubes are discussed and at the end toughening mechanisms of nano-modified systems are stated.

Clays

Clays are alumino silicates or hydrous silicates containing silicon, aluminum or magnesium, oxygen, and hydroxyl with various cations. *Azeez et al.* reviewed works of other scientists on clay modified epoxies. They state that three different groups of clay minerals exist, based on silicon to alumina sheet ratio which are hydrophilic in nature and prior to using them modification by organic modifiers, such as ammonium or phosphonium ions, should be done. [47]

Based on processing techniques, clay modifier, and curing agents different morphologies can be seen in the final product which affects the mechanical and thermal properties. Figure 2.27 schematically illustrates theses morphologies. *Gam et al.* claimed that exfoliation morphology leads to significant improve in modulus of nanoclay modified epoxy. [48]

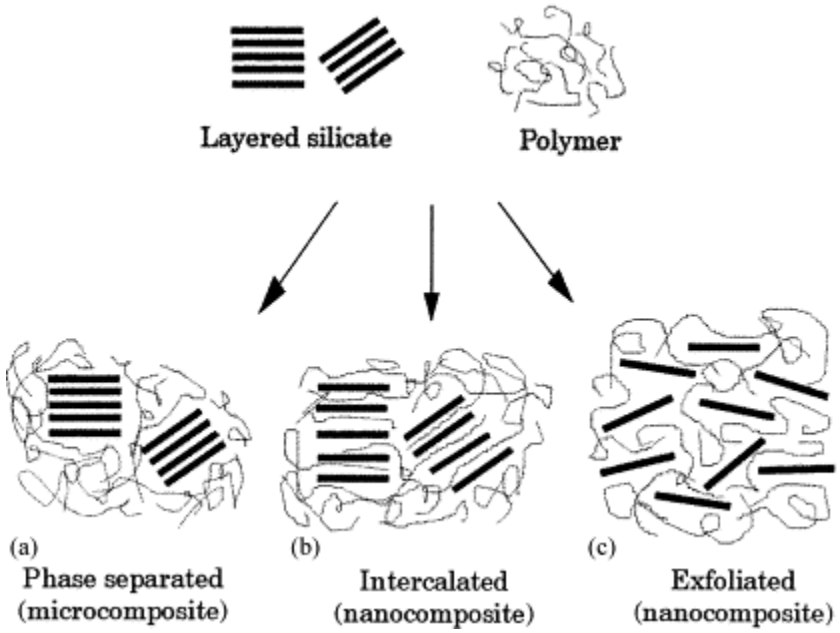

Figure 2.27 Schematically showing different types of composites arising from the interaction of layered silicates and polymers [49]

If clay particles are dispersed well in the matrix they can enhance tensile modulus noticeably, and beside that storage modulus and tensile strength. Reason for that is claimed to be high aspect ratio of dispersed particles and their high modulus and mechanism is suggested by *Chan et al.* to be interlocking and bridging effect. These properties increase by increasing concentration of the nanoclays and then at a specific concentration, due to agglomeration of clay particle, there is a drop in mechanical properties. [47]

Silica

Lean et Pearson studied nanocomposites of epoxy and nanosilica particles. They used two types of nanosilica with different particle sizes of 20 nm and 80 nm and claimed that there was no difference between two types in toughening epoxy. Modulus of the nanocomposite was increased by increasing the amount of nanosilica with no significant change in T_g. They observed up to 17.4 % increase in fracture toughness which was not observed when using micron size silica particles. Zone shielding mechanism is suggested by them as toughening mechanism. [50]

Sprenger studied the effects of nanosilica used with elastomer simultaneously to modify epoxy resins. He concluded that nanosilica can compensate the loss in Young's modulus due to rubbers, so a tough and stiff epoxy can be formulated. But no increase in T_g and losses in strength was claimed by him. He stated synergistic effect because of higher toughness of hybrid systems. Also fatigue properties was improved and he suggested composition of 5–10 wt% core–shell elastomer or 5–15 wt% reactive liquid rubber with 5–10 wt% of silica nanoparticles for the best performance. [51] *Gam et al.* also suggested the similar results in the case of core shell rubbers and nanoclays. Toughening mechanisms suggested by them was cavitation of CSR, while crack bifurcation, deflection, and crack bridging were also observed. [48]

Liu et al. studied epoxy system modified with nanosilica based core–shell nanoparticles and stated to have 39.4 % increase in impact strength by using 2.0 wt% of nanofillers. Beside they reported slight decrease in the glass transition temperature. Suggested reinforcing mechanisms by them were crazing, formation of microcracks, and debonding of nanoparticles from the matrix. [52] *Ngah and Taylor* studied effects of core-shell rubber (CSR) and nanosilica on modifying glass fiber composites. They claimed that CSR are better modifiers because they all cavitated and caused the full toughness transfer. On the other hand just some of the nanosilica particle debonded from the matrix. [53]

Carbon Nanotubes

Carbon nanotubes (CNTs) have distinctive properties such as high Young's modulus, high aspects ratio, high tensile strength, and also electrical and thermal conductivity which have made them interesting additives for modified systems. CNT consists of three different types: single-walled CNT (SWCNT), double-walled CNT (DWCNT) and multi-walled CNT (MWCNT) which are schematically shown in figure 2.28. Chemical vapor deposition, arch discharge, laser ablation, and plasma torch are some methods of CNTs synthesization.

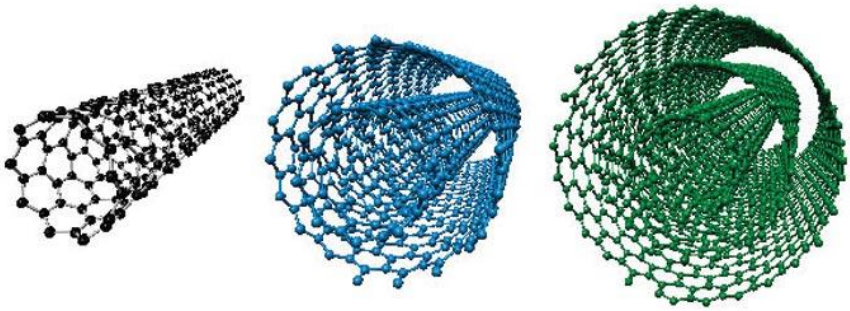

Figure 2.28 ball and stick illustrations of SWCNTs, DWCNTs, and MWCNTs. [54]

Dispersity of nanofillers and interfacial adhesion between matrix and them are main parameters affecting the mechanical properties of the modified systems. In general CNTs with higher specific surface area (SSA) have higher agglomeration and lower degree of dispersion, in other words, better dispersion in the case of MWCNTs. Figure 2.29 shows the relation between surface volume ratio and diameter in different materials.

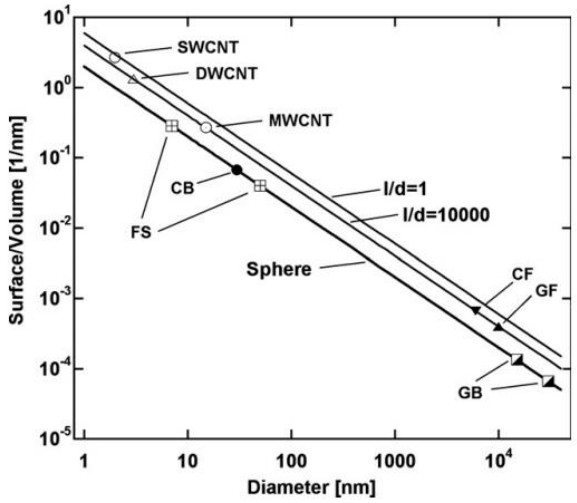

Figure 2.29 Relation between surface/volume ratio and diameter for different materials. [55]

But on the other hand interface is important because of stress transfer and higher SSA will help having better interfaces to transfer stress. Also if the area of the CNTs is functionalized with some groups it will lead to better interaction between them and matrix. [56] Figure 2.30 shows different methods for CNTs modification.

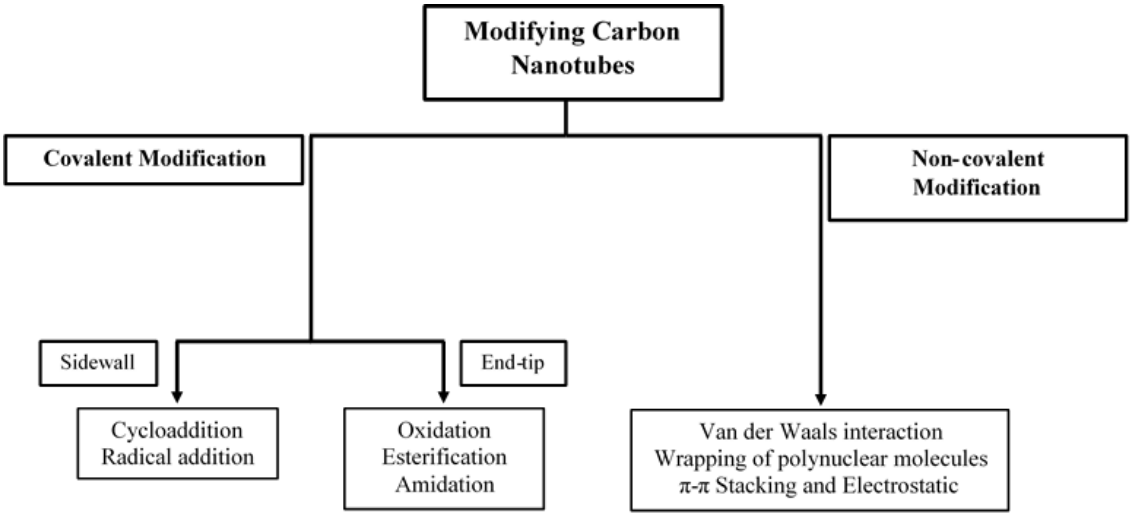

Figure 2.30 Different methods of modifying carbon nanotubes. [57]

Fiedler et al. worked on fundamental aspects of nano-reinforced composites which have CNTs as nanofillers. They studied effects of particle size, surface properties, volume content, and other properties of CNTs on the mechanical properties of the CNT/epoxy blend. Some the challenges they have mentioned for using CNTs as toughening agents are length of the tubes and their entanglement, attraction between nanotubes and high matrix viscosity. How the nanofillers are dispersed affects so much the properties of final blend. Three ways of dispersion was studied by them: sonication, stirring, and mini calendaring. Sonication is good for little amount of sample which have low viscosity and mini calendaring is a complex process, compared to other two ways. Stirring with the proper shape and speed of stirrer can give the required shear stress to the solvent and disperse the nanofillers very well, especially in case of MWCNTs. [55]

They state that plastic zone of brittle matrix is small and when nanofillers are used many particles happen to be in these zones and improve the toughness, which is not the case of micron sized or bigger particles and justifies the difference of toughening by them. In general based on the volume fraction of particles, their shape, and size toughening mechanisms are different and can be localized plastic deformation and void nucleation, particle debonding, crack deflection, crack pinning, crack tip deformation, and particle deformation or breaking at the crack tip. They claim 45% increase in K_{IC} by adding just 0.3 wt% amino-functionalized double-walled carbon nanotubes. [55]

In another study on carbon nanotube reinforced epoxy composites *Gojny et al.* studied DWCNTs/epoxy system produces by calendaring technique. They showed better dispersion of nanotubes compared to sonication technique, and also 18% improvement in K_{IC} by just using 0.1 wt% DWCNT but decrease in tensile strength. They also showed that amino functionalizing nanotubes gives even better properties. [58]

A year later they did a comparative study of effects of different carbon nanotube on DGEBA based epoxy

matrix system. They concluded to have the most significant improvements of strength (+10%), stiffness (+15%) and, fracture toughness (+43%) were just 0.5 wt% of amino-functionalized DWCNTs were used. [59] Results of their study is shown in figure 2.31.

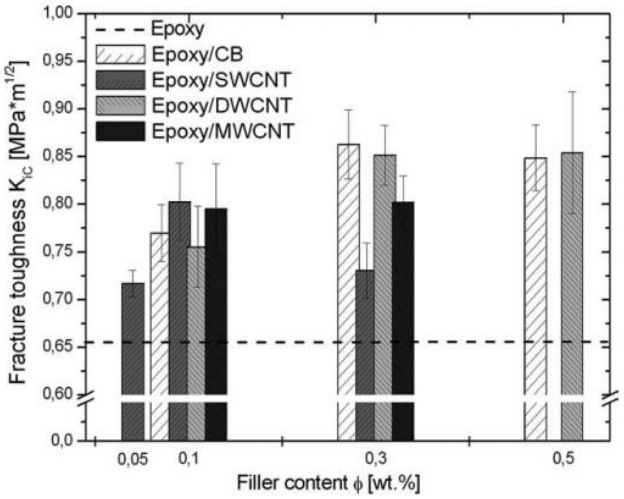

Figure 2.31 Results of carbon black and different type of CNTs on fracture toughness of DGEBA based epoxy resins. [59]

Allaoui et al. studied mechanical and electrical properties of MWCNTs/epoxy system. They state a twofold increase in Young's modulus and threefold enhancement in yield strength by using 1 wt% MWCNTs. [60] *Li et al.* also studied the same subject and claimed the highest increase in fracture toughness to occur at 0.7 wt% CNTs. They state that there is a decrease in fracture toughness value after the amount of CNTs reaches a specific amount. Major toughening mechanism was claimed to be shear banding and minor mechanisms suggested to be plastic void growth and bridging. [61]

Domun et al. reviewed the status of toughening epoxy system using nanomaterials until 2015. They concluded CNTs show a good toughening effect in low loadings, 0.1-2.0 wt%, which is a great help in processing the mixture due to low effect on viscosity. Fracture toughness of these mixture can be improved more by using rubbers but it will damage Young's modulus. Some drawbacks of CNTs as nanofillers is mentioned by them as being expensive and containing large amount of impurities. [62] Figure 2.32 summarizes concentration effect of different nano particles of fracture toughness, Young's modulus, and

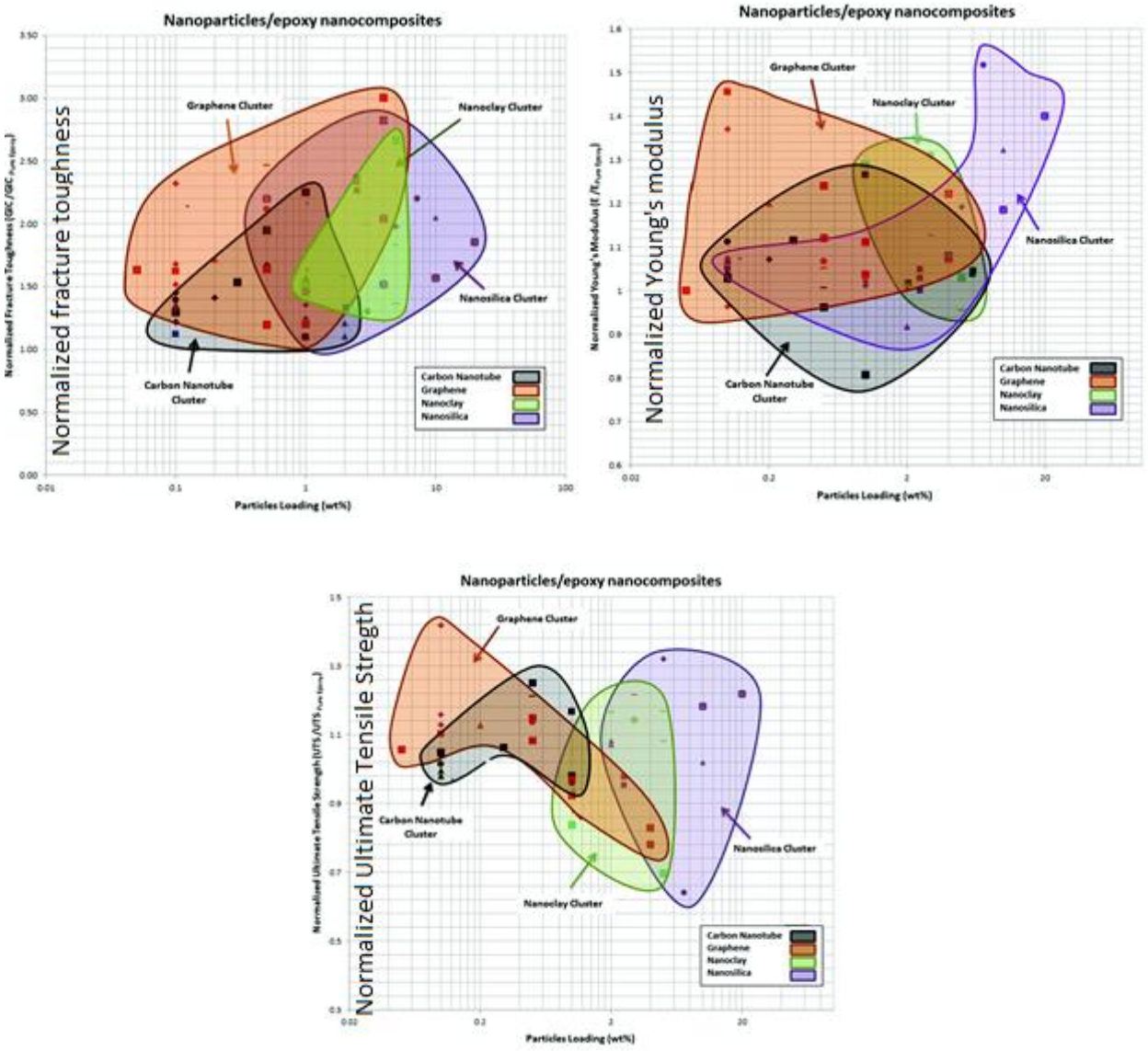

Figure 2.32 Effects of different amounts of particle loading on different mechanical properties. [62]

Toughening Mechanisms of nano-modified systems

Some of the toughening mechanisms mentioned by scientists in their works are crack deflection, crack pinning, plastic shear bands, and debonding of the matrix from nanoparticles which causes plastic void growth. In the next paragraphs these micro mechanisms are discussed and some images are shown to illustrate how they appear on fracture surfaces under SEM observations.

Crack Deflection

This mechanism is more or less the same at the one discussed in thermoplastic toughening mechanisms in previous parts. The basic of this fracture toughening is that when a crack is deflected it has more fracture

surface area which results in more energy needed for it to propagate. Also when a crack is deflected, it makes the crack to grow under mixed modes of I/II or I/III except for pure K_{Ic} mode. [63]

Again in reference [18] *Faber and Evans* has given the formula below to calculate the effect of crack deflection on fracture toughness by increasing the fracture surface area

$$\frac{G_{Ic}}{G_{Ic,m}} = \frac{1}{2}\left(1 + \frac{\sqrt{\left(\Delta/2\right)^2 + r^2}}{\Delta/2}\right)$$

Where G_{Ic} is the fracture energy of the modified system, $G_{Ic,m}$ is the fracture energy of the epoxy matrix, r is the radius of nano particles, and Δ is the distance between the centers of the particles. [43]

Crack Pinning

Crack pinning mechanism is the same as discussed in previous parts for thermoplastic modified systems. The basic of this mechanism suggested by *Lange* is that hard rigid well-bonded particles are pinning points in the way of crack propagation, which shows itself like "tail" under SEM observations. [42] These cracks consume more energy to propagate due to pinning. Figure 2.33 (A) shows a crack pinning observed by SEM in epoxy systems modified with TiO_2 nanoparticles.

When the particle size is even smaller it will result in crack front bowing which is illustrated in figure 2.33 (B). The basic of this mechanism is the same as crack pinning and just due to smaller size it occurs.

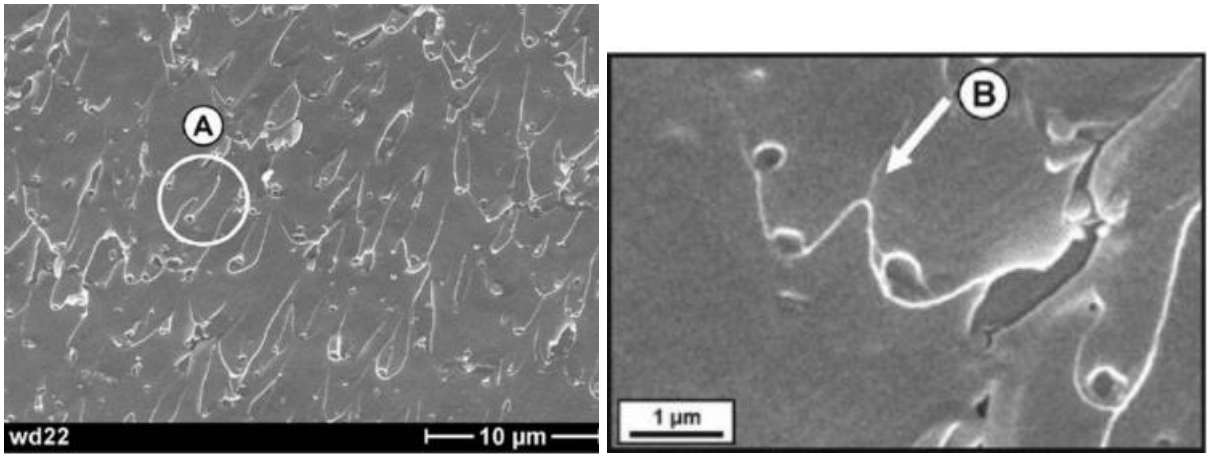

Figure 2.33 Crack pinning (A) and crack front bowing (B) in epoxy nanocomposites. [42]

Debonding

Depending on the adhesion between nanoparticles and matrix; debonding can occur when sample is under a load. Debonding improves the fracture toughness either by plastic void growth or the energy used to pull-out the particles. [63] *Opelt et al.* stated in their article that when cracks reach nanoparticles; at the first stage these particles increase the fracture toughness by crack bridging. Crack bridging was discussed in

thermoplastic modified epoxies part, but here because the particles are not ductile, after the first stage they are forced to pull-out. [64] Figure 2.34 schematically illustrates these two stages.

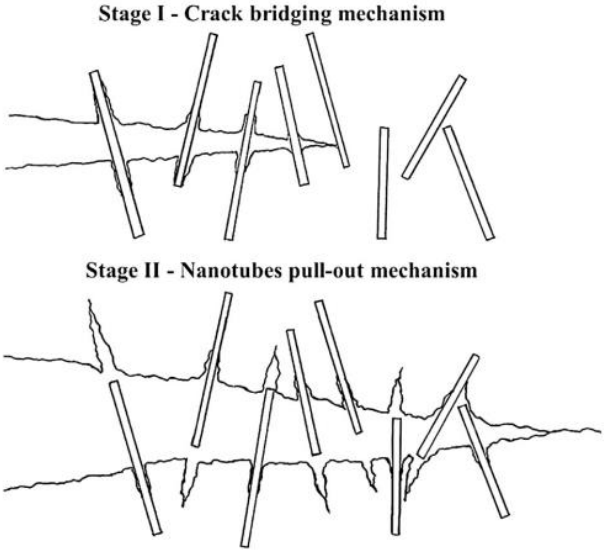

Figure 2.34 Schematic of two stages happening while nanoparticles are pulling out. [64]

Specifically talking about CNTs, *Gojny et al.* schematically described processes and mechanism that might happen in thermoset polymer modified MWCNTs. As can be seen in figure 2.35 they have claimed 4 different processes depending on both CNTs mechanical properties and interfacial adhesion properties. In case of poor adhesion pull-out occurs, Fig. 2.35 (b), while if the adhesion is way stronger then mechanical properties of CNTs rupture will occur, 2.35 (c), or just the outer wall(s) will rupture and initial wall(s) will pull-out. Spatial bonding will result in crack bridging, 2.35 (e). [59]

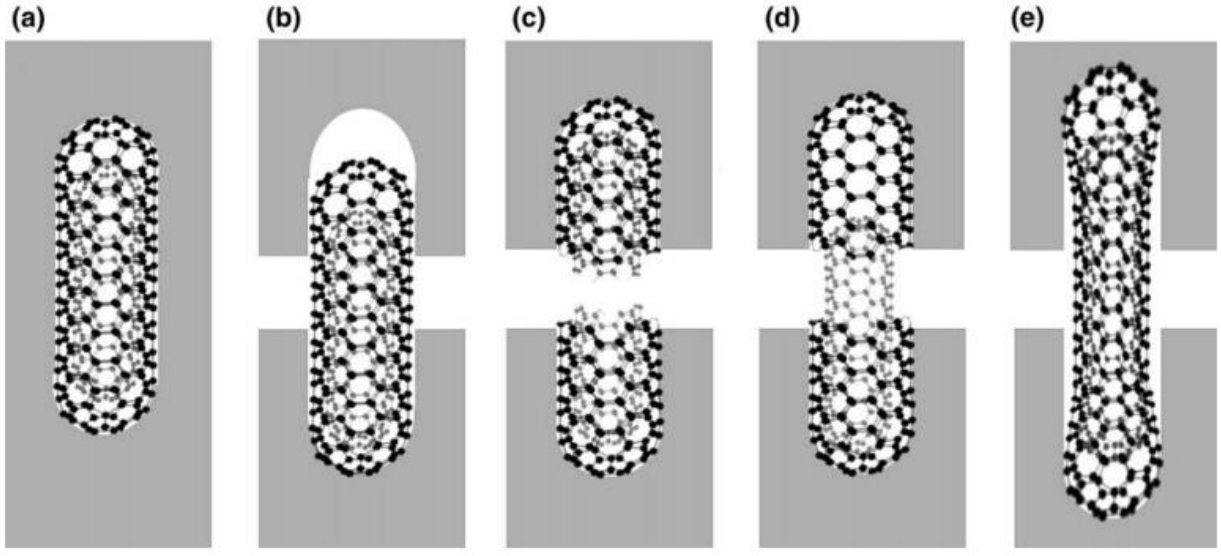

Figure 2.35 Schematic of different possible processes and mechanism to toughen a thermoset polymer with MWCNTs. [59]

Particles pull-out might result in microcracks and their linkage with main crack increases the crack length which means increasing the absorbed energy or improving fracture toughness. Figure 2.36 shows pulled-out nanotubes and voids around nanotubes after they are pulled in thermoset epoxy polymer modified with 0.5 wt% MWCNTs. [65]

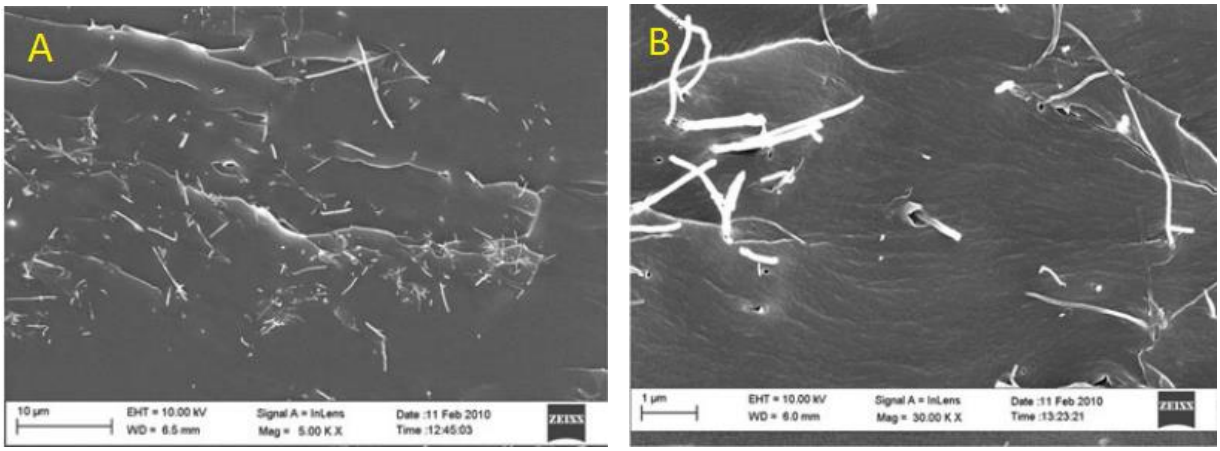

Figure 2.36 Nanotubes pull-out (A) and voids around nanotubes in epoxy polymer modified with 0.5 wt% MWCNTs [65]

The Shear-Banding Mechanism

Shear bands are inhomogenous localized plastic deformations occuring during severe deformation because of intense shear strains in those zones. [66] They were observed and also stated as toughening mechanism in rubber modified systems and also systems modified with micron-sized silica and years later at 2010 *Hsieh et al*. managed to observed it by nonlocal observations. [67] Figure 2.37 shows and image of shear bands around agglomeration of amino functionalized DWCNTs inside modified epoxy system.

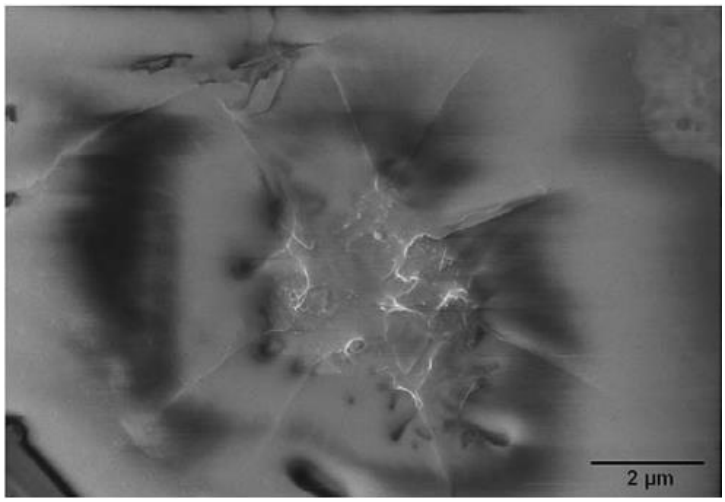

Figure 2.37 shear-bands around the agglomerates DWCNT–NH_2/epoxy composites. [59]

Ternary Systems

In the previous paragraphs, systems that were modified with only one material and method were discussed. Scientists have also studied some systems that two different materials, like rubbers and hard inclusions, are used at the same time to increase the toughness of the epoxy based systems. In the coming paragraphs some of these works are reviewed.

Chozhan et al. studied thermo mechanical behavior of unsaturated polyester (UP) toughened epoxy–clay hybrid nanocomposites. They claimed that when only added UP or clays to the system the mechanical properties were improved. To examine the synergy of both additives, they added clays to the already UP toughened epoxy system and observed of 26.3 % increase in the impact strength when 3 wt% clay and 10 wt% UP were added to epoxy; more increasing compared with systems modified with only clay or UP. [68] On the other hand, *Zeng et al.* studied improvement in the interlaminar fracture toughness of epoxy composites modified with nano-rubbers or nano-silica. They claimed that system modified with both nano-rubbers and nano-silica has fracture toughness higher than system containing only nano-silica, but lower than the system modified with just nano-rubbers, total amount of the additives in compared systems were kept constant. Figure 2.38 illustrates the mechanical results of their study. By using SEM observations on the fracture surfaces they state that cavitation of nano-rubbers, void growth and debonding of nano-silica from epoxy matrix are interlaminar toughening mechanisms. [69]

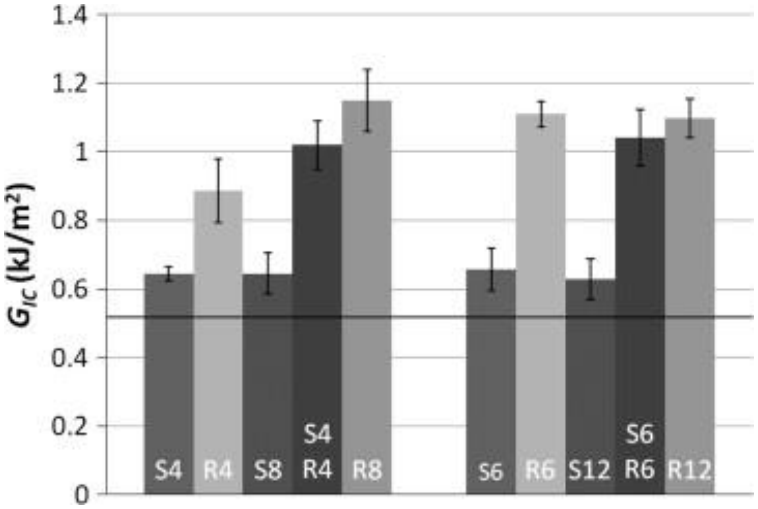

Figure 2.38 Comparison of the delamination toughness of samples with binary and ternary matrices. S stands for nano-silica and R is for nano-rubber. Numbers are weight percentage and the black bold line is the delamination toughness of the sample with neat epoxy. [69]

Fröhlich and Mülhaupt studied epoxy hybrid nanocomposites containing organophilicly modified layered silicates and liquid poly-(propylene oxide-block-ethylene oxide) (PPO) systems and claimed no exfoliation and decrease of T_g of the cured sample. Also they stated 71% of fracture toughness (K_{Ic}) but with the expense of 19% reduction of stiffness. They added that when the solubility of rubber in the cured epoxy

was decreased, fracture toughness improved up to 200% while stiffness decreased only 10%, with 1.5 wt% of organo-silicate and 13.5 wt% of PPO. [70]

Abadyan et al. explored the tensile strain energy absorption of hybrid modified epoxies containing either amine terminated butadiene acrylonitrile (ATBN) and hollow glass spheres (HGS) or ATBN and recycled tire particles. They claimed that in some compositions for both hybrid systems synergistic effect on fracture toughness improvement exists, for instance 245% increase of fracture toughness in sample with 7.5wt % ATBN and 2.5 wt% HGS which is more than sample with 10 wt% ATBN or with 10 wt% HGS. [71] Also *Azimi et al.* studied hybrid systems of epoxy modified with CTBN and HGS. They claimed synergistic effect in static fracture toughness by micro-cracking and shear banding mechanisms. [72]

Chatterjee et al. studied mechanical properties of hybrid epoxy composites modified with graphene nanoplatelets (GnP) and carbon nanotubes (CNTs). They claim that there is a synergistic effect between the fillers, especially between the bigger size of GnP and when the ratio of CNTs: GnP is 9:1, total amount of nanofillers is 0.5 wt%. Fracture toughness vale was near to the sample containing only 0.5 wt% CNTs, but flexural modulus showed a huge increase in this ratio compared to other samples. [73]

Cheng et al. examined the effect of epoxidized castor oil (ECO) and nano-$CaCO_3$ on thermal and mechanical properties of ternary system of DGEBA/ECO/nano-$CaCO_3$. They claimed that the impact strength of the system was increased and also suggested shear deformations observed by SEM prevent cracks from propagation and increase fracture toughness of the ternary system. [74]

Asif et al. studied ternary epoxy system modified with poly (ether ether ketone) with pendant methyl group (PEEKMOH) and clay. They stated that even for samples with high amount of nano clay the structure was exfoliated, tensile modulus and flexural modulus were improved by addition of clay, and ternary system showed higher fracture toughness than neat epoxy. Main toughening mechanisms suggested by them are crack path deflection, ductile nature of crack, and plastic deformation of the matrix. They even observed that high contents of clay, 8 phr, causes the gelation too happen before the occurrence of phase separation. [75]

Mirmohseni and Zavareh studied synergy between poly(acrylonitrile-*co*-butadiene-*co*-styrene) (ABS), clay as layered nanofiller, and nano-TiO_2 as particulate nanofiller on thermal and mechanical properties of epoxy based systems. They examined both ternary and quadric systems and claimed that the quaternary nanocomposite with 4 wt% of ABS, 2.5 wt% of clay, and 3 wt% of nano-TiO_2 showed the 168% and 64% improve in impact and tensile strength, respectively. They also stated that for the impact strength synergistic effect exists between the additives in quaternary system. [76]

Tang et al. studied ternary epoxy systems modified with MWCNTs and spherical particles, either soft submicron rubber or rigid nano-silica particles. They claimed that the ternary system had superior electrical

properties alongside with a good balance the stiffness, strength, fracture toughness, and T_g. Figure 2.39 shows the mechanical results of their study. For ternary system containing nano-silica they suggested pull-out of MWCNTs and matrix plastic deformation because of the debonded silica nanoparticles as toughening mechanisms. While for the other ternary system containing submicron rubbers the main toughening mechanisms were shear banding and void growth. [77]

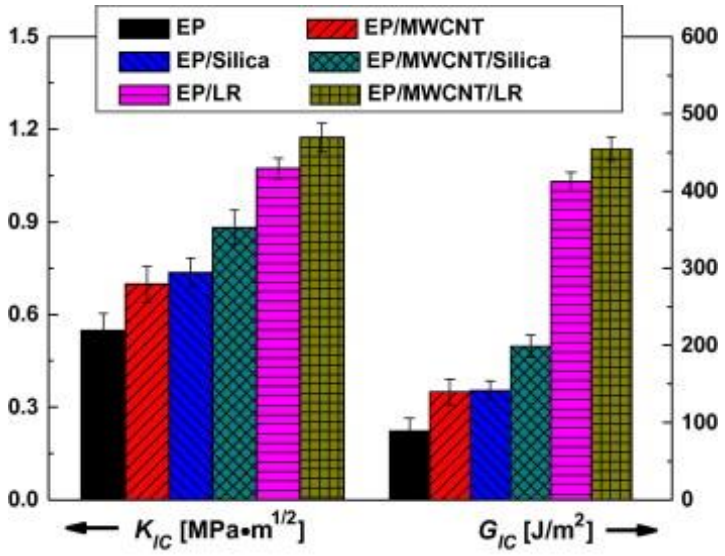

Figure 2.39 Fracture toughness of neat epoxy and epoxy nanocomposites with various compositions, 1 wt% of MWCNTs and/or 10 wt% of nano-silica and/or 10 wt% of liquid rubber. [77]

Cao et al. worked on the ternary system of epoxy/polyester/nano-Al_2O_3 particles. They prepared this composite by adding nano-Al_2O_3 particles to binary system of epoxy/polyester. Maximum impact and tensile strength was observed by addition of 8 phr nano-Al_2O_3 and Young's modulus increased linearly with increasing the amount of nano-Al_2O_3 particles. They claimed that all related properties of the ternary composite were "remarkably superior" compared with binary systems or neat epoxy. [78]

Liu et al. studied effects of silica and rubber on epoxy based systems. The stated that while silica nano-particles improves both fracture toughness and Young's modulus; rubber nano-particles decrease the Young's modulus, even though they increase fracture toughness more than silica nano-particles. They examined the hybrid system of both nanofillers and concluded that hybridization can help to have a good balance of Young's modulus and fracture toughness properties in the modified system. Debonding and bridging before complete pull out of silica nano-particles and nano-rubber cavitation and matrix plastic shearing were suggested by them as toughening mechanisms. They claimed that no synergistic effect were found in hybrid nanocomposites. [79]

Works done at UC Louvain

In the coming paragraphs three latest works done on toughening of epoxy systems at Université catholique de Louvain are reviewed.

Van Velthem et al. have studied influence of thermoplastic diffusion on delamination toughness of RTM6 epoxy based composites. Thermoplastics studied in their work were poly(ether sulfone) (PES),T_g = 220 ° C, and phenoxy, T_g = 84 ° C. Thermoplastic layers with thickness of 40 μm were placed at the mid plane and every interlayer. Also two other kinds of samples were made with layers of 80 μm thick. The highest increase in critical strain energy release rate (G_{Ic}) was observed in sample modified with in-plane 80 μm phenoxy films. On the other hand PES decreased the G_{Ic} a bit. The reason they suggested was difference in interdiffusion and reactivity of PES and phenoxy. [80]

Later in another work, *Van Velthem et al.* have studied the application of phenoxy nanocomposites films as carriers for delivery of nanofiller, either MWCNTs or nanoclays, in epoxy matrix for resin transfer molding composites. Based on their model studies, during heating nanofillers can be passively transported by interdiffusion gradient of phenoxy up to 800 μm. These nanocomposite films were placed between every odd carbon layer of preform. They claim that carbon fibers had filtered the fully transporting of CNTs and this caused a negative effect on the fracture toughness of the composite; while on the other hand in the case of nanoclays fracture toughness was slightly improved. [81]

In the most recent not yet published article *Van Velthem et al.* have studied highly crosslinked TGDDM epoxy composited modified with four different tougheners, MAM block copolymer, CTBN rubber, PES, and phenoxy, all samples containing 10 wt% of additives. They stated that high T_g amorphous thermoplastics PES and phenoxy improved interlaminar fracture toughness by 66% and 80%, respectively. On the other side, soft tougheners, MAM and CTBN, were less effective, 30% and 38% of increase, respectively. After SEM observations of the fracture surfaces, they concluded that fine dispersion of toughener and strong matrix-toughener and matrix-CF interfaces are essential for effective toughening of composite panels. [82]

Cordenier et al. studied the addition of both phenoxy and block copolymer (MAM) carbon fiber epoxy matrix composite processed by RTM. They claimed an existence of the synergistic effect on the out-of-plane fracture toughness of manufactured composite. They suggested two steps for the increase in fracture toughness: first interdiffusion of the phenoxy/MAM filament and RTM6 resin, and second step is because of the different microstructures of the panels. [83]

CHAPTER 3 MATERIALS AND EXPERIMENTAL DETAILS

In this chapter, first all materials that were used in this thesis and some of their properties are stated. Then two different methods of mixing the materials and making samples are shown. Finally, at the end of this chapter, characterization techniques are presented.

Materials

Tetra functional epoxy resins were used in this thesis with commercial name Araldite® MY 721 and chemical formula N,N,N',N'-Tetraglycidyl-4,4' methylenebisbenzenamine made by Huntsman® company to fabricate high-temperature performance composites. This brownish liquid resin has low viscosity, 300 mPas at 70 ° C, and long pot life, minimum two years for temperatures below 4 ° C. Some other advantages of this product, as mentioned in the datasheet, are extremely low shrinkage, excellent chemical resistance, extremely high glass transition temperatures, low moisture uptake, and good long-term high-temperature performance. Table 3.1 shows some properties of this resin. [84]

Table 3.1 Typical properties of Araldite® MY 721 epoxy resin.

Property	Value
Epoxy value	0.86 - 0.91 eq/100g
Density	1177 kg/m^3
Pot life –at 50 °C **–at 70 °C**	23 hr 7 hr
Mix viscosity –at 50 °C **–at 70 °C**	1000 mPas 300 mPas
Gel time at 150 °C	21 min

4,4' diamino diphenyl sulfone (DDS), a hazardous white chemical powder made by Huntsman® company under the commercial name Aradur® 9664-1 NL, were used as hardener. Figure 3.1 shows the chemical structure of DDS. It is a stable powder which decomposes at 200 ° C. [85] As stated in previous chapter, in order to reach the highest possible properties the hardener and resin should be mixed exactly at stoichiometric ratio which was 100:53 for epoxy: DDS ratio.

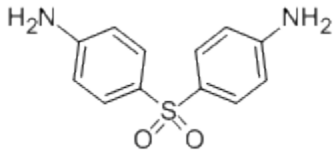

Figure 3.1 Chemical structure of 4,4' diamino diphenyl sulfone (DDS, used as hardener. [86]

Nanotubes used in this thesis were multiwall carbon nanotubes (MWCNTs) produced by Nanocyl® company under the name NC7000 via catalytic chemical vapor deposition process. UV resistance, good processability, retention of key mechanical properties, and best cost in use ratio are some of the advantages. [87] It is a solid odorless black powder containing 90 wt% of carbon nanotubes. Amongst the 10 wt% impurities were the remaining parts of the catalysts used to produce this product. Low density of this material, 60 g/L, made them to have big volume percentages even in mixtures with low weight percentage of MWCNTs. Figure 3.2 shows structure of these nanotubes under transmission electron microscopy (TEM).

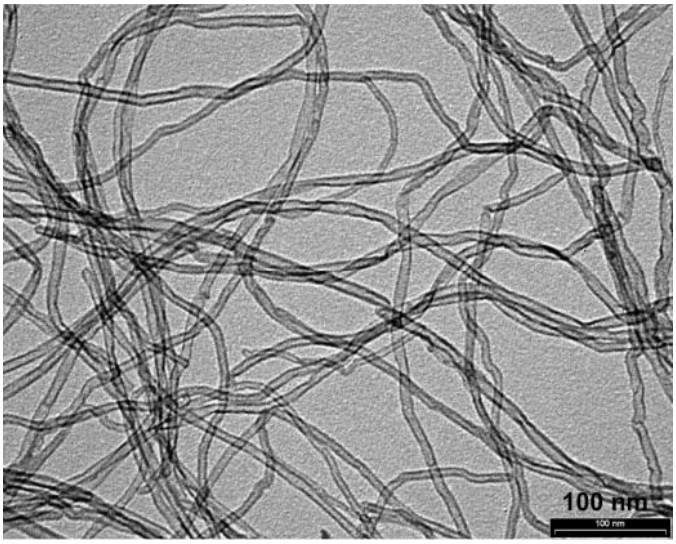

Figure 3.2 TEM image of MWCNTs used for the preparation of different blends. [87]

Some characteristic of NC7000 are listed in table 3.2.

Table 3.2 Typical characteristics of MWCNTs used. [87]

Property	Value
Average diameter	9.5 nm
Average length	1.5 µm
Density	60 g/L
Carbon purity	90 %
Surface area	250-300 m^2/g
Volume resistivity	10^{-4} Ω.cm

PKHP-200 powder were phenoxy resins used for sample preparation. It is produced by Gabriel Performance Products chemical supplier. As can be seen on table below phenoxy is more viscous than epoxy and after adding it viscosity of the mixture increase so much.

Table 3.3 Typical properties of PKHP-200 phenoxy resins. [88]

Property	Value
Particle size	<200 µm
Ave. particle size	110 µm
Specific gravity	1.17-1.19
Nonvolatile	>99 wt%
Molecular weight, M_n	10-16 kg/mol
Molecular weight, M_w	50-60 kg/mol
Melt viscosity at 200 ^{0}C	46.5 Pas

Finally the last material used was nanocomposite based of phenoxy with different concentration of MWCNTs (NC7000), 1, 3, 6, and 10 wt% concentrations of MWCNTs made by Nanocyl® Company. These material are in the form of pellets with height of 2 mm. It takes a lot of time for them to get dissolved completely in epoxy resin, so they were grinded and then added to epoxy resins.

Blends Preparation

Three different types of epoxy blends were made. One was containing only CNTs, another one containing CNTs and phenoxy added separately, and the last one containing nanocomposites of phenoxy and CNTs. All of these methods were done at elevated temperature and with the same stirrer shape and speed, so the shear force in each sample was equal. In order to reach elevated temperatures a beaker was put inside a container full of oil held on the heater. Set point of the heater was 130 ° C, which was reached at the last stage of mixing. Table 3.4 shows the composition of different blends.

Table 3.4 Composition of different epoxy blends made in the experimental part.

No. of sample	Composition	wt% of CNTs	wt% of phenoxy
1	Epoxy[1]	0	0
2	Epoxy/CNTs	0.1	0
3	Epoxy/CNTs	0.3	0
4	Epoxy/CNTs	0.6	0
5	Epoxy/CNTs	1.0	0
6	Epoxy/CNTs	1.2	0
7	Epoxy/CNTs/phenoxy	0.1	9.9
8	Epoxy/CNTs/phenoxy	0.3	9.7
9	Epoxy/CNTs/phenoxy	0.6	9.4
10	Epoxy/CNTs/phenoxy	1.0	9.0
11	Epoxy/CNTs/phenoxy NC[2]	0.1	9.9
12	Epoxy/CNTs/phenoxy NC	0.3	9.7
13	Epoxy/CNTs/phenoxy NC	0.6	9.4
14	Epoxy/CNTs/phenoxy NC	1.0	9.0

1: Epoxy blends are made by addition of stoichiometric portion of TGDDM and DDS.

2: NC means sample is made by using grinded nanocomposites of phenoxy and CNTs.

To make blends with just CNTs first desired amount of TGDDM epoxy was heated up to 100 ° C and then at this temperature specific amount of CNTs were added and stirred in beaker for twenty minutes. Finally DDS was added and stirred for twenty minutes to have a homogenous mixture.

As also stated in previous parts, two methods were used to make blends containing CNTs and phenoxy. In the first method again TGDDM resins were heated inside the beaker up to 100 ° C. Then CNTs were added and stirred for twenty minutes and after that phenoxy powder was added and stirred for twenty more minutes. At the end DDS was added and homogenous mixture was reached after twenty minutes of stirring.

Another way was using nanocomposites. As mentioned the original pellets were big and taking so much time to get completely dissolved in epoxy; so they were grinded. Then again TGDDM was heated inside the beaker and when the temperature was 100 ° C those grinded nanocomposites were added and stirred for forty minutes. After that DDS powder was added to the black looking homogenous solution and stirred for twenty minutes.

After mixing was finished, beaker was put inside the oven connected to vacuum pomp in order to do degassing. Temperature inside the oven was in the range of 115-125 ° C based on the viscosity of sample, higher temperatures for more viscous mixtures. Degassing was done by manipulating pressure inside the oven and being careful about not outpouring the solution out of the beaker.

After degassing the mixture, while it was still hot and less viscous, it was poured into two molds, which had been wet with releasing agent five minutes earlier. Rest of the mixture was poured in a sample cup and kept inside freezer to remain uncured. After molding the curing cycle was set on the oven and molds were put inside it.

Curing cycle was consisted of different stages. First pre heating of sample at 80 ° C for one hour, then heating up to 100 ° C and keeping samples there for two hours. After that curing at 150 ° C for four hours, and finally post-curing at 200 ° C for seven hours to be sure high percentage of curing, >95%, had been achieved. Figure 3.3 is the illustration of the curing cycle temperature versus time.

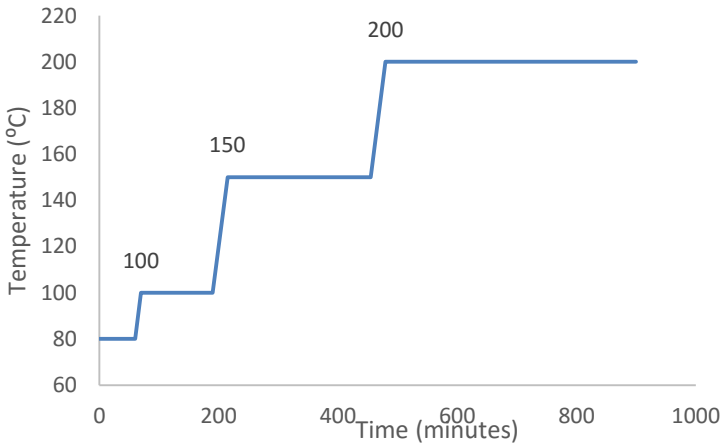

Figure 3.3 Tempereture versus time diagram of thr curing cycle of the blends

Characterization techniques

After curing four rigid cuboid samples were made. As stated in previous part to measure the fracture toughness by SENB test, samples must have special dimensions. So cured samples were machined and ready to be tested, as shown in figure 3.4.

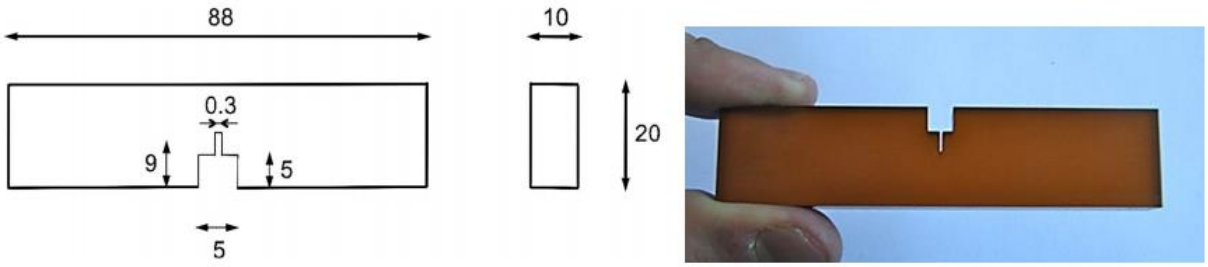

Figure 3.4 Cured and machined SENB sample and its dimensions. [89]

As samples should have precracks for three point test; with the help of razor and hammer precracks were made at the end of nudge. Figure 3.5 shows an image of this procedure and also an image of the precrack made in the nudge of the sample.

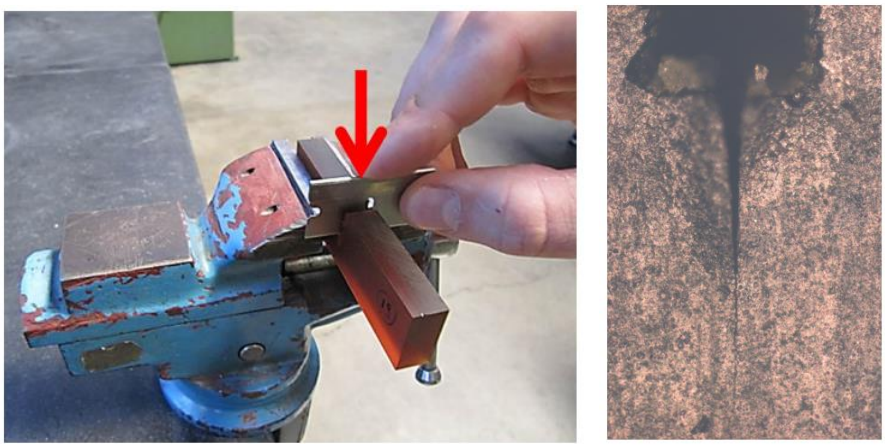

Figure 3.5 Using razor to make a pre-crack in the sample,left, and optical microscopy image the pre-crack, right. [89]

An image of the three point flexural test on the SENB sample is illustrated in figure 3.6 (a). To calculate the fracture toughness of the sample relation of the length of the crack and with of the sample ($\frac{a}{W}$) is important. Optical microscopy on the fracture surface of the sample was used to measure the length of the crack, figure 3.6 (b).

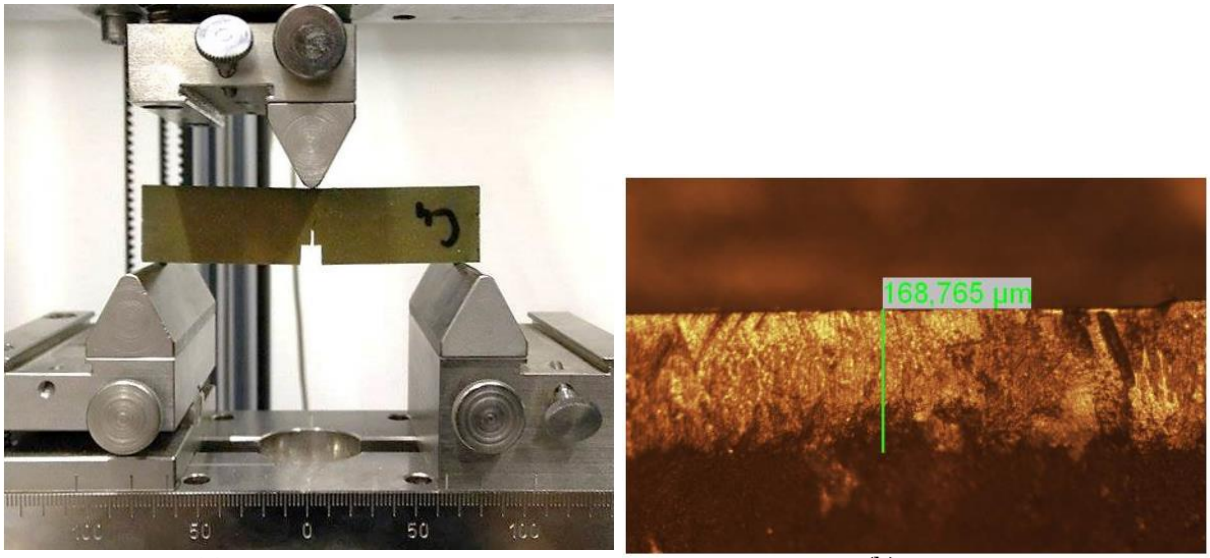

(a) (b)

Figure 3.6 Three point test, (a), and precrack measurement by optical microscopy, (b), to determine fracture toughness of samples. [89]

After measurements of the cracks' length this formula was used to calculate fracture toughness:

$$K_Q = \frac{P_Q}{B\sqrt{W}f(a/W)}$$

Where P_Q is the a critical load used to determine the conditional fracture toughness, B is the thickness of the specimen, W is the width of specimen, a is the length of the crack, and $f(a/W)$ is a formula as:

$$f\left(\frac{a}{W}\right) = \frac{3\frac{S}{W}\sqrt{\frac{a}{W}}}{2\left(1+2\frac{a}{W}\right)\left(1-\frac{a}{W}\right)^{3/2}}\left[1.99 - \frac{a}{W}\left(1-\frac{a}{W}\right)\left\{2.15 - 3.93\left(\frac{a}{W}\right) + 2.7\left(\frac{a}{W}\right)^2\right\}\right]$$

Figure 3.7 (a) schematically shows the dimensions and their defining parameters and figure 3.7 (b) shows different states of choosing P_Q on the load-displacement graphs. [90]

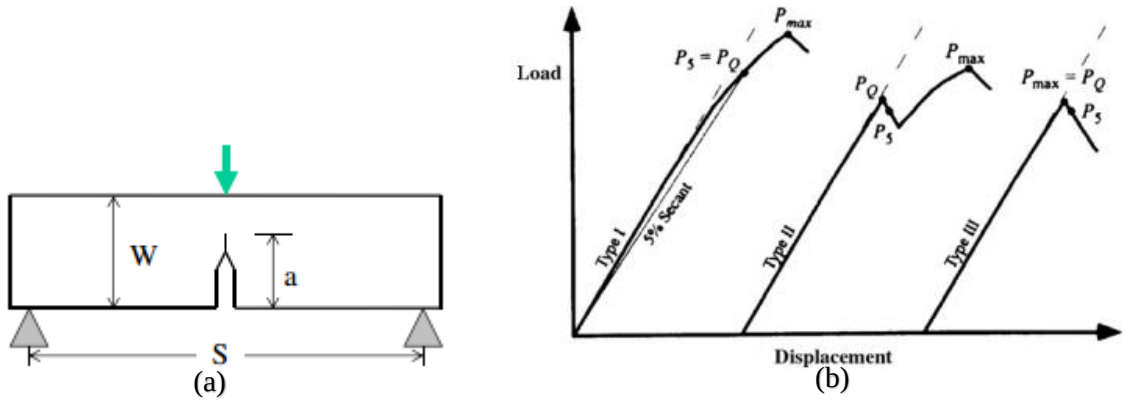

Figure 3.7 Schematic of the SENB sample with a pre-crack, (a), and different types of critical load for calculating fracture toughness, (b). [90]

After toughness measurements, samples were cut by diamond knives to have thickness around 95 nm and diameters less than 3mm and then mounted with carbon grids to be prepared for transmission electron microscopy (TEM). LEO 922 microscope with 120 KV voltage was used to study morphology of samples and figure out dispersion of additives in the bulk, qualitatively and quantitatively. Also optical microscopy, in both bright field and phase separated modes, was used to have images with lower magnifications to help better understanding the morphology and dispersion in larger scales.

Generally the operating principles are more or less similar to optical microscopy, except in TEM electron beam is used instead of light wave and due to lower wavelength of electrons; higher resolutions are attainable. A beam of electrons is generated by a filament, LaB_6 in LEO 922, in electron gun part and then the condenser focuses a small coherent beam on the specimen. Depending on the thickness and electron transparency of the specimen, some parts of the beam are transmitted. The transmitted part is then focused by objective length and enlarged by projector lens. The final image can be shown either on phosphor screen or on monitor by using charge coupled device (CCD) camera. Figure 3.8 illustrates the LEO 922 TEM microscope and the schematics of TEM basis. [91]

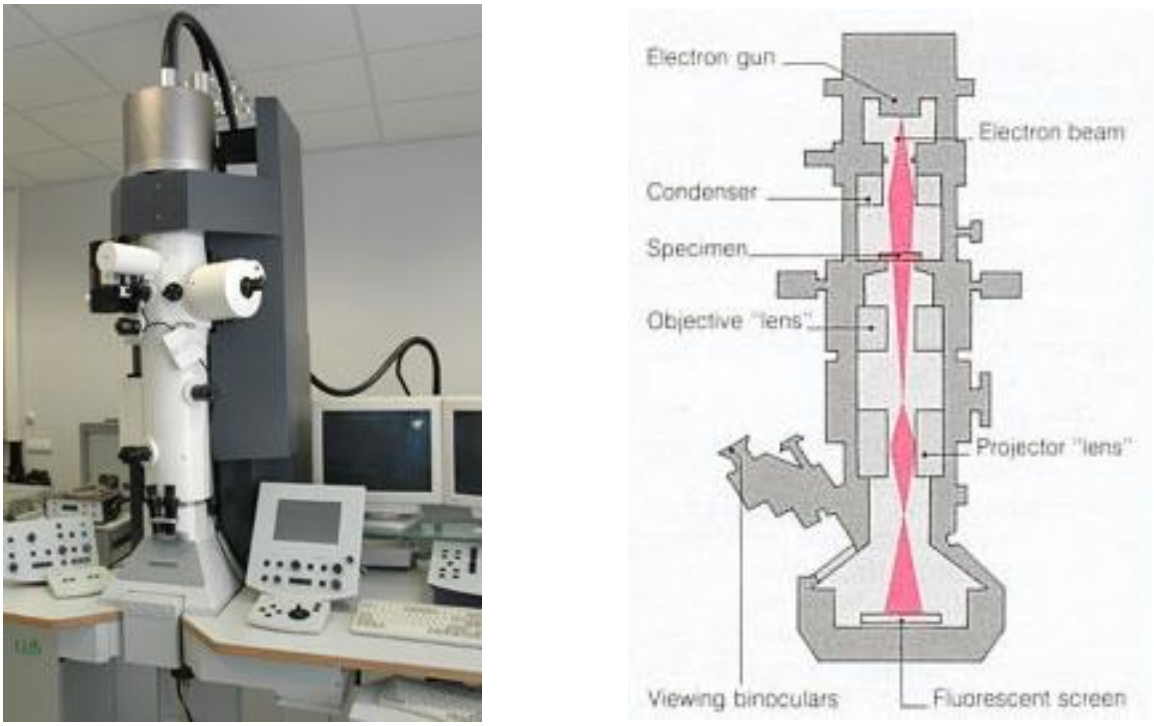

Figure 3.8 LEO 922 TEM microscope, left, and the schematics of different parts of TEM structure, right. [92, 93]

In order To understand toughening mechanisms, fracture surfaces of samples were studied by scanning electron microscopy (SEM). To do so; a small part from fracture surface of the SENB samples were cut and then coated with chromium by sputtering in a Cressington 280 HR chamber. JEOL 7600F was used in 15 KV voltage and images with magnifications in the range of 500x to 50000x of the samples in chamber with low pressure were captured.

SEM principles is similar to TEM but here the scattered electrons are studied, instead of transmitted electrons, so there is no need of thin samples and sample preparation is easier. Again here beam of electrons generated by electron gun and passes condenser and different electromagnet lenses and reaches the surface of the sample. As illustrated in image 3.9 there are different results of electron-specimen interaction. Among all these interactions, secondary electrons and backscattered electrons are usually used for imaging, secondary electrons for showing morphology and topography of the surface and backscattered electrons for showing contrasts in different phases in multiphase specimens. Secondary electrons detector (SED) detects these electrons and after amplifying them shows the result on the monitor. [94]

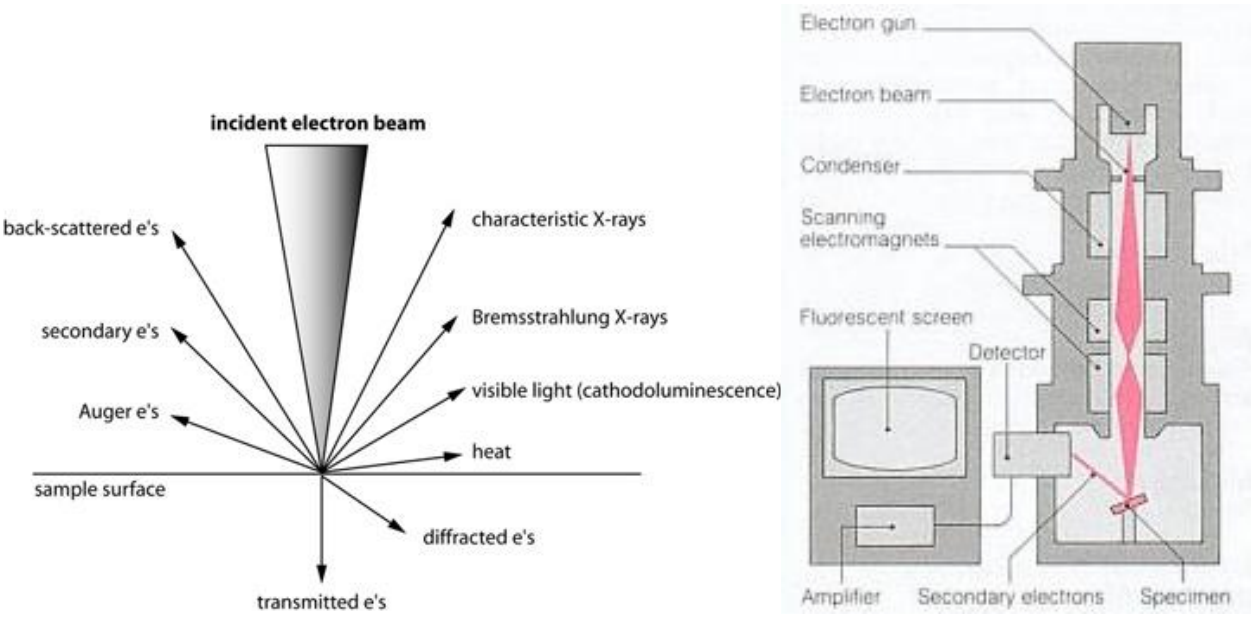

Figure 3.9 Different types of interaction between electrons and sample, left, and schematics of different parts of scaning electron microscope (SEM), right. [95, 93]

Uncured samples which were kept in freezer had been used in rheology tests to calculate gelation time. Figure 3.10 illustrates the Bohlin Gemini rheometer used for this purpose. The test was isothermal and done at temperature 150 ° C with the frequency of 1 Hz. Gelation time was chosen as a time when complex viscosity (η^*) of samples start to increase rapidly.

As it is schematically shown in figure 3.10, an amount of sample is placed on the horizontal plate which is connected to heater and another plate is placed on it. The basic idea of this method is to measure the force required to rotate an object in fluid at specific speed and frequency, and through this the viscosity is measured. The outcome of this test is the complex viscosity (η^*) versus time.

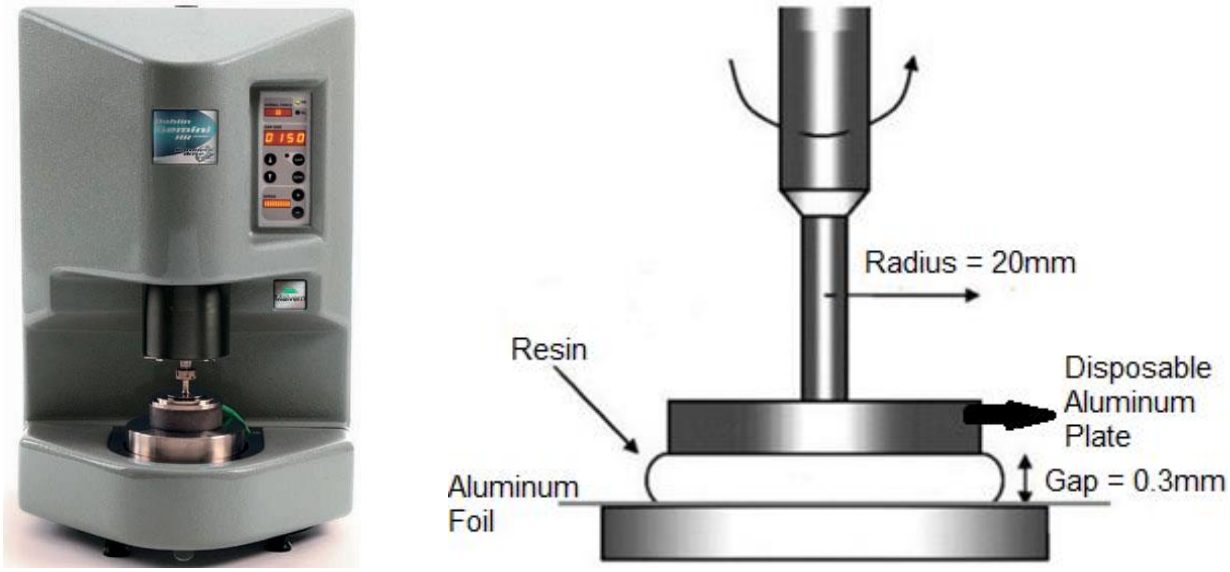

Figure 3.10 Bohlin Gemini rheometer, left, and schematic of the dimensions of the gap and radius of plates in the test, right.. [96, 89]

When samples are going to be loaded on aluminum foil on the horizontal lower plate; it should be taken into account that the correct form is as illustrated in figure 3.10. If the amount of the sample is lower, under filled, or higher, over filled, than the required amount to just fill the gap, it will affect the measured torque by the other place and the data will be incorrect.

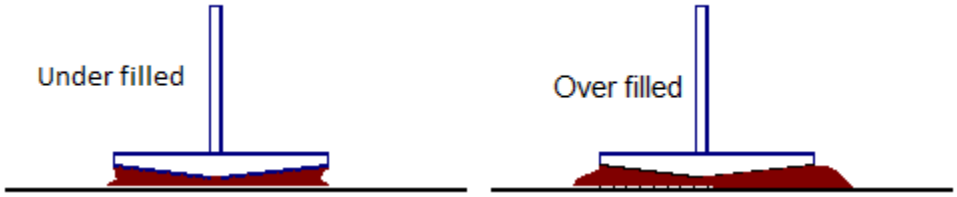

Figure 3.11 Incorrect examples of sample loading: lower amount, left, and higher amount, right, of the sample that is required in rotationary rheometry. [97]

Finally a small amount of frozen uncured sample, less than 20mg, was used in differential scanning calorimetry (DSC) analysis to measure the glass transition temperature (T_g) and enthalpy of the polymerization. In this technique difference in the required heat to increase the temperature of the specimen and reference, which has a specific heat capacity, is measured as a function of temperature. Figure 3.12 shows schematically the structure of DSC machine. [98]

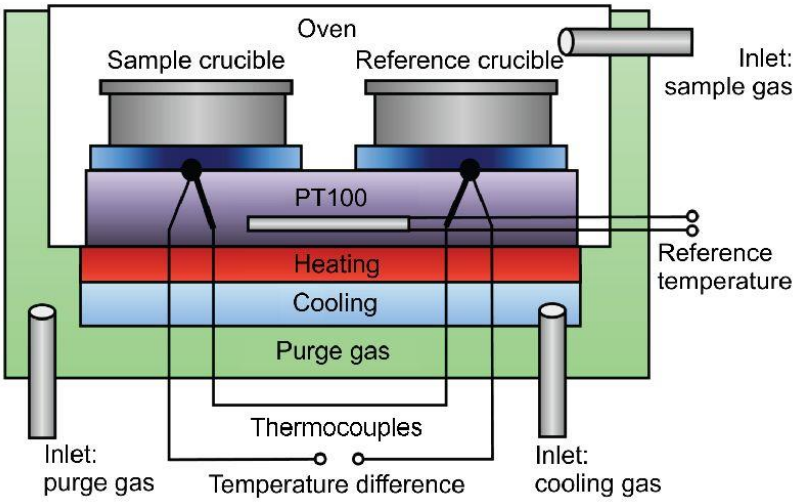

Figure 3.12 Schmatics of the structure of DSC analysis instrument. Temperatures of both reference and sample crucibles are changed and the heat flow is measured by thermocouples. [98]

The result of the DSC analysis is the heat flux curve versus temperature or time. Figure 3.13 illustrates the curves obtained by the DSC analysis. As shown in the previous image there are two chambers, one for reference and one for sample. After the analysis two curves are obtained, one for reference (q_r) and one for sample (q_s). The reference is a well-defined materials with a known specific heat, so a third curve based on the difference between the heat flows (Δq) of two other curves can be illustrated which might contain peaks showing the exothermic reactions in the sample. Integration of the related peaks will be the enthalpy of the reaction. [99]

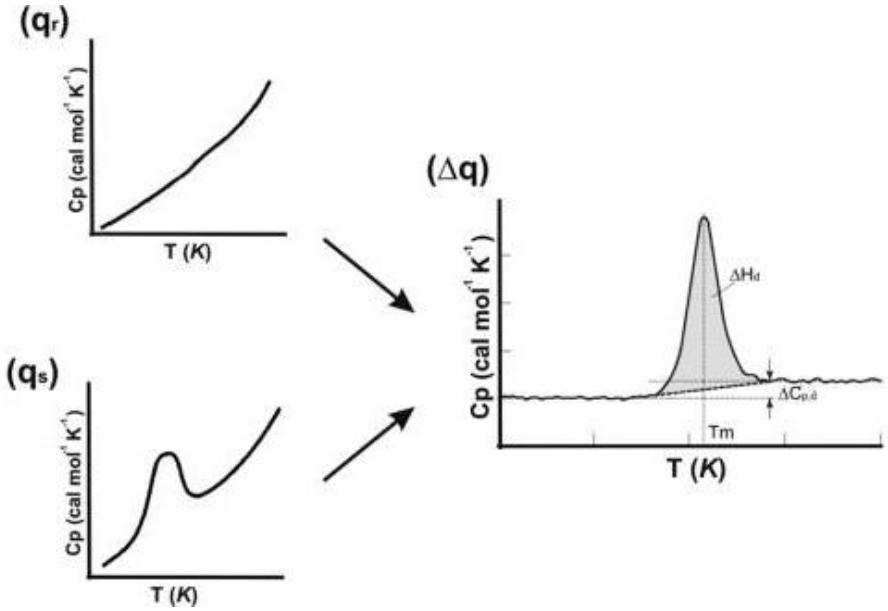

Figure 3.13 DSC curves shows the amount of heat needed to increase the tempereture of reference (q_r) and of sample (q_s). Sunstracting q_r from q_s (Δq) shows the excess heat changes as function of temperature. T (K), Temperature, kelvin; ΔH_d, change in enthalpy; $\Delta C_{p,d}$, change in C_p; T_m, transition and melting point [100]

CHAPTER 4 RESULTS AND DISCUSSION

In this chapter effects of unfunctionalized multi-walled carbon nanotubes (MWCNTs) and thermoplastic phenoxy on high performance epoxy resins are discussed. As mentioned in the first chapter the objectives of this master are to see if there is synergistic effect between modifiers and also to find the composition(s) that in them synergy exist. Beside these main objectives, effects of additives on glass transitions temperature (T_g) and gelation time of the uncured mixtures are studied.

In the following paragraphs first the effects on T_g and gelation time are discussed. Discussions are made based on DSC analysis and rheometry measurements. After that effects on mechanical property of fracture toughness are discussed. To do so, first effects of just using MWCNTs are stated and compared with the results stated in second chapter, state of the art.

Then simultaneous effects are discussed. First samples modified with separately added MWCNTs and phenoxy are discussed with the same structure used for the samples containing only MWCNTs. Synergistic effects are also studied for each composition.

Finally results of the samples modified with nanocomposites of phenoxy and MWCNTs are mentioned and studied. Again first effects on the fracture toughness are discussed and then followed by TEM and SEM results to link microstructures and morphologies to mechanical results. Also differences between modification with nanocomposites or adding separately are discussed.

Results from optical microscopy and transmission electron microscopy (TEM) are used to have understanding about microstructures of the bulk of samples. Scanning electron microscopy (SEM) results of fracture surfaces are discussed and toughening mechanisms have been claimed with the help of articles reviewed in second chapter.

Effects on T_g and Gelation Time

Remaining amounts of the mixtures that were not used in curing cycle to make SENB samples were kept in freezer, to avoid curing at room temperature, and used to measure T_g and gelation time. Figure 4.1 shows the evaluation of the heat flow as function of temperature, measured by DSC for three samples with different compositions.

In figure 4.1, the green curve is for reference epoxy sample, TGDDM/DDS, with the producing conditions as same as modified samples. Blue curve is for the sample containing 1 wt% CNTs and the orange curve is for epoxy system modified with 0.2 wt% CNTs and 9.8 wt% phenoxy added separately.

As it is illustrated, there is not a huge difference between the curves and they all look the same. Only differences are that T_g is around 13 ^{o} C for reference sample, which is slightly decreased by adding toughening agents, it is 11 ^{o} C for both samples with 1.0 wt% CNTs and with 0.2 wt% CNTs + 9.8 wt% phenoxy. On the other hand the exothermal peak for three samples occurs at 235 ^{o} C and normalized

integral values which is the energy released during polymerization per gram of the sample are almost the same for each sample and around 530 J/g. These results prove that toughening agents do not affect the thermodynamic of polymerization process.

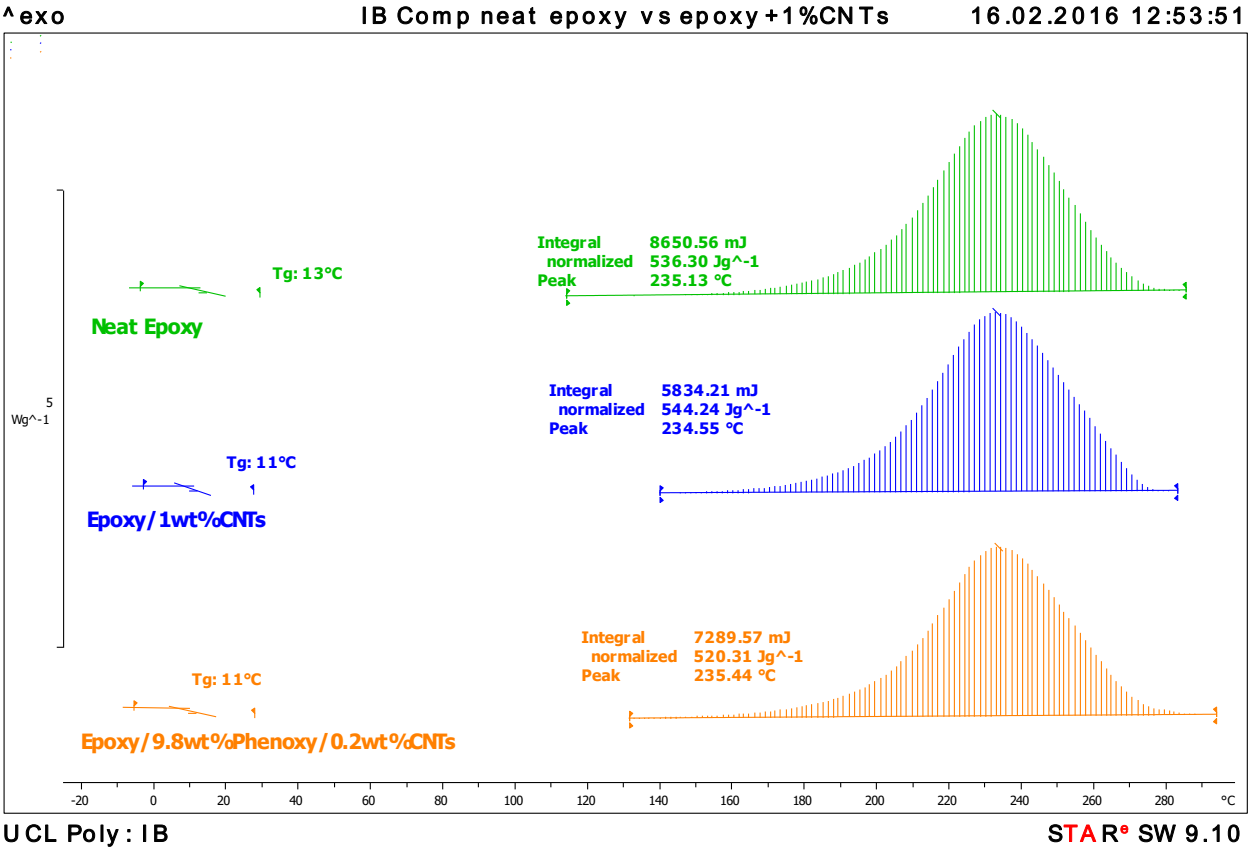

Figure 4.1 Effects of CNTs and phenoxy on T_g and enthalpy of curing. As it shows the peak temperature is exactly the same for all samples and T_g has not changed drastically.

Figure 4.2 shows normalized results of rheology tests for different samples at 150 ° C. Again samples here are reference and two extreme samples which were used for DSC analysis. Reference sample has the gelation time around 55 minutes. It is observed that 1 wt% CNTs slightly increases the gelation time, around 58 minutes, and on the other hand sample with 0.2 w% CNTs + 9.8 wt% phenoxy has lower gelation time, 52 minutes. These slight changes of gelation times for extreme samples prove that there is not a significant effect of CNTs and phenoxy on gelation time.

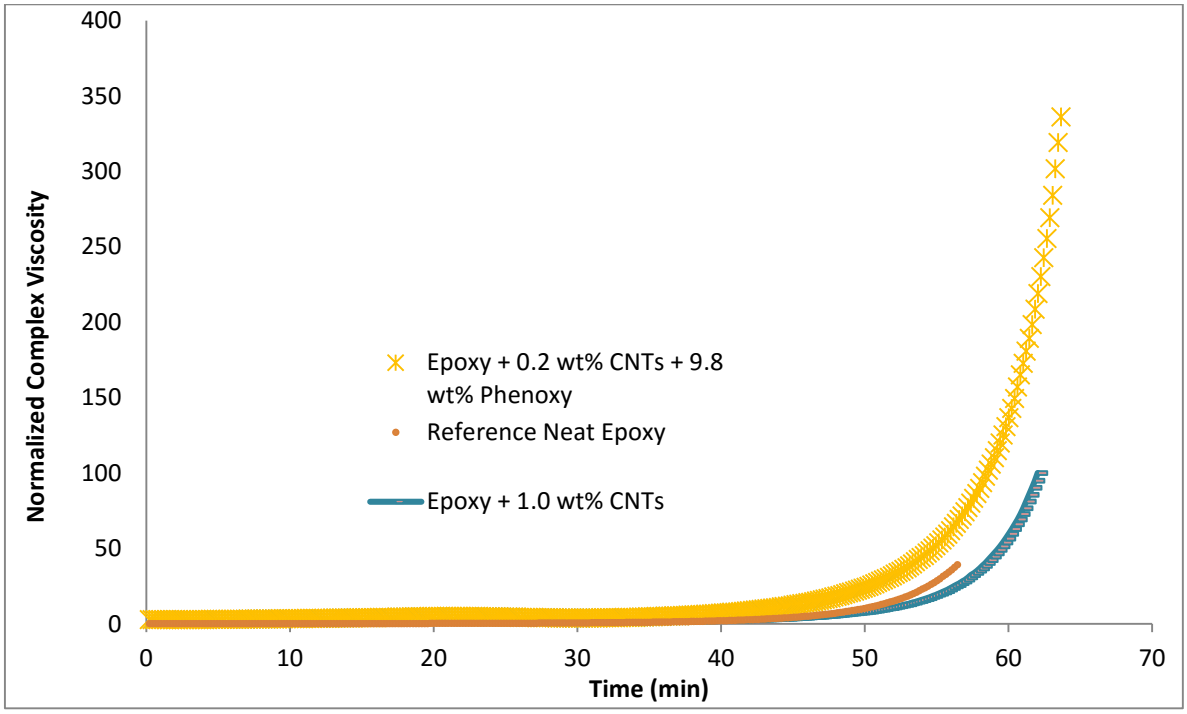

Figure 4.2 Effects of CNTs and phenoxy on gelation time

CNTs Concentration and Fracture Toughness

In this part of the chapter effects of MWCNTs on fracture toughness of epoxy resins are discussed. Single edge notch bending (SENB) samples of epoxy systems modified with different concentrations of CNTs were used in three point bending tests and strain energy release rate (G_{Ic}) were calculated in order to compare the fracture toughness. Optical microscopy beside TEM and SEM observations were also used for a better understanding of effects.

Figure 4.3 shows effects of CNTs concentration on fracture toughness. In general, the graph shows an increase in toughness until a specific amount of CNTs concentration, 0.6 wt%, and then after that it drops. 103 % improvement of G_{Ic} is achieved by using just 0.6 wt% CNTs. The general trend of the graph is as claimed by other scientists such as *Li et al.* in reference [61]; they also have stated decrease in fracture toughness after 0.7 wt% concentration.

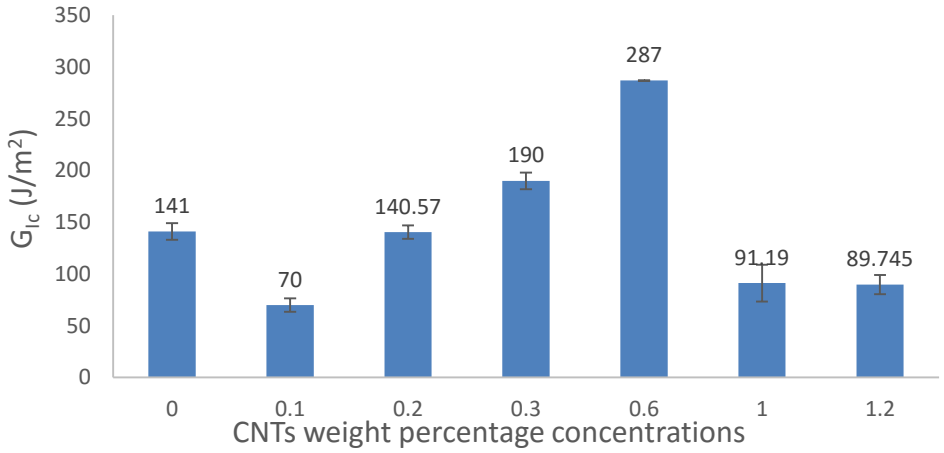

Figure 4.3 Effect of CNTs concentration on fracture toughness

But on the other hand, none of the articles reviewed in chapter two [59-62] have stated decrease in fracture toughness at small concentration of CNTs. TEM observations of the bulk of this sample have been applied to discuss this unexpected result. As shown in figure 4.4, the dispersion is so bad and there are wide areas of the sample with almost no nanotubes and in some parts there are agglomeration of CNTs. These TEM images prove that our methodology, mechanical stirring, is not good to prepare well dispersed samples containing low amounts of CNTs. The lines in these images are due to diamond knife used to cut the sample and prepare it for observation.

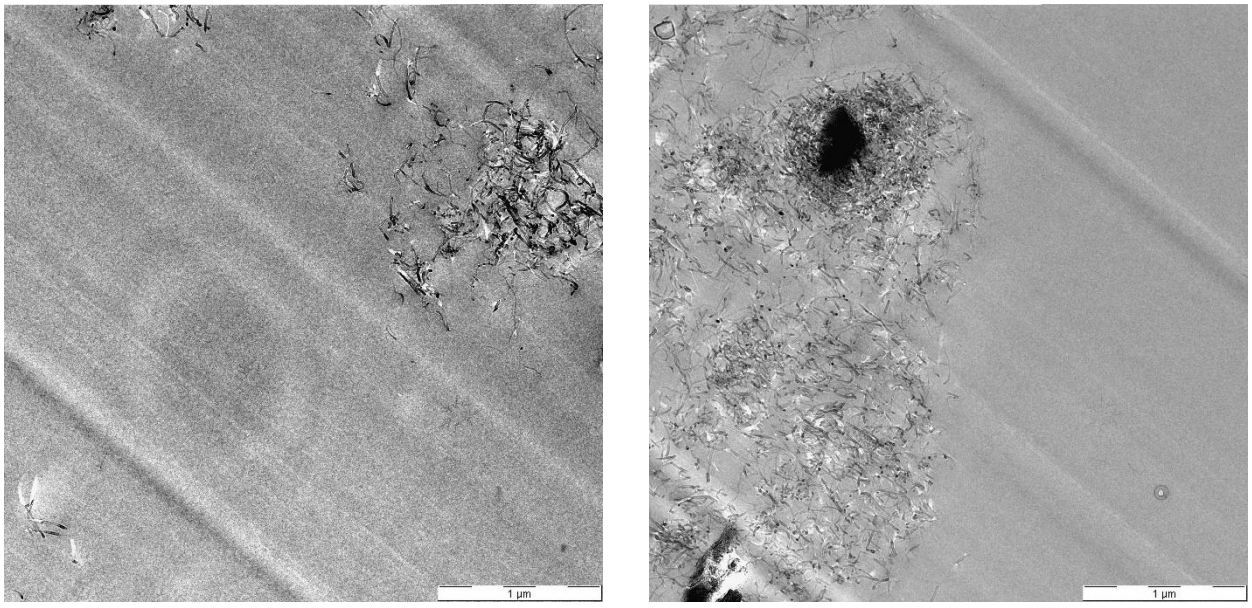

Figure 4.4 TEM images of epoxy + 0.1 wt% CNTs

To have a better understanding of the reason for decreasing of G_{Ic} after 0.6 wt% concentration, TEM images of samples with 0.6 wt% CNTs and with 1.0 wt% CNTs are shown in figure 4.5. Comparison of these images shows better dispersion of CNTs in sample with 0.6 wt% CNTs rather than the one 1.0 wt% CNTs. More and bigger agglomerations observed by TEM in samples with 1.0 wt% CNTs might be the reason for lower fracture toughness than samples with 0.6 wt% CNTs. Results like this are also claimed by *Li et al.* [61] and other scientists.

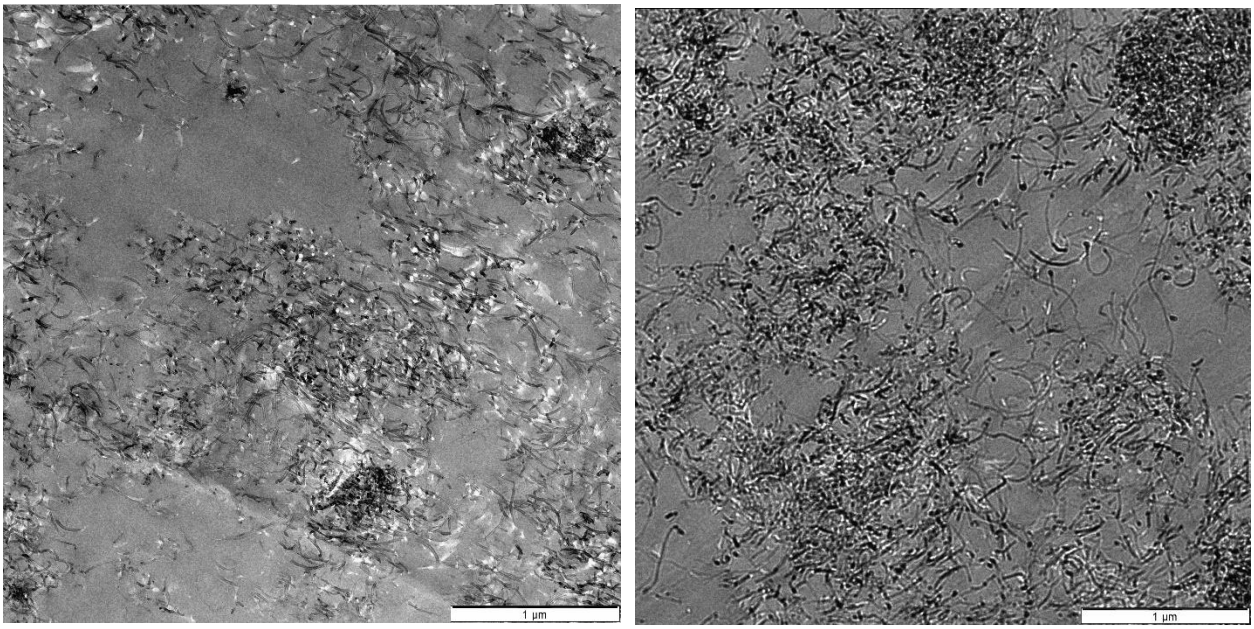

Figure 4.5 TEM images of sample with 0.6 wt% CNTs, left, and of the one with 1.0 wt% CNTs, right. It should be taken into account that the right image shows dispersion of CNTs in just one of the agglomerations.

Figure 4.5 shows CNTs in one agglomerated part of the sample and in order to have a better idea about the dispersity of CNTs and their agglomerations; optical microscopy is done. Figure 4.6 is optical microscopy image of sample with 1.0 wt% with lower magnification than TEM image and clearly illustrates bad dispersion and agglomerations of CNTs in the bulk of the sample.

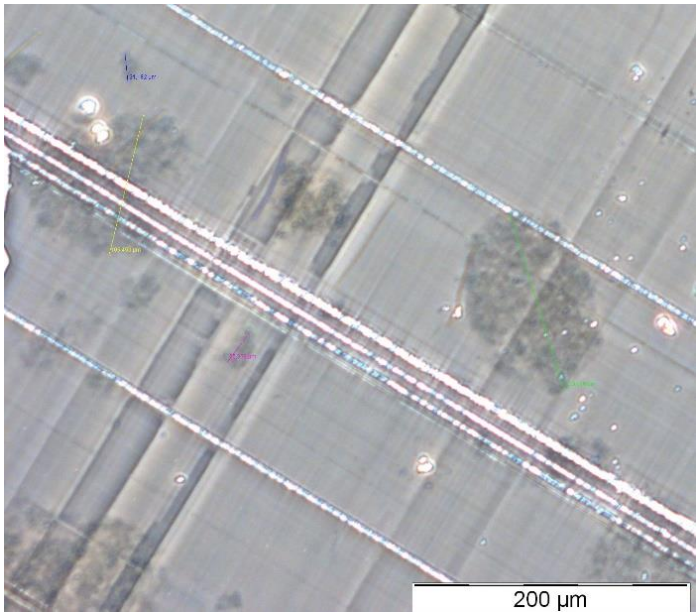

Figure 4.6 Optical microscopy image of sample with 1.0 wt% CNTs

Fracture surface analyses help better understanding of toughening mechanisms. Figure 4.7 shows SEM images of samples with different concentrations. Comparison between image 4. 7 (a) and (b) shows that in the case of 0.1 wt% CNTs there are no interactions between cracks and fillers, figure 4.7 (a), but in the other image for 0.3 wt% CNTs interactions between cracks and CNTs are evident. These interactions are also clear in figure 4.7 (c) for the sample modified with 0.6 wt% CNTs. But images of sample with 1.0 wt% CNTs didn't show any interaction and were reflective which can be proofs of low fracture toughness.

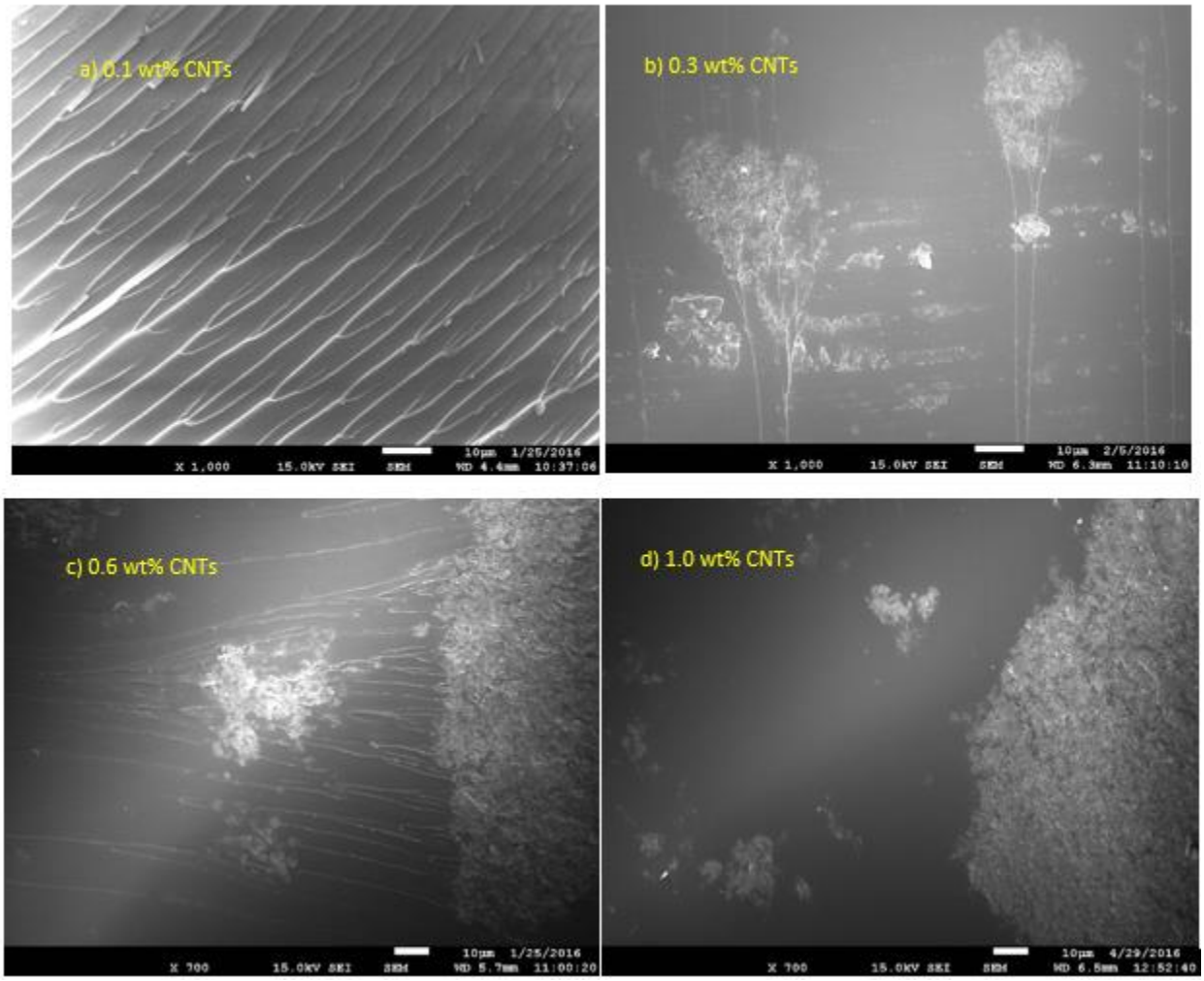

Figure 4.7 SEM images of fracture surfaces of samples modified with CNTs. Amount of the CNTs are shown on each photo.

Images with higher magnifications of fracture surface are helpful to have an idea about toughening mechanisms in modified samples. Figure 4.8 shows two images of fracture surface of sample with 0.6 wt% CNTs. Existence of the bright lines and dots on the image on the right is a strong reason for debonding and nanotubes pull-out as a toughening mechanisms, as also stated in reference [65]. The other image on the left shows a very a good interaction between cracks and CNTs which is a reason why this sample has such a high G_{Ic}.

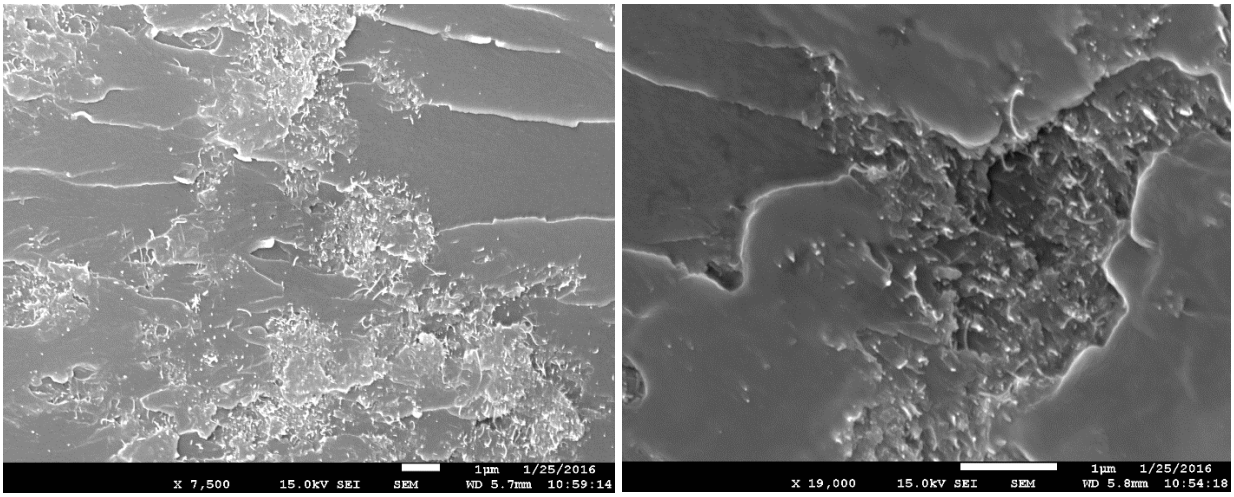

Figure 4.8 SEM images of fracture surface of epoxy + 0.6 wt% CNTs

After studying the effect on CNTs on the fracture toughness of epoxy modified blends, samples of containing both thermoplastic phenoxy phase and CNTs are examined. The next parts of this chapter is dedicated to studying these samples. First in the next part samples modified with separately added CNTs and phenoxy are studied and after that in the final part results of modifying samples by nanocomposites are discussed.

Separately Added CNTs and Phenoxy

In this part the main objective of this master thesis, which is to find the existence of synergistic effect between CNTs and phenoxy, is discussed. To do so first samples of separately added CNTs and phenoxy are studied. Three different samples were made containing 0.1, 0.3, and 0.6 wt% CNTs and 9.9, 9.7, and 9.4 wt % phenoxy, respectively. Also one sample with 10.0 wt% phenoxy was made to be used as reference in comparisons for synergistic effects. At the end TEM and SEM images were studied to understand microstructures morphology and toughening mechanisms.

Figure 4.6 shows the effect of toughening agents added separately on fracture toughness. Total amount of additives is kept 10 wt% in order to have a better comparison. Again here the sample containing 0.1 wt% CNTs + 9.9 wt% phenoxy has lower fracture toughness than sample with 10 wt% phenoxy. Reason for this can be also related to bad dispersion of nanotubes. Figure 4.6 shows that highest increase in fracture toughness, while total amount of additives is 10 wt%, is achieved when sample has 0.3 wt% CNTs and 9.7 wt% phenoxy.

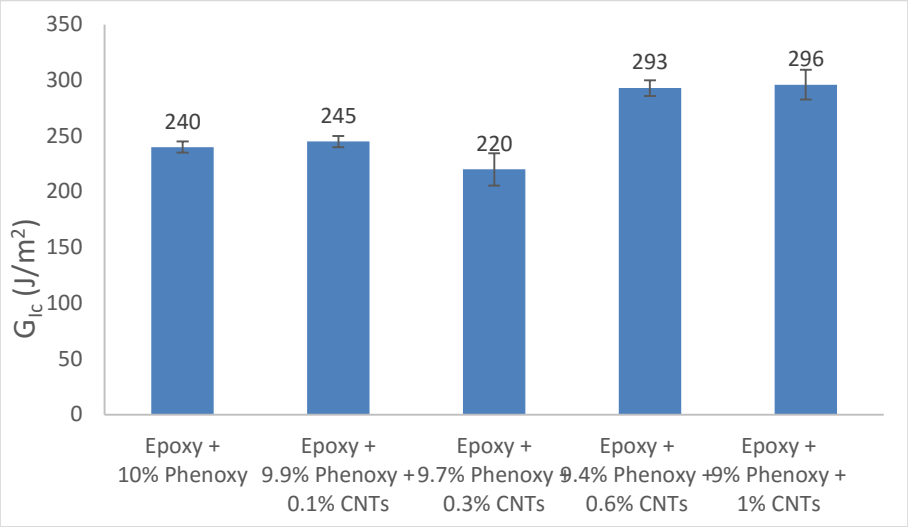

Figure 4.9 Simultaneous effect of separately added CNTs and phenoxy on fracture toughness of epoxy blends.

In order to check synergistic effects of additives on fracture toughness four samples are compared with each other, neat epoxy, epoxy + CNTs, epoxy + CNTs + phenoxy, and epoxy + 10 wt% phenoxy. Figure 4.10 shows fracture toughness of two reference samples and also two modified samples which contain 0.1 wt% CNTs and 0.1 wt% CNTs + 9.9 wt% Phenoxy. As it can be seen fracture toughness of the modified samples are lower than references and no synergistic effect exists.

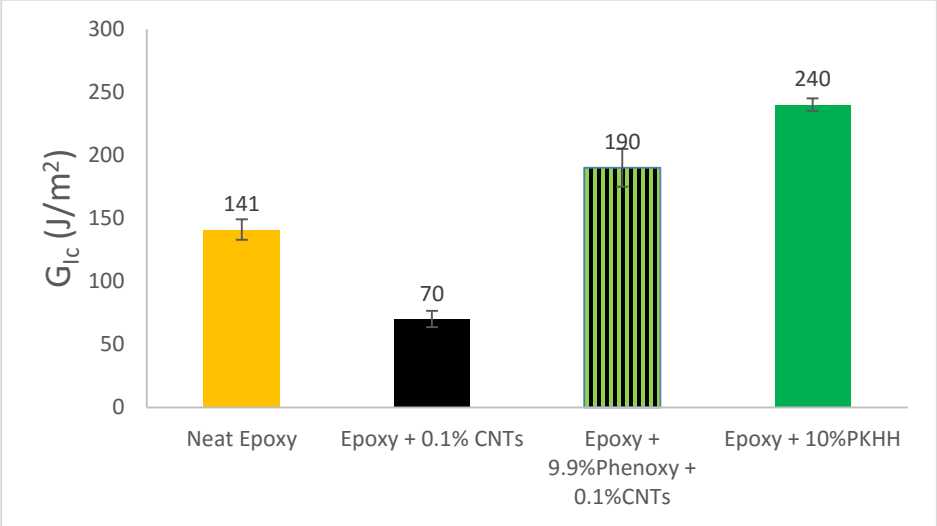

Figure 4.10 Simultaneous effect of separately added 0.1 wt% CNTs and 9.9 wt% phenoxy.

Figure 4.11 shows fracture toughness of two reference samples and also two modified samples which contain 0.3 wt% CNTs and 0.3 wt% CNTs + 9.7 wt% Phenoxy. Sample containing both of the modifiers has G_{Ic} value higher than both sample with only 0.3 wt% CNTs and sample with only 10.0 wt% phenoxy. It is a reason to claim that in this case, 0.3 wt% CNTs and 9.7 % phenoxy added separately, synergistic effect between CNTs and phenoxy exists.

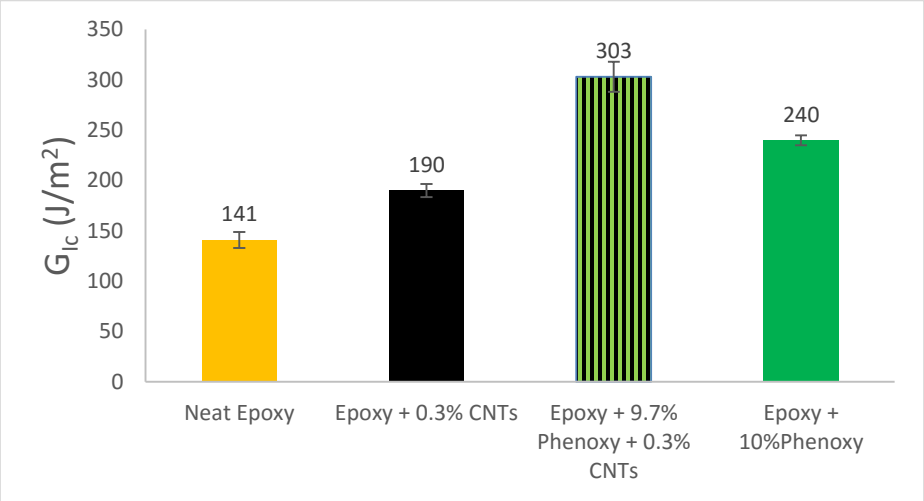

Figure 4.11 Simultaneous effect separately added of 0.3 wt% CNTs and 9.7 wt% phenoxy.

Figure 4.12 shows fracture toughness of two reference samples and also two modified samples which contain 0.6 wt% CNTs and 0.6 wt% CNTs + 9.4 wt% Phenoxy. Because G_{Ic} values of samples with 0.6 wt% CNTs and the other sample modified with 0.6 wt% CNTs + 9.4 wt% phenoxy is close to each other, 287 and 295 J/m^2, respectively; we can claim that in this case no specific synergistic effect exists.

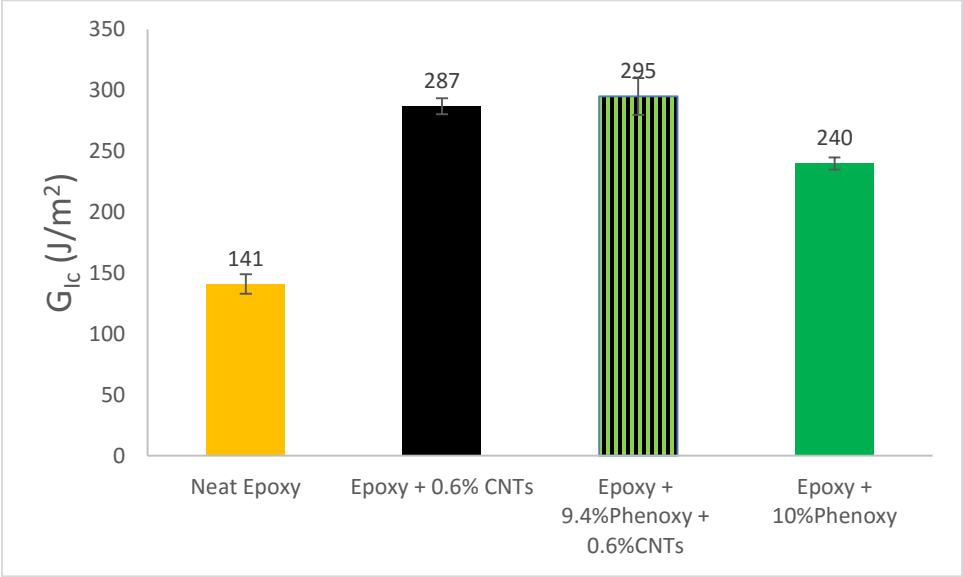

Figure 4.12 Simultaneous effect of separately added 0.6 wt% CNTs and 9.4 wt% phenoxy.

TEM and SEM observations were also done on these samples. Figure 4.13 illustrates TEM images for sample containing 0.3 wt% CNTs + 9.7 wt% phenoxy. There are some areas that almost just phenoxy nodules exist and some other areas that both CNTs and thermoplastic phenoxy phase exist. It might be a good reason why in this sample synergistic effect between different fillers exists; because inside sample in

some areas thermoplastic additives are dominant and toughening mechanisms related to them exist and some other areas nanotubes exist and help toughening

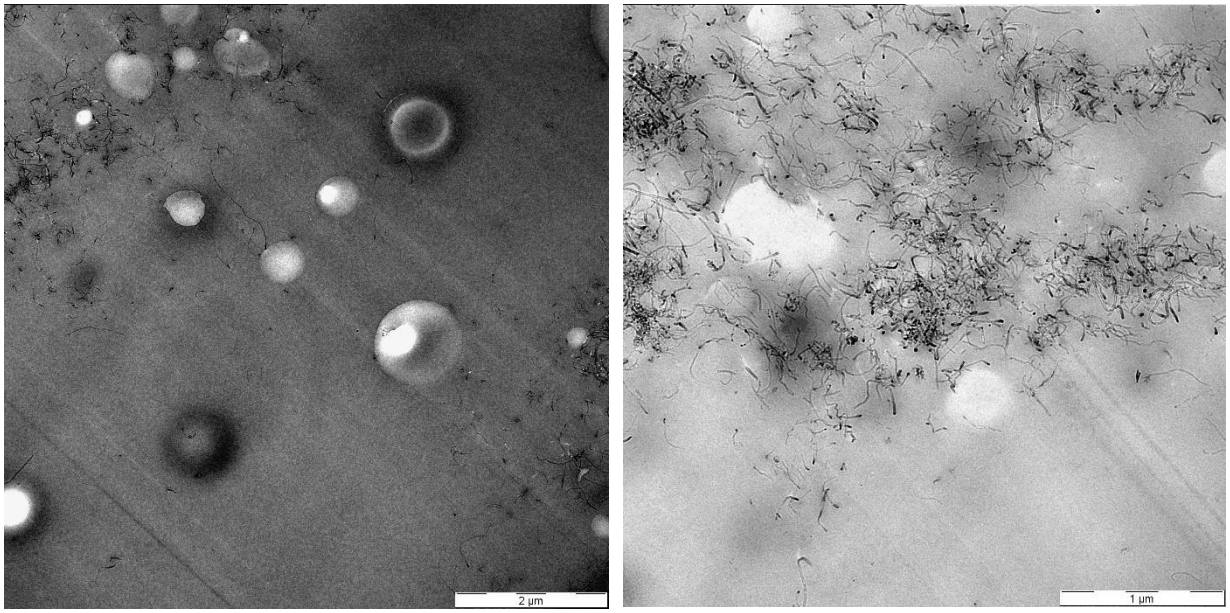

Figure 4.13 TEM images of epoxy + 0.3 wt% CNTs + 9.7 wt% phenoxy, added separately.

Figure 4.14 shows the TEM images of sample with 0.6 wt% CNTs + 9.4 wt% phenoxy. Due to two times more concentration of CNTs in this sample, compared to previous one, no such areas that thermoplastic phenoxy phase is dominant were observed. TEM images illustrate dispersion of CNTs and phenoxy nodules in the bulk of the sample.

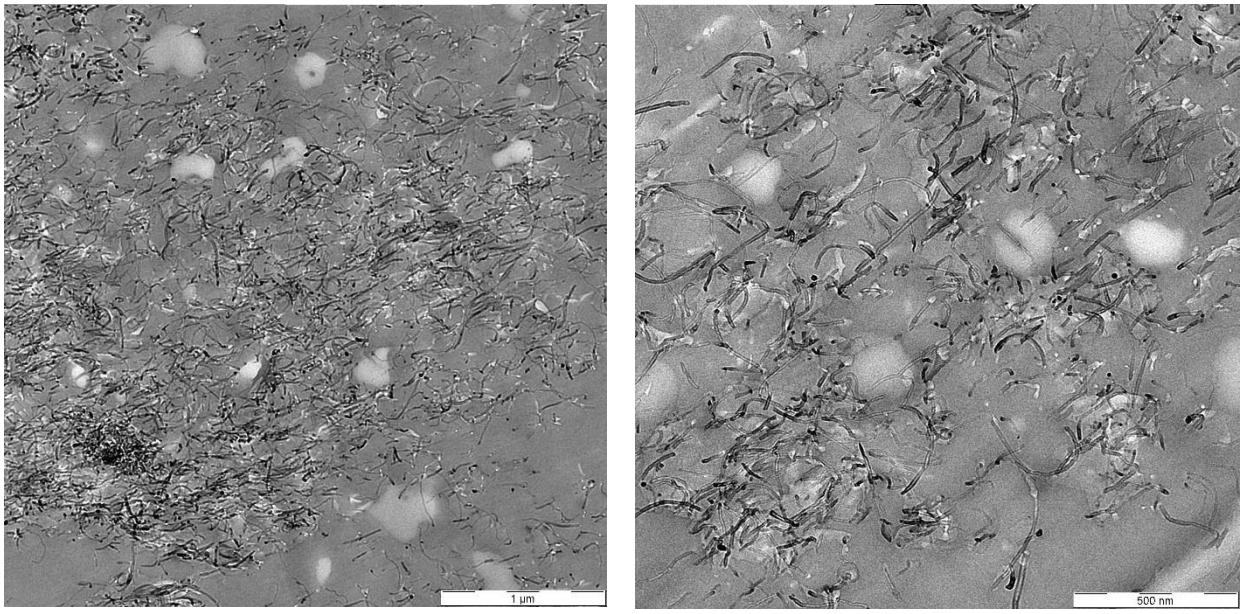

Figure 4.14 TEM images of epoxy + 0.6 wt% CNTs + 9.4 wt% phenoxy, separately added.

SEM results of fracture surfaces of these samples are also used to understand toughening mechanisms. Figure 4.15 shows fracture surface images of sample containing 0.3 wt% CNTs + 9.7 wt% phenoxy with different magnifications. Low magnification image like 4.15 (a) shows crack deflection, as seen in reference [44], and crack pinning, as reference [41], due to phenoxy nodules as toughening mechanisms.

Higher magnified images of fracture surface, 4.15 (b) to (d), more and more prove the toughening mechanisms due to nanoparticles. Figure 4.15 (d) perfectly illustrates nanotubes pull-out as toughening mechanism; so similar to the image in reference [65].

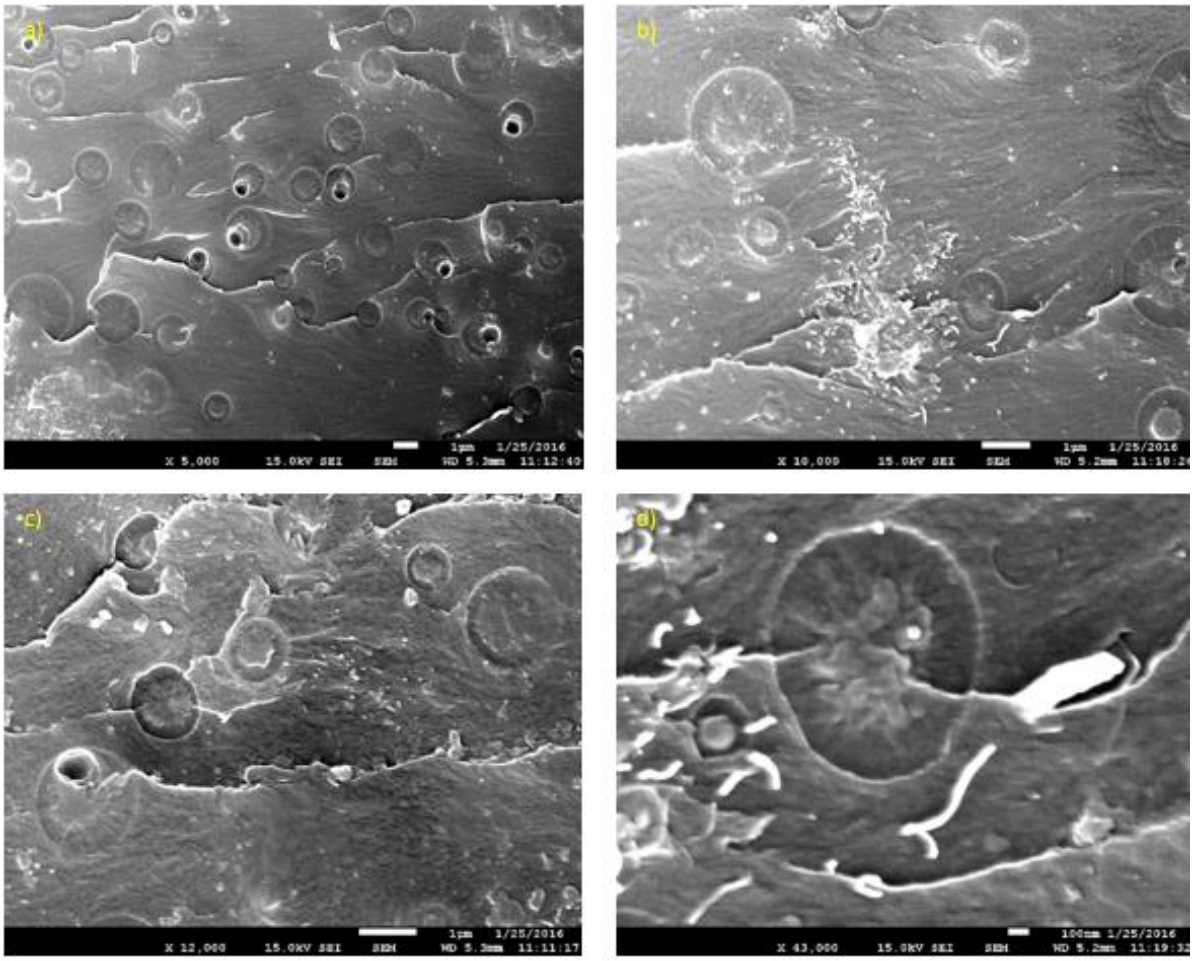

Figure 4.15 SEM images of fracture surface epoxy + 0.3 wt% MWCNTs + 9.7 wt% phenoxy, added separately.

Figure 4.16 shows the same results but for the sample modified with 0.6 wt% CNTs and 9.4 wt% phenoxy with different magnifications. Even in an image with lowest magnification, (a), existence of CNTs at the surface is clear by brighter parts. This image beside image (b) shows clearly the combination of toughening mechanism of both thermoplastic phase and nanotubes.

If compared with the figure 4.15, because concentration of CNTs is twice in this sample, they have greater role in toughening of epoxy in this sample. Especially differences between figures 4.15 (a) and 4.16 (a)

show how much the portion of toughening due to thermoplastic phase is lower in this case. This might be the reason why fracture toughness of this sample is close to the one containing only 0.6 wt% MWCNTs, G_{Ic} = 295 and 287 J/m^2, respectively.

Figure 4.16 (d) shows how thermoplastic nodules of phenoxy are improving fracture toughness by their plastic deformation and induced shear banding, as seen in reference [45], also as a toughening mechanism.

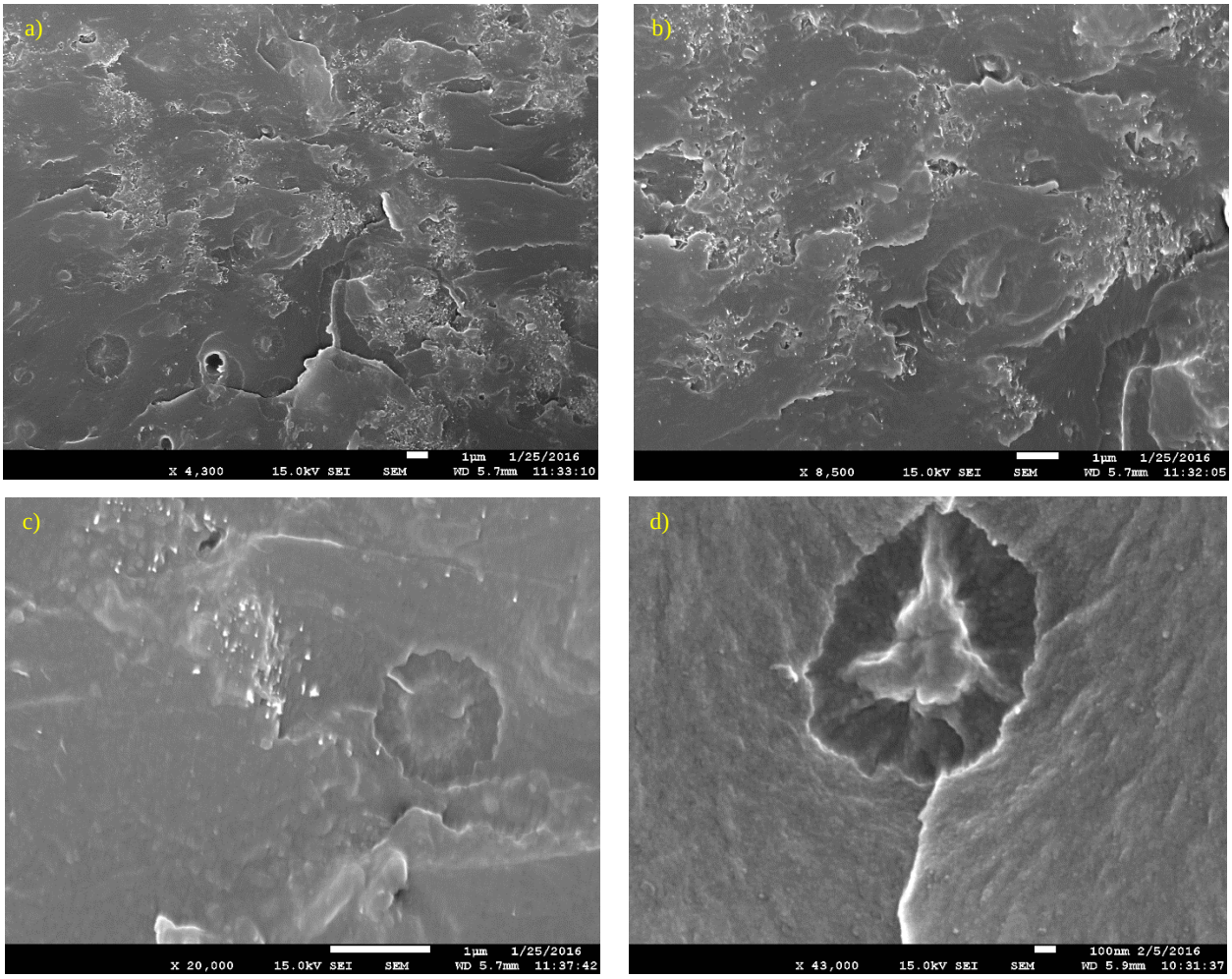

Figure 4.16 SEM images of fracture surface of epoxy + 0.6 wt% MWCNTs + 9.4 wt% phenoxy, added separately.

Nanocomposites of Phenoxy and CNTs

In the previous part samples modified by separately adding CNTs and phenoxy were studied. As mentioned in the third chapter also nanocomposites of phenoxy and CNTs were used in modified samples. In these paragraphs the effects of this type of samples are studied. The structure here is also the same as previous part, first mechanical results and then TEM and SEM results are discussed.

Figure 4.17 shows results of fracture toughness of samples with different amounts of CNTs. Also here in each sample total concentrations of modifiers is kept at 10 wt%. The graph shows that CNTs increase the

fracture toughness until 0.6 wt% and after that there is no significant increase in fracture toughness by increasing amount of CNTs.

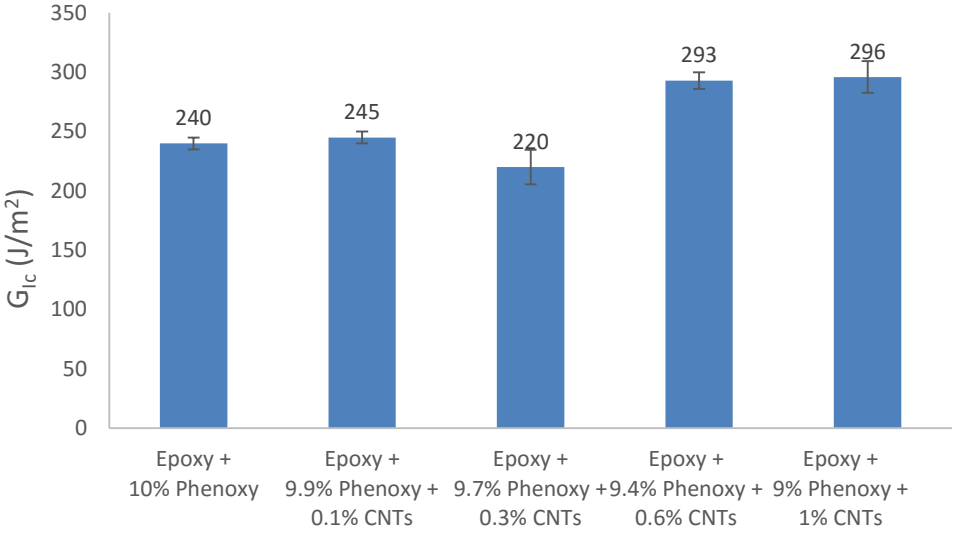

Figure 4.17 Fracture toughness of samples with 10 wt% nanocomposites of different CNTs concentration.

Table 4.1 shows the measured values of G_{Ic} for samples modified with CNTs and phenoxy in both ways. Comparing these results with each other shows some interesting points. First there is no reduction of G_{Ic} in the case of 0.1 wt% CNTs + 9.9 wt% phenoxy, which might be a proof for better dispersion on nanotubes. Second, in case of 0.6 wt% CNTs + 9.4 wt% phenoxy both numbers are near to each other and there is not a huge difference, 295 J/m^2 and 293 J/m^2 for adding separately and using nanocomposites, respectively. Finally in the case of 0.3 wt% CNTs + 9.7 wt% phenoxy there is a huge difference between G_{Ic} values of these samples made in different ways. TEM images might be helpful to discuss this big amount of difference. As TEM images shows when nanocomposites are used, CNTs are preferably at interfaces of phenoxy nodules and epoxy matrix and if the concentration of CNTs is high they will disperse in other parts of the sample also. It can be stated that in sample with 0.3 wt% CNTs, some amounts of CNTs are at the interface of phenoxy nodules and epoxy matrix, figure 4.22 (b). The remaining amount of CNTs, less than 0.3 wt%, is dispersed in the bulk of the sample and it affects similar to samples which had 0.1 wt% CNTs, that's why fracture toughness is decreased.

Table 4.1 Simultaneous effect of CNTs and phenoxy on G_{Ic} (J/m^2)

Composition	Added separately	Added by nanocomposites
0.1 wt% CNTs + 9.9 wt% phenoxy	190	245
0.3 wt% CNTs + 9.3 wt% phenoxy	303	220
0.6 wt% CNTs + 9.4 wt% phenoxy	295	293
1.0 wt% CNTs + 9.0 wt% phenoxy	--------	296

After studying fracture toughness of samples modified by nanocomposites, synergistic effect of CNTs and phenoxy is tested the same way used for separately added toughening agents. Figure 4.18 show the results for sample containing 0.1 wt% CNTs + 9.9 wt% phenoxy. G_{Ic} value is not so higher than the case of 10 wt% phenoxy, so no significant synergistic effect exists in this case.

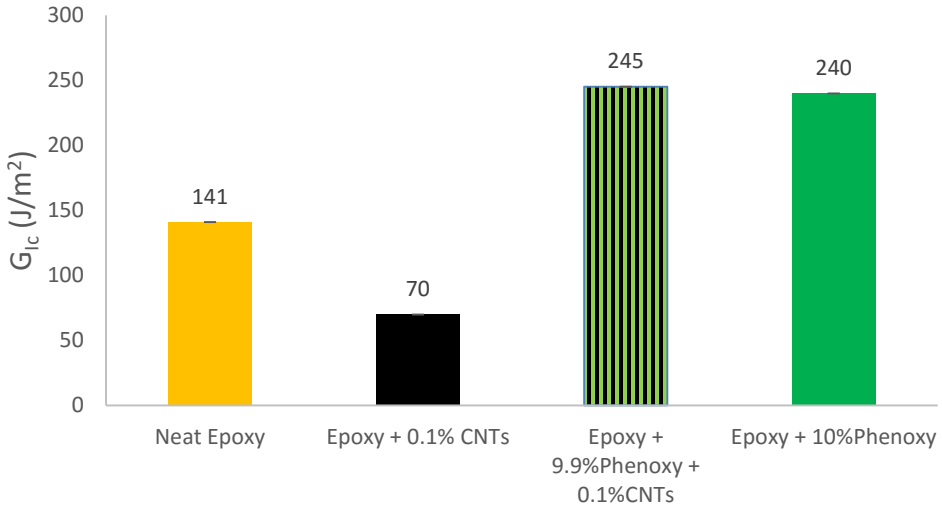

Figure 4.18 Simultaneous effect of 0.1 wt% CNTs and 9.9 wt% phenoxy using nanocomposites.

Figure 4.19 shows that in case of 0.3 wt% CNTs and 9.7 wt% phenoxy no synergy is observed and the fracture toughness of the sample made by nanocomposites is lower than sample containing 10 wt% phenoxy; but, higher than sample with just 0.3 wt% of CNTs.

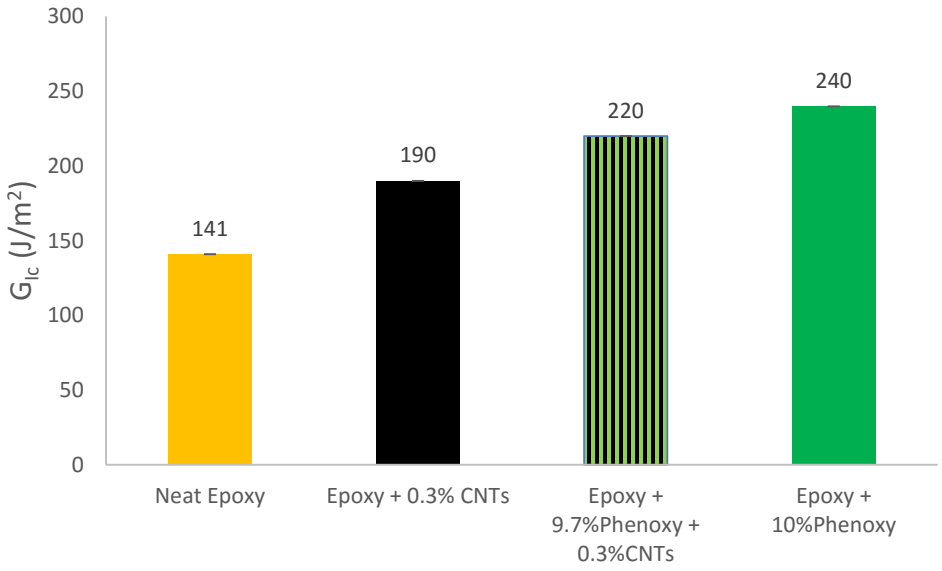

Figure 4.19 Simultaneous effect of 0.3 wt% CNTs and 9.7 wt% phenoxy using nanocomposites.

Based on figure 4.20, when 0.6 wt% CNTs and 9.4 wt% phenoxy is used, by dissolving nanocomposites, fracture toughness does not increase so much more than the case modified with only 0.6 wt% CNTs. So in this case no significant synergistic effect exists.

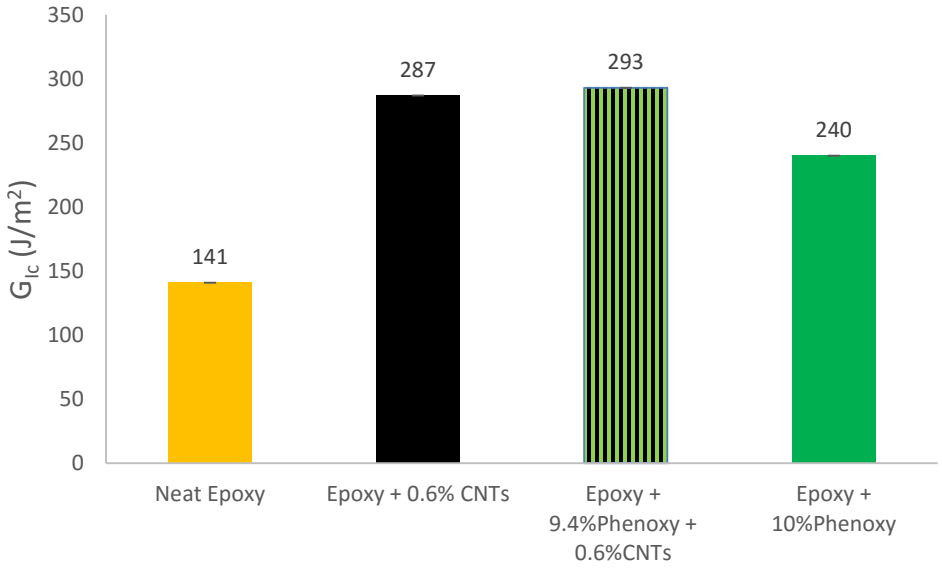

Figure 4.20 Simultaneous effect of 0.6 wt% CNTs and 9.4 wt% phenoxy using nanocomposites.

When 1 wt% of CNTs + 9 wt% is present in the sample, unlike sample with only 1 wt% CNTs, fracture toughness is significantly increased. Fracture toughness is also higher than sample modified with 10 wt% phenoxy which proves the existence of synergistic effect between CNTs and phenoxy. It is clearly shown in figure 4.21.

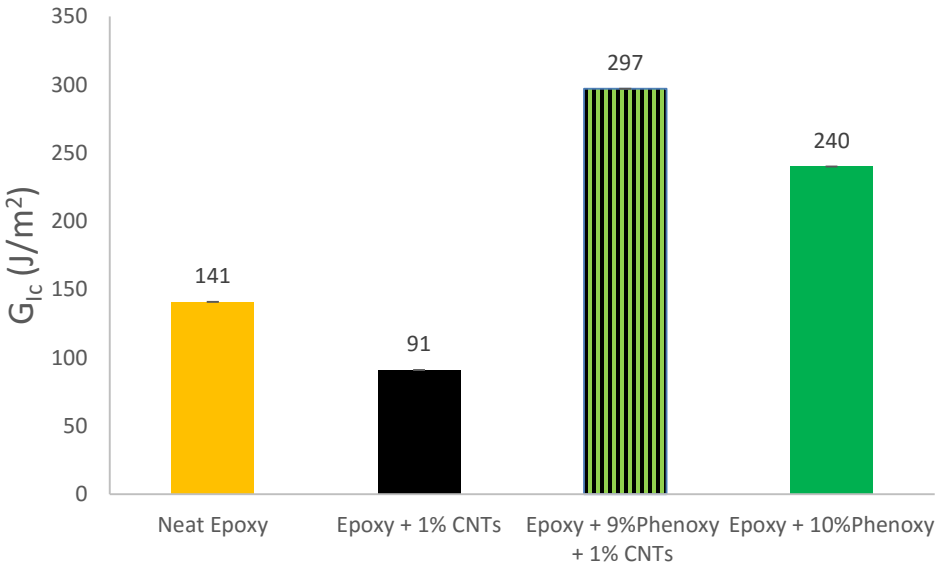

Figure 4.21 Simultaneous effect of 1.0 wt% MWCNTs and 9.0 wt% phenoxy using nanocomposites.

Finally microstructures of samples modified by using nanocomposites are shown in this part. Figure 4.22 shows TEM images of these samples with different concentration of CNTs and phenoxy. As seen in the photos nanotubes are mainly at the interface of phenoxy nodules and epoxy matrix. From figure 4.22 (a) to (d) CNTs concentration increases which causes more and more CNTs in the bulk. Figure 4.22 (a) shows that almost all the CNTs are located in the interfaces of phenoxy nodule and epoxy matrix, but in figure 4.22 (d) where CNTs concentration is 10 times more, we see CNTs in the bulk and also CNTs agglomerations.

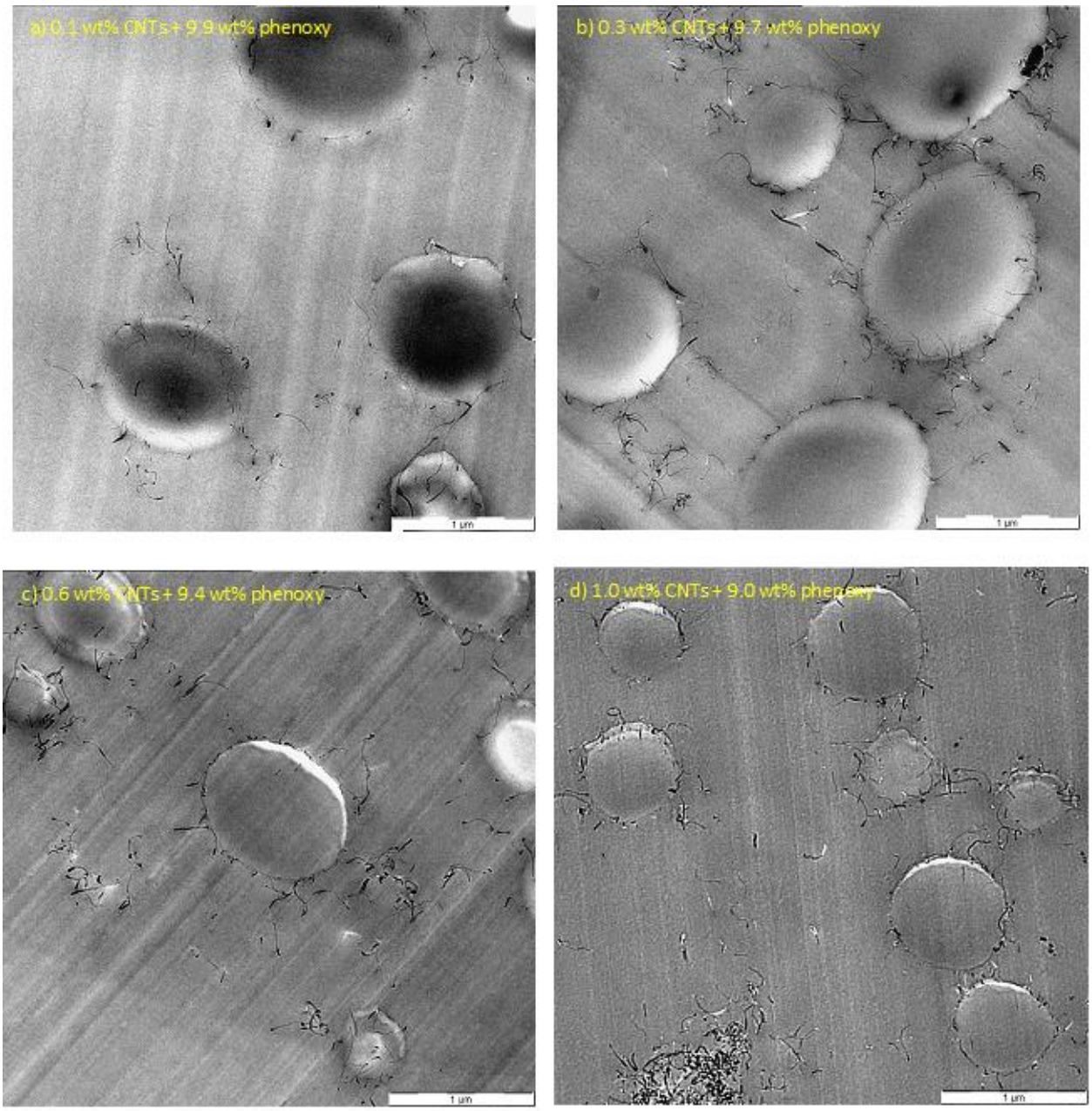

Figure 4.22 TEM images of samples modified with nanocomposites with different compositions

Knowing the microstructure of sample with 0.1 wt% CNTs + 9.9 wt% phenoxy, figure 4.22 (a), and also comparing the measured G_{Ic} value for this sample with the sample containing 10 wt% phenoxy; 245 and 240 J/m^2, respectively; shows that if CNTs are at the interface they do not improve fracture toughness so huge and the role of thermoplastic phase is dominant in improving fracture toughness.

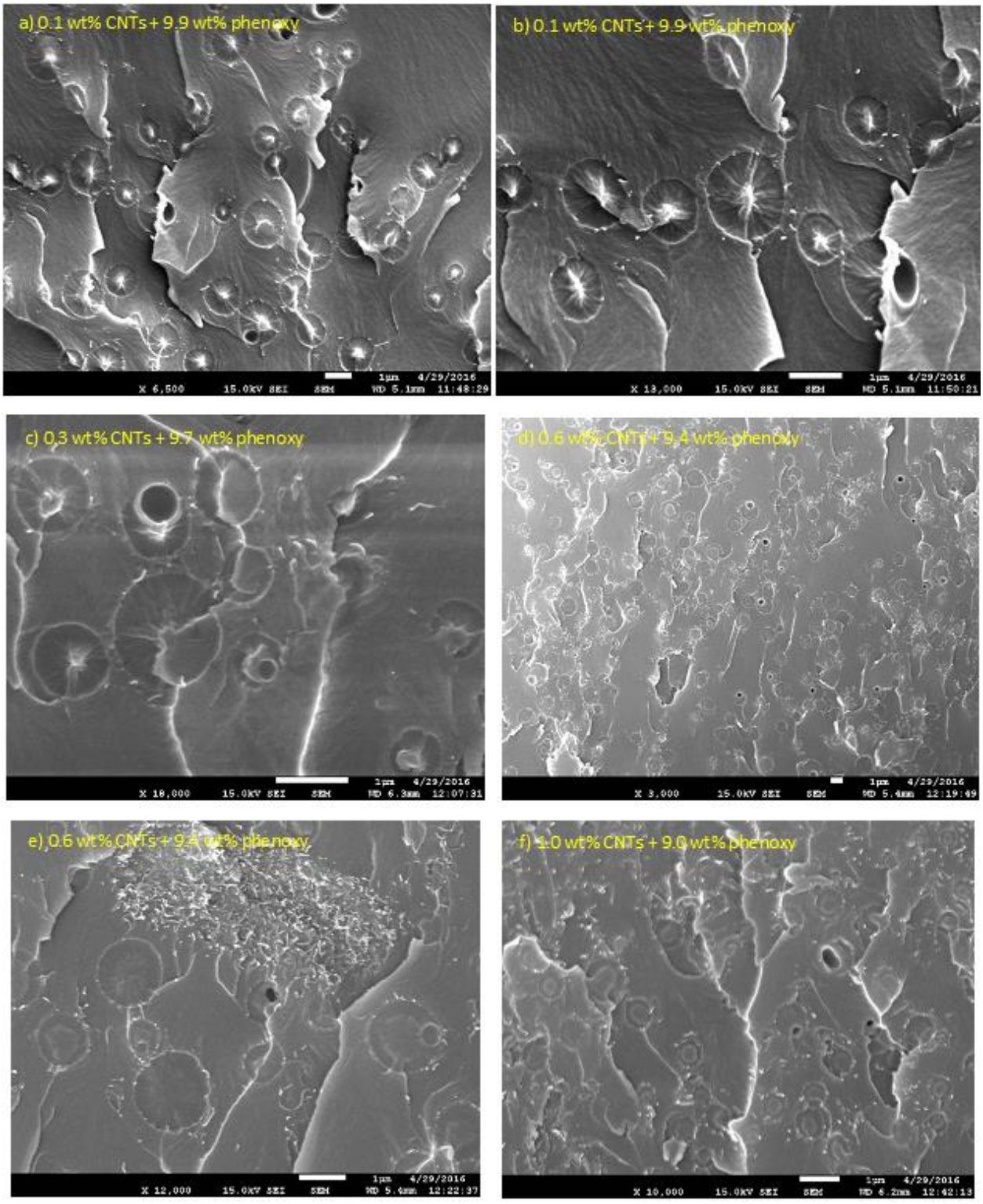

Figure 4.23 SEM images of fracture surface of epoxy samples modified with different nanocomposites of phenoxy and CNTs.

Figure 4.23 illustrates SEM images of fracture surfaces of different samples modified with nanocomposites. Toughening mechanisms look the same as samples modified with separately added toughening agents. Figure 4.23 (a) shows that in really low concentration of CNTs, 0.1 wt%, main toughening mechanism is as the one for systems modified with thermoplastics. This figure looks like the one in reference [26] for crack path deflection.

In figure 4.23 (b) pull-out of nanotubes is observed, similar to reference [65]. Because these pull-outs are at the interface of thermoplastic phenoxy phase, around the crack, they don't increase fracture toughness so much.

Figure 4.23 (d) shows a good overview over fracture surface containing different toughening mechanisms such as crack path deflection and crack pinning; as well as pull-out of nanotubes which results in brighter lines and dots. Figure 4.23 (e) illustrates a part of samples that CNTs are dominantly interacting with crack, not just being in the interface of phenoxy nodules, and this can be the reason for higher G_{Ic} value for this sample.

CHAPTER 5 CONCLUSIONS AND PROSPECTIVES

Polymer matrix composites are attractive alternatives for sustainable developping future. Epoxy resins due to their properties such as high mechanical properties, low density, and excellent chemical resistance are widely used in automotive and aerospace industries. One of the barriers in using epoxy based composites is their limited fracture toughness and impact resistance.

Since 1960s many different methods and materials are used and studied to make them less brittle and increase the fracture toughness. These methods were discussed in the second chapter. It was shown that most of the conventional methods increase the fracture toughness but with the expense of decreasing other properties like Young's modulus, tensile strength, and glass transition temperature which results in limited working temperature.

Among all these methods toughening by thermoplastics and nanoparticles are more interesting because they are compatible with highly crosslinked and brittle epoxy matrix, unlike rubbers, and also they don't decrease other properties. One more interesting aspect of using nanoparticles is that high improvements in fracture toughness can be achieved by low amount of fillers. Thermoplastic phenoxy phase and carbon nanotubes (CNTs) have been well studied by other scientist and are proved to be good modifiers.

Phenoxy and CNTs have different toughening mechanisms and if they both exist in the ternary system it is probable the synergistic effects between them will make the modified system to reach even higher amounts of fracture toughness than binary systems. To validate this idea samples containing both multi-walled CNTs and phenoxy were made in two different ways adding CNTs and phenoxy separately to epoxy or adding nanocomposites of phenoxy and CNTs to epoxy resins. Also samples of just containing CNTs and sample of epoxy modified with 10 wt% phenoxy were made.

After curing the blends, three point bending tests were done on SENB samples and strain energy release rate (G_{Ic}) were measured. An unwanted decrease was observed in samples modified with 0.1 wt% CNTs, 50% decrease, and sample containing separately added 0.1 wt% CNTs and 9.9 wt% phenoxy, 21% decrease. It might be due to bad dispersion of CNTs, agglomerations were observed by TEM, which proves mechanically stirring additives and applying shear force is not a good method of dispersion for samples with low CNTs concentrations.

Generally when only CNTs were used G_{Ic} was increasing until 0.6 wt% CNTs (G_{Ic}=287J/m^2, 103% increase) and after that it was decreased. The main toughening mechanisms in this case are thought to be debonding and pull-out of CNTs.

In case of separately added phenoxy and CNTs highest G_{Ic} was reached when 0.3 wt% CNTs and 9.7 wt% phenoxy were used, G_{Ic}=303J/m^2, 114% increase. The main toughening mechanisms for this sample are crack path deflection, crack pinning, and nanotubes pull-out.

Finally when nanocomposites of phenoxy and CNTs were used completely different morphologies from previous samples were observed. CNTs were preferably at the interfaces of the phenoxy nodules and epoxy matrix and if the concentration was high they were also seen in the bulk. Highest fracture toughness in this case was reached in sample modified with 1.0 wt% CNTs and 9.0 wt% phenoxy, G_{Ic}=296J/m^2, 111% increase. Toughening mechanisms in these samples were also the same as before, crack path deflection, crack pinning, and nanotubes pull-out. But because of the more existence of nodules around phenoxy nodules CNTs had smaller role in toughening mechanism.

The main objective of this master thesis was to find if there is a synergistic effect between CNTs and phenoxy of fracture toughness of epoxy. It was observed that is some specific formulation there is synergistic effect between them. Synergy was observed is samples when 0.3 wt% CNTs and 9.7 wt% phenoxy is added separately or when nanocomposites are used to add 0.6 wt% and 9.4 wt% phenoxy.

At the end, some perspectives might be checking the Young's modulus and operating temperature for samples by DMTA analysis. Also testing the effect of additives on electrical conductivity and threshold of materials. Especially the sample modified with nanocomposites because of having more nanotubes at the nodules interfaces might be interesting in electrical properties.

CHAPTER 6 REFERENCES

1. Stein, Jasmin. *Toughening of highly crosslinked epoxy resin systems*. Diss. University of Manchester, 2013.
2. Rebsdat, S. and Mayer, D. 2001. Ethylene Oxide. Ullmann's Encyclopedia of Industrial Chemistry.
3. P. K. Mallick. Fiber-Reinforced Composites. Taylor & Francis/CRC, Boca Raton, 2008.
4. Pham, H. Q., and M. J. Marks. "Epoxy resins. Ullmann's encyclopedia of industrial chemistry." (2005).
5. Menard, Kevin P. *Dynamic mechanical analysis: a practical introduction*. CRC press, 2008.
6. Bruce Prime, R. *Thermoset Characterization Part 4: Introduction to Gelation* http://polymerinnovationblog.com May 5, 2014
7. "Fracture Toughness". *NDT Resource Center.* Available from: https://www.nde-ed.org/EducationResources/CommunityCollege/Materials/Mechanical/FractureToughness.htm
8. Sagar Vijay Gade, "Selective property enhancement by modification of epoxy". Missouri University of Science and Technology http://coatings.mst.edu/v12i1/v12i1/
9. Bagheri, R., B. T. Marouf, and R. A. Pearson. "Rubber-toughened epoxies: a critical review." Journal of Macromolecular Science®, Part C: Polymer Reviews 49.3 (2009): 201-225.
10. Arias, María L., Patricia M. Frontini, and Roberto JJ Williams. "Analysis of the damage zone around the crack tip for two rubber-modified epoxy matrices exhibiting different toughenability." Polymer 44.5 (2003): 1537-1546.
11. Pearson, R. A., and A. F. Yee. "Toughening mechanisms in elastomer-modified epoxies." Journal of materials science 24.7 (1989): 2571-2580.
12. He, J., et al. "The influence of elastomer concentration on toughness in dispersions containing preformed acrylic elastomeric particles in an epoxy matrix." Polymer 40.8 (1999): 1923-1933.
13. Dong, Lina, et al. "A Carboxyl-Terminated Polybutadiene Liquid Rubber Modified Epoxy Resin with Enhanced Toughness and Excellent Electrical Properties." Journal of Electronic Materials (2016): 1-10.
14. Baiuk, Amad-Adeen, Riyadh Al-Ameri, and Bronwyn Fox. "Bond properties of rubber modified epoxy." (2014): 175.
15. Yahyaie, Hossein, et al. "Toughening mechanisms of rubber modified thin film epoxy resins." Progress in Organic Coatings 76.1 (2013): 286-292.
16. Abadyan, Mohamadreza, et al. "Loading rate-induced transition in toughening mechanism of rubber-modified epoxy." Journal of Macromolecular Science, Part B 49.3 (2010): 602-614.
17. Qi, Guicun, et al. "The study of rubber-modified plastics with higher heat resistance and higher toughness and its application." Polymer Chemistry 2.6 (2011): 1271-1274.
18. Ballout W, Horion J, Velthem P.V. "UCL report – Toughening of Epoxy Resins: a Review"
19. Dean, Jennifer M., et al. "Nanostructure toughened epoxy resins." Macromolecules 36.25 (2003): 9267-9270.

20. Dean, Jennifer M., et al. "Mechanical properties of block copolymer vesicle and micelle modified epoxies." Journal of Polymer Science Part B: Polymer Physics 41.20 (2003): 2444-2456.
21. Li, Tuoqi, et al. "Engineering superior toughness in commercially viable block copolymer modified epoxy resin." Journal of Polymer Science Part B: Polymer Physics 54.2 (2016): 189-204.
22. Downey, Markus A., and Lawrence T. Drzal. "Toughening of aromatic epoxy via aliphatic epoxy copolymers." Polymer 55.26 (2014): 6658-6663.
23. Romeo, Hernán E., et al. "From spherical micelles to hexagonally packed cylinders: The cure cycle determines nanostructures generated in block copolymer/epoxy blends." Macromolecules 46.12 (2013): 4854-4861.
24. Redline, Erica M., et al. "Effect of block copolymer concentration and core composition on toughening epoxies." Polymer 55.16 (2014): 4172-4181.
25. Hodgkin, J. H., G. P. Simon, and R. J. Varley. "Thermoplastic toughening of epoxy resins: a critical review." Polymers for Advanced Technologies 9.1 (1998): 3-10.
26. Francis, Bejoy, et al. "Poly (ether ketone) with pendent methyl groups as a toughening agent for amine cured DGEBA epoxy resin." Journal of materials science 41.17 (2006): 5467-5479.
27. Girard-Reydet, Emmanuel, et al. "Reaction-induced phase separation mechanisms in modified thermosets." Polymer 39.11 (1998): 2269-2279.
28. Williams, Roberto JJ, Boris A. Rozenberg, and Jean-Pierre Pascault. "Reaction-induced phase separation in modified thermosetting polymers." *Polymer Analysis Polymer Physics*. Springer Berlin Heidelberg, 1997. 95-156.
29. MacKinnon, Alexander J., et al. "A dielectric, mechanical, rheological and electron microscopy study of cure and properties of a thermoplastic-modified epoxy resin." Macromolecules 25.13 (1992): 3492-3499.
30. Deng, Shiqiang, et al. "Thermoplastic–epoxy interactions and their potential applications in joining composite structures–A review." Composites Part A: Applied Science and Manufacturing 68 (2015): 121-132.
31. Gilbert, A. H., and C. B. Bucknall. "Epoxy resin toughened with thermoplastic." Makromolekulare Chemie. Macromolecular Symposia. Vol. 45. No. 1. Hüthig & Wepf Verlag, 1991.
32. Grishchuk, S., et al. "Structure and toughness of polyethersulfone (PESU)-modified anhydride-cured tetrafunctional epoxy resin: Effect of PESU molecular mass." Journal of Applied Polymer Science 123.2 (2012): 1193-1200.
33. Aravand, Mohammadali, Stepan V. Lomov, and Larissa Gorbatikh. "Morphology and fracture behavior of POM modified epoxy matrices and their carbon fiber composites." Composites Science and Technology 110 (2015): 8-16.
34. Giannotti, M. I., et al. "Morphology and fracture properties relationship of epoxy-diamine systems simultaneously modified with polysulfone and poly (ether imide)." Polymer Engineering & Science 45.9 (2005): 1312-1318.
35. Teng, Kun-Chun, and Feng-Chih Chang. "Single-phase and multiple-phase thermoplastic/thermoset polyblends: 1. Kinetics and mechanisms of phenoxy/epoxy blends." Polymer 34.20 (1993): 4291-4299.

36. Teng, Kun-Chun, and Feng-Chih Chang. "Single-phase and multiple-phase thermoplastic/thermoset polyblends: 2. Morphologies and mechanical properties of phenoxy/epoxy blends." Polymer 37.12 (1996): 2385-2394.
37. Wong, Doris Wai-Yin. Toughening of epoxy carbon fibre composites using dissolvable phenoxy fibres. Diss. Queen Mary University of London, 2013.
38. Pearson, Raymond A., and Albert F. Yee. "Toughening mechanisms in thermoplastic-modified epoxies: 1. Modification using poly (phenylene oxide)." Polymer 34.17 (1993): 3658-3670.
39. Cardwell, B. J., and Albert F. Yee. "Toughening of epoxies through thermoplastic crack bridging." Journal of materials science 33.22 (1998): 5473-5484.
40. Przystupa, M. A., and T. H. Courtney. "Fracture in equiaxed two phase alloys: part ii. Fracture in alloys with isolated plastic particles." Metallurgical Transactions A 13.5 (1982): 881-887.
41. Chaudhary, Saurabh, et al. "Simple toughening of epoxy thermosets by preformed thermoplastics." Society of Plastics Engineers (2014).
42. Lange, F. F. "The interaction of a crack front with a second-phase dispersion." *Philosophical Magazine* 22.179 (1970): 0983-0992.
43. Faber, K. T., and A. G. Evans. "Crack deflection processes—I. Theory."*Acta Metallurgica* 31.4 (1983): 565-576.
44. Gao, Chengde, et al. "Enhancement mechanisms of graphene in nano-58S bioactive glass scaffold: mechanical and biological performance." *Scientific reports* 4 (2014).
45. Kim, Sung C., and Hugh R. Brown. "Impact-modified epoxy resin with glassy second component." *Journal of materials science* 22.7 (1987): 2589-2594.
46. Wong, Doris Wai-Yin. Toughening of epoxy carbon fibre composites using dissolvable phenoxy fibres. Diss. Queen Mary University of London, 2013.
47. Azeez, Asif Abdul, et al. "Epoxy clay nanocomposites–processing, properties and applications: A review." *Composites Part B: Engineering* 45.1 (2013): 308-320.
48. Gam, K. T., et al. "Fracture behavior of core-shell rubber–modified clay-epoxy nanocomposite." *Polymer Engineering & Science* 43.10 (2003): 1635-1645.
49. Alexandre, Michael, and Philippe Dubois. "Polymer-layered silicate nanocomposites: preparation, properties and uses of a new class of materials." Materials Science and Engineering: R: Reports 28.1 (2000): 1-63.
50. Liang, Y. L., and R. A. Pearson. "Toughening mechanisms in epoxy–silica nanocomposites (ESNs)." *Polymer* 50.20 (2009): 4895-4905.
51. Sprenger, Stephan. "Epoxy resins modified with elastomers and surface-modified silica nanoparticles." *Polymer* 54.18 (2013): 4790-4797.
52. Liu, Songlin, Xiaoshan Fan, and Chaobin He. "Improving the Fracture Toughness of Epoxy with Nanosilica-Rubber Core-Shell Nanoparticles." Composites Science and Technology (2016).
53. Ngah, Shamsiah Awang, and Ambrose C. Taylor. "Toughening performance of glass fibre composites with core–shell rubber and silica nanoparticle modified matrices." Composites Part A: Applied Science and Manufacturing 80 (2016): 292-303.
54. Belle Dumé. "Scientists delve deeper into carbon nanotubes" http://physicsworld.com/ Visited on 31 May 2016
55. Fiedler, Bodo, et al. "Fundamental aspects of nano-reinforced composites." *Composites science and technology* 66.16 (2006): 3115-3125.

56. Gojny, Florian H., et al. "Influence of nano-modification on the mechanical and electrical properties of conventional fibre-reinforced composites." *Composites Part A: Applied Science and Manufacturing* 36.11 (2005): 1525-1535.
57. Sprenger, Stephan. "Epoxy resins modified with elastomers and surface-modified silica nanoparticles." *Polymer* 54.18 (2013): 4790-4797.
58. Gojny, F. H., et al. "Carbon nanotube-reinforced epoxy-composites: enhanced stiffness and fracture toughness at low nanotube content." *Composites Science and Technology* 64.15 (2004): 2363-2371.
59. Gojny, Florian H., et al. "Influence of different carbon nanotubes on the mechanical properties of epoxy matrix composites–a comparative study." *Composites Science and Technology* 65.15 (2005): 2300-2313.
60. Allaoui, Aïssa, et al. "Mechanical and electrical properties of a MWNT/epoxy composite." *Composites Science and Technology* 62.15 (2002): 1993-1998.
61. Li, Xiaoyan, et al. "Investigation into the toughening mechanism of epoxy reinforced with multi-wall carbon nanotubes." *e-Polymers* 15.5 (2015): 335-343.
62. Domun, Nadiim, et al. "Improving the fracture toughness and the strength of epoxy using nanomaterials–a review of the current status." *Nanoscale* 7.23 (2015): 10294-10329.
63. Zhao, Su, et al. "Mechanisms leading to improved mechanical performance in nanoscale alumina filled epoxy." *Composites Science and Technology* 68.14 (2008): 2965-2975.
64. Opelt, Carlos V., et al. "Reinforcement and toughening mechanisms in polymer nanocomposites–Carbon nanotubes and aluminum oxide." *Composites Part B: Engineering* 75 (2015): 119-126.
65. Hsieh, T. H., et al. "The toughness of epoxy polymers and fibre composites modified with rubber microparticles and silica nanoparticles." *Journal of materials science* 45.5 (2010): 1193-1210.
66. Wikipedia contributors. "Shear band." *Wikipedia, The Free Encyclopedia*. Wikipedia, The Free Encyclopedia, 17 Mar. 2014. Web. 2 Jun. 2016.
67. Quaresimin, M., et al. "Toughening mechanisms in polymer nanocomposites: From experiments to modelling." *Composites Science and Technology* 123 (2016): 187-204.
68. Chozhan, Chinnakkannu Karikal, et al. "Thermo mechanical behaviour of unsaturated polyester toughened epoxy–clay hybrid nanocomposites."Journal of Polymer Research 14.4 (2007): 319-328.
69. Zeng, Ying, et al. "Improving interlaminar fracture toughness of carbon fibre/epoxy laminates by incorporation of nano-particles." Composites Part B: Engineering 43.1 (2012): 90-94.
70. Fröhlich, Jörg, Ralf Thomann, and Rolf Mülhaupt. "Toughened epoxy hybrid nanocomposites containing both an organophilic layered silicate filler and a compatibilized liquid rubber." Macromolecules 36.19 (2003): 7205-7211.
71. Abadyan, M., et al. "Exploring the tensile strain energy absorption of hybrid modified epoxies containing soft particles." Materials & Design 32.5 (2011): 2900-2908.
72. Azimi, H. R., R. A. Pearson, and R. W. Hertzberg. "Fatigue of hybrid epoxy composites: epoxies containing rubber and hollow glass spheres." Polymer Engineering & Science 36.18 (1996): 2352-2365.

73. Chatterjee, S., et al. "Size and synergy effects of nanofiller hybrids including graphene nanoplatelets and carbon nanotubes in mechanical properties of epoxy composites." Carbon 50.15 (2012): 5380-5386.
74. Chen, Ju-Long, Fan-Long Jin, and Soo-Jin Park. "Thermal stability and impact and flexural properties of epoxy resins/epoxidized castor oil/nano-CaCO3 ternary systems." Macromolecular Research 18.9 (2010): 862-867.
75. Asif, A., et al. "Hydroxyl terminated poly (ether ether ketone) with pendant methyl group-toughened epoxy clay ternary nanocomposites: Preparation, morphology, and thermomechanical properties." Journal of applied polymer science 106.5 (2007): 2936-2946.
76. Mirmohseni, A., and S. Zavareh. "Preparation and characterization of an epoxy nanocomposite toughened by a combination of thermoplastic, layered and particulate nano-fillers." *Materials & Design* 31.6 (2010): 2699-2706.
77. Tang, Long-Cheng, et al. "Fracture toughness and electrical conductivity of epoxy composites filled with carbon nanotubes and spherical particles." *Composites Part A: Applied Science and Manufacturing* 45 (2013): 95-101.
78. Cao, Y. M., J. Sun, and D. H. Yu. "Preparation and properties of nano-Al2O3 particles/polyester/epoxy resin ternary composites." Journal of Applied Polymer Science 83.1 (2002): 70-77.
79. Liu, Hong-Yuan, et al. "On fracture toughness of nano-particle modified epoxy." *Composites Part B: Engineering* 42.8 (2011): 2170-2175.
80. Van Velthem, Pascal, et al. "Influence of thermoplastic diffusion on morphology gradient and on delamination toughness of RTM-manufactured composites." *Composites Part A: Applied Science and Manufacturing* 72 (2015): 175-183.
81. Van Velthem, Pascal, et al. "Phenoxy nanocomposite carriers for delivery of nanofillers in epoxy matrix for resin transfer molding (RTM)-manufactured composites." *Composites Part A: Applied Science and Manufacturing* 76 (2015): 82-91.
82. Van Velthem, Pascal, et al. "Morphology and Fracture Properties of Toughened Highly Crosslinked Epoxy Composites: A Comparative Study between high and low Tg Toughness."
83. Cordenier, François, et al. "ADDITION OF A BLOCK COPOLYMER INTO CARBON FIBERS/EPOXY COMPOSITES PROCESSED BY RTM: MICROSTRUCTURES AND MECHANICAL PROPERTIES."
84. "Araldite® MY 721". Product datasheet, *Ciba specialty chemicals*, http//:www.lindberg-lund.com/files/Tekniske%20datablad/VAN-**MY721**-TD.pdf
85. "Aradur® 9664-1", *Technical DataSheet*, Supplied By Huntsman. http://adhesives.specialchem.com
86. "4,4'-Diaminodiphenylsulfone". *CAS DataBase List.* Chemical Book http://www.chemicalbook.com/ChemicalProductProperty_EN_CB0152851.htm
87. "NANOCYL® NC7000". *Technical Data Sheet*, 25 January 2016. http://www.nanocyl.com/product/nc7000/
88. "PKHP-200 Powder". Product data by Gabriel Performance Products. Visited on 18 May 2016 http://www.gabrielchem.com/products/phenoxy-resin/products/standard-solid-grades/pkhp-200-powder/

89. Sacrez, Joachim. “Influencé de différents additifs polymères en vue d'améliorer la ténacité d'une résine epoxy de haute performance.” *Travail de fin d'études présenté en vue de l'obtention du grade d'ingénieur civil en science des matériaux*, UC Louvain, August 2015
90. Zhu, Xian-Kui, and James A. Joyce. "Review of fracture toughness (G, K, J, CTOD, CTOA) testing and standardizationXian-Kui Zhu." (2012).
91. Leadley, D. “Transmission Electron Microscopy (TEM)” Department of Physics, University of Warwick.https://www2.warwick.ac.uk/fac/sci/physics/current/postgraduate/regs/mpags/ex5/techniques/structural/tem/
92. “Equipment catalog”. Mica Platform, Institut de la matière condensée et des nanosciences (IMCN) http://sites.uclouvain.be/mica/index.php?page=catalogue&l=en
93. “Electron Microscopes”. A Review of the Universe - Structures, Evolutions, Observations, and Theories https://universe-review.ca/R11-13-microscopes.htm#electron
94. Swapp, S. “Scanning Electron Microscopy (SEM)”. *Geochemical Instrumentation and Analysis*, *University of Wyoming.* *http://serc.carleton.edu/research_education/geochemsheets/techniques/SEM.html*
95. Henry, D. “Electron-Sample Interactions”. *Geochemical Instrumentation and Analysis, Louisiana State University.* *http://serc.carleton.edu/research_education/geochemsheets/electroninteractions.html*
96. Bohlin Gemini II Rheometer. *Malvern Instruments*. http://www.aimil.com/product-Bohlin_Gemini_II_Rheometer-810.aspx Visited on 19 May 2016
97. “A Basic Introduction to Viscometers & Viscometry”. Rheosys LLC. http://www.rheosys.com/intro.html
98. W. Steinmann et al. “Thermal Analysis of Phase Transitions and Crystallization in Polymeric Fibers” Applications of Calorimetry in a Wide Context - Differential Scanning Calorimetry, Isothermal Titration Calorimetry and Microcalorimetry, (2013) DOI: 10.5772/54063. Available from: http://www.intechopen.com/books/applications-of-calorimetry-in-a-wide-context-differential-scanning-calorimetry-isothermal-titration-calorimetry-and-microcalorimetry/thermal-analysis-of-phase-transitions-and-crystallization-in-polymeric-fibers
99. Wikipedia contributors. "Differential scanning calorimetry." *Wikipedia, The Free Encyclopedia*. Wikipedia, The Free Encyclopedia, 19 May. 2016. Web. 6 Jun. 2016.
100. Gill, Pooria, Tahereh Tohidi Moghadam, and Bijan Ranjbar. "Differential scanning calorimetry techniques: applications in biology and nanoscience." *J Biomol Tech* 21.4 (2010): 167-193.